PROJECT 202
AG

MARINE TECHNOLOGY DEVELOPMENT GROUP PROJECT

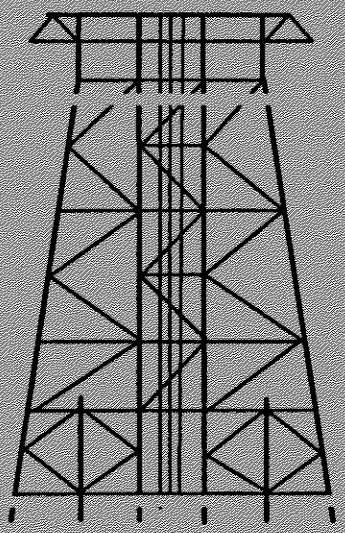

Screening Methodologies for Use in Platform Assessments and Requalifications

Final Report

by

Mehrdad Mortazavi
&
Professor Robert G. Bea

Department of Civil Engineering
University of California, Berkeley

June 1995

Table of Contents

Acknowledgments

This research has made extensive use of the software USFOS provided by SINTEF (trondheim, Norway), the SESAM pre and post processors for USFOS provided by Det Norske Veritas (DNV, Oslo, Norway and Houston, Texas). The implementation and initial application of this software on a RISK 6000 365 was performed by a visiting research scholar from SINTEF, Mr. Øyvind Hellan. The authors would like to acknowledge the assistance, guidance and instruction provided by SINTEF, DNV, and Mr. Øyvind Hellan in performing this study.

Appreciation is expressed to the sponsors including ARCO Exploration Co., Exxon Production Research Co., UNOCAL Corp., Shell Oil Co., Mobil Research and Development Co., the U.S. Minerals Management Service and the California State Lands Commission. Support and assistance have also been provided by Chevron Petroleum Technology Co., Amoco Production Co., and Phillips Petroleum Co.

Executive Summary

With the oil economics of today and new technology extending the life of the old oil fields, many existing offshore platforms are called upon for extended service. This makes the need to assess and requalify them a high priority concern.

During the past three decades, an immense amount of effort has been devoted to development of sophisticated computer programs to enable the assessment of storm wind, wave, and current loadings and the ultimate limit state capacity characteristics of conventional, pile-supported, template-type offshore platforms. The programs developed to help engineers perform such analyses require high degrees of expertise to operate properly, are expensive to purchase and maintain, and require large amounts of manpower and time to complete the analyses. Due to the sophistication of these programs, experience has shown that it is easy to make mistakes that are difficult to detect and that can have significant influences on the results.

The objective of this research was to develop and verify a simplified quantitative method for assessment of structural reliability of steel template-type offshore platforms subjected to severe storm conditions.

Verification of these procedures has been accomplished by comparing the results from the simplified analyses with the results from three dimensional, nonlinear analyses of a variety of template-type platforms. Good agreement between results from the two type of analyses has been developed for the evaluations of capacities. There is also a reasonable degree of verification of the simplified methods with the observed performance of platform in the field during intense hurricane storm loadings.

A computer program has been developed to perform the simplified analyses based on ultimate limit state limit equilibrium analysis (ULSLEA) techniques. Reasonable simplifications and high degrees of user friendliness have been employed in development of the software to reduce the engineering effort, expertise, and costs associated with the analyses.

ULSLEA can be used in the process of screening platforms that are being evaluated for extended service. In addition, it can be used to help verify results from complex analytical models that are intended to determine the

ultimate limit state loading capacities of platforms. Lastly, ULSLEA can be applied as a preliminary design tool for design of new platforms.

List of Figures

List of Tables

1. Introduction

1.1 Problem Statement

The offshore industry is relatively young by structural standards; the first steel platforms were installed in 1947 in the Gulf of Mexico. Since then they have been extensively used in development of offshore fields around the world. Today, there are over 7,000 offshore structures worldwide with more than 3,800 in the Gulf of Mexico. It was not until 1969 that the industry had its first offshore design standards with the publication of the first edition of API RP 2A (American Petroleum Institute Recommended Practice for Planning, Designing and Constructing Fixed Offshore Platforms). The design criteria for these platforms has changed significantly over the past four decades.

With the oil economics of today on one hand and new technology extending the life of the old oil fields on the other hand, many of these structures are now called upon for extended service. This makes the need to assess and requalify them a high priority concern; hurricanes of considerable magnitude and with significant impact have highlighted this need (Hilda and Betsy in the 1960's, Camille in 1974 and Andrew in 1992). In addition, interest in safety assessment and maintaining the safety of offshore platforms against loss of life, environmental pollution, and loss of resources and property has recently increased due to the awareness of the public of the consequences of their failure.

Assessment of existing facilities is not unique to offshore industry. The electric power generation industry and the chemical industry have been addressing the problem. The 1971 San Fernando, 1989 Loma Prieta, and 1994 Northridge earthquakes in California have repeatedly focused the attentions on existing infrastructure. In particular, questions were raised concerning safety of buildings and bridges.

During the past three decades, an immense amount of effort has been devoted to development of sophisticated computer programs to enable the assessment of storm wind, wave, and current loadings and the ultimate limit state capacity characteristics of conventional, pile-supported, template-type offshore platforms. There are many alternatives in modeling the structure and its components and in interpreting the results. There is very little validation of software, either against large scale test results, or by comparison with other

analytical results. The few existing studies indicate relatively large deviations and inconsistencies among the results of different software packages. Quite different results are demonstrated in the literature, in terms both of failure mode and capacity for the same structure (Billington et. al. 1993).

In addition to structural modeling uncertainties, large uncertainties are associated with environmental conditions (wave height, wind and current speed), calculated forces, and structure and foundation condition and capacities. These uncertainties add another dimension to the complexity of the process of assessment and requalification of offshore platforms.

Nevertheless, state of the art structural reliability evaluations based on nonlinear finite element analyses are the best we know to analytically deal with the problem. However, the programs developed to help engineers perform such analyses require high degrees of expertise to operate properly, are expensive to purchase and maintain, and require large amounts of manpower and time to complete the analyses. Due to the sophistication of these programs, experience has shown that it is easy to make mistakes that are difficult to detect and that can have significant influences on the results.

These facts and the large number of platforms that need to be assessed and requalified highlight the need for a practical methodology for safety assessment of existing platforms.

1.2 Project Description and Objective

The fundamental question is whether it is possible to develop a rational simplified method for a majority of existing platforms so that a complete reevaluation for each structure be unnecessary. The objective of this research was to develop and verify a simplified quantitative method for structural safety evaluation of steel template-type offshore platforms subjected to severe storm conditions.

This report documents the development of such a method. Simplified procedures have been developed to estimate the storm loadings on and lateral loading capacities of template-type offshore platforms.

Verification of these procedures has been accomplished by comparing the results from the simplified analyses with the results from three dimensional,

linear and nonlinear analyses of a variety of template-type platforms. The verification platforms have included four-leg well protector and quarters structures and eight-leg drilling and production Gulf of Mexico structures that employed a variety of types of bracing patterns and joints. Several of these structures were subjected to intense hurricane storm loadings during hurricanes Andrew, Camille, and Hilda. Within the population of verification platforms are several that failed or were very near failure.

A computer program has been developed to perform the simplified analyses based on ultimate limit state limit equilibrium analysis (ULSLEA) techniques. Reasonable simplifications and high degrees of user friendliness have been employed in development of the software to reduce the engineering effort, expertise, and costs associated with the analyses.

1.3 Organization of Report

Chapter 2 summarizes the background of platform reassessment and requalification process developed at University of California at Berkeley and that developed by American Petroleum Institute.

The modeling and simplified aero- and hydrodynamic loading calculation procedures are detailed in Chapter 3. Capacity formulations for the three structural components that comprise fixed platforms (deck, jacket and foundation) are discussed in Chapter 4. The basic concept of a simplified pushover analysis is presented and discussed in Chapter 5.

Taking into account the uncertainties associated with loadings and capacities, a simplified structural reliability analysis method is introduced, discussed, and implemented in Chapter 6.

Chapter 7 contains the results of a literature survey on Ultimate and Residual Strength of Damaged and Repaired Tubular Members. The modified capacity equations integrated into ULSLEA are also documented in this chapter.

Chapter 8 is devoted to the verification studies performed during this project. The loadings on and capacities of 5 GOM Platforms have been estimated using both the simplified ULSLEA and the nonlinear finite element analysis programs USFOS and SEASTAR.

Chapter 9 contains a summary of the developments and findings of this research. Potential research topics and need for further investigation are also identified and discussed in this chapter.

1.4 Notations

A_p	area of pile tip
A_{sh}	embedded area of pile shaft
A_d	effective cross-sectional area of dent section
A_0	cross-sectional area of undamaged member
A_{st}	cross-sectional area of the steel
A_s	cross-sectional area of the soil plug in pile
D, D_o	outside diameter of tubular member
D_i	inside diameter of tubular member
dd	dent depth
Δ	deck bay drift
ΔY	primary out-of-straightness of a dented member
ΔY_0	$=0.001\ L$
E	Young's modulus
f_{av}	ultimate average shear yield force per unit surface area of pile
f_y	yield stress
ϕ	angle of friction of soil
F_L	batter component of leg force
γ_{st}	submerged specific weight of the steel
γ_s	submerged specific weight of the soil
I_d	effective moment of inertia of dent cross-section
I_0	moment of inertia of undamaged cross-section
K_0	effective length factor of undamaged member
K	effective buckling length factor
L	unbraced member length
L_p	embedded length of the pile
λ	slenderness ratio
λ_d	slenderness parameter of a dented member = $(P_{ud}/P_{Ed})^{0.5}$
M_u	ultimate moment capacity
M_{cr}	critical moment capacity (local buckling)
M_p	plastic moment capacity of undamaged member
M_{ud}	ultimate negative moment capacity of dent section
M-	negative moment for dent section

$M+$	positive moment for dent section
M^*	neutral moment for dent section
n	# of platform supporting legs
P	axial compression
P_{crd}	critical axial buckling capacity of a dented member ($\Delta/L>0.001$)
P_{crd0}	critical axial buckling capacity of a dented member ($\Delta/L=0.001$)
P_E	Euler load of undamaged member
P_u	axial compression capacity
P_{ud}	axial compression capacity of a short dented member
P_{crl}	axial local buckling capacity
P_{cr}	axial column buckling capacity
P_y	tensile capacity
Q	total deck load
q	normal end yield force per unit of pile-end area
R	resistance
r	radius of gyration
R_p	ultimate end bearing capacity
R_s	ultimate shaft capacity
S	load
S_u	undrained shear strength of clay
t	member wall thickness
UC	unity check
w_p	submerged weight per unit of length of the pile and the soil plug
Z	plastic section modulus

2. Background

During 1988 through 1990, The University of California at Berkeley undertook and completed research on the requalification of platforms located in the Gulf of Mexico. This research resulted in a four level requalification approach which is based on a progressive screening process involving four cycles of analyses of increasing detail and difficulty (Figure 2.1):

- **Cycle 1:** qualitative scoring factors are used to evaluate the platform capacity and loadings and the potential consequences associated with the failure of the platform.
- **Cycle 2:** coarse quantitative analyses are used to define the capacity and loadings and the potential consequences of failure.
- **Cycle 3:** detailed quantitative state-of-the-practice analyses of platform capacity, loadings and potential consequences are performed.
- **Cycle 4:** very detailed quantitative state-of-the-art analyses are used to evaluate platform performance characteristics, the probabilistic aspects of the loadings and capacities, and the likelihood and consequences associated with failure.

This four cycle assessment approach is thought to be a rapid mean that can be used for a periodic reassessment and evaluation of the safety and serviceability of platforms. In this way platforms can be qualified at the earliest possible cycle and a detailed evaluation of the reserve strength and consequence levels is required for only a few platforms.

In early 1992, the American Petroleum Institute (API) initiated an effort to develop a Recommended Practice (RP) for Assessment of Existing Platforms. An API task group was charged with developing procedures for inspection and acceptance criteria. The initial draft of the API RP 2A Section 17 was published in 1993 encompassing a global framework and recommending a multi-level screening approach. Based on this working draft, a document was ballot released for a one year review/comment to assist the process of acceptance and use.

Incorporating industry feedback received at the International Workshop on Reassessment and Requalification of Offshore Production Structures, held in New Orleans in December 1993, and a trial application of the Section 17

process on a number of existing platforms by several organizations, API will officially issue a draft Supplement 1 for both the WSD and LRFD versions of API RP 2A. Figure 2.2 shows the Platform Assessment Process for Metocean Loading as contained in Section 17 (Digre et. al. 1995).

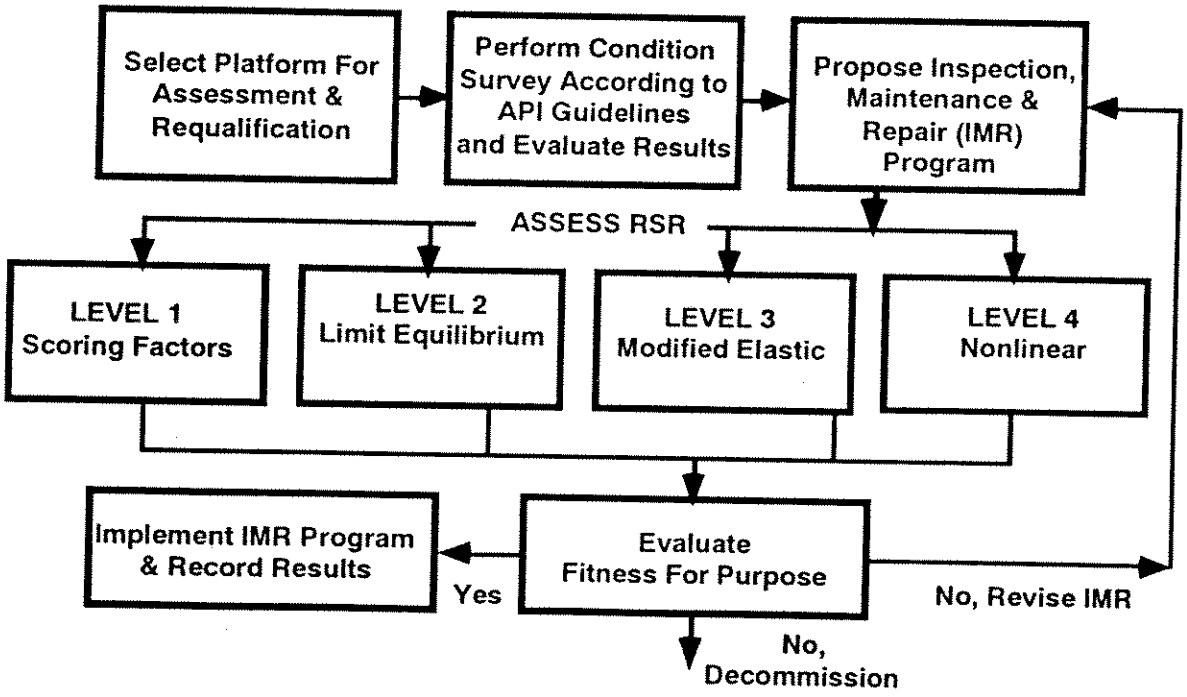

Figure 2.1: Assessment and Requalification Approach Based on RSR

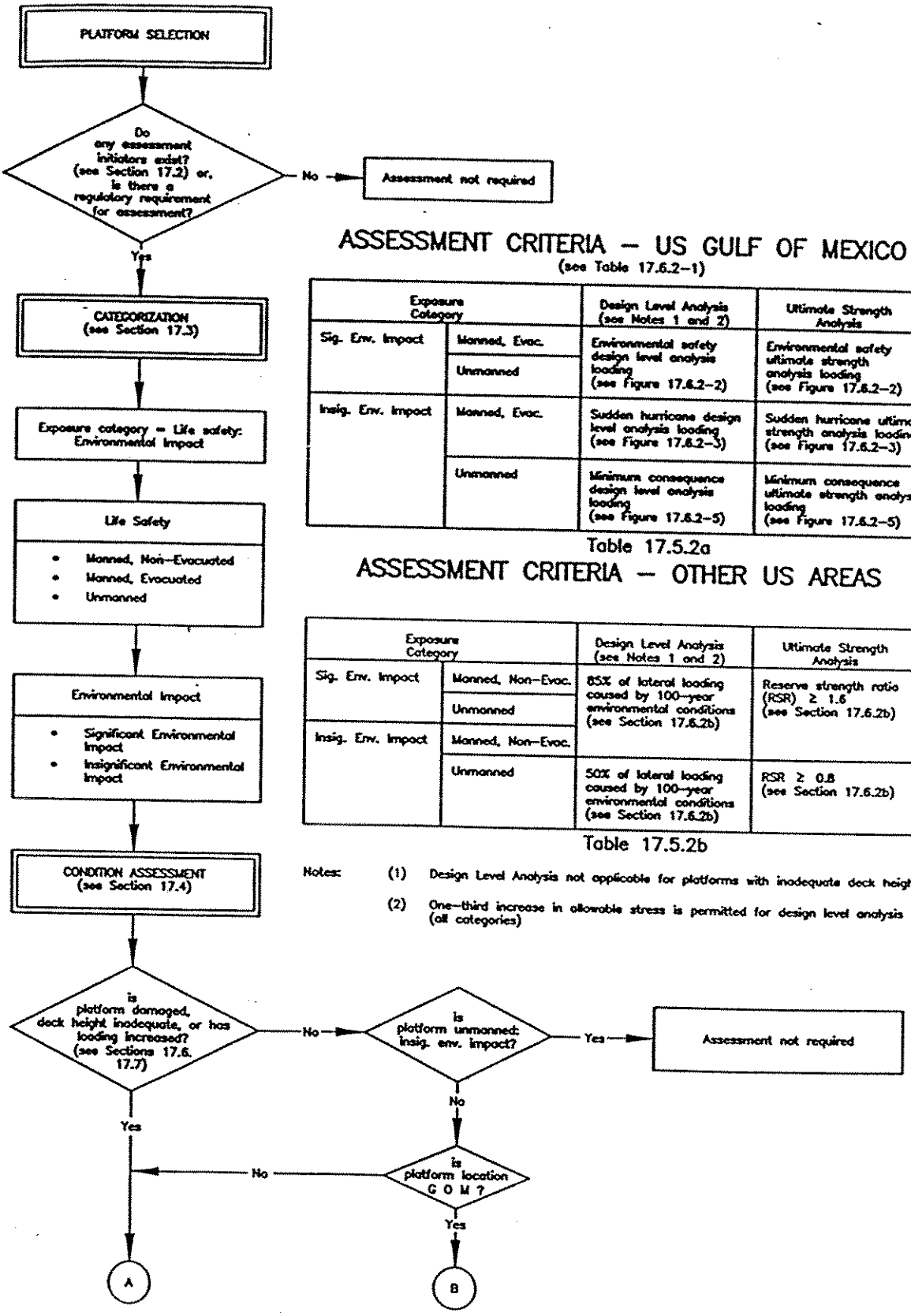

ASSESSMENT CRITERIA — US GULF OF MEXICO

(see Table 17.6.2–1)

Exposure Category		Design Level Analysis (see Notes 1 and 2)	Ultimate Strength Analysis
Sig. Env. Impact	Manned, Evac.	Environmental safety design level analysis loading (see Figure 17.6.2–2)	Environmental safety ultimate strength analysis loading (see Figure 17.6.2–2)
	Unmanned		
Insig. Env. Impact	Manned, Evac.	Sudden hurricane design level analysis loading (see Figure 17.6.2–3)	Sudden hurricane ultimate strength analysis loading (see Figure 17.6.2–3)
	Unmanned	Minimum consequence design level analysis loading (see Figure 17.6.2–5)	Minimum consequence ultimate strength analysis loading (see Figure 17.6.2–5)

Table 17.5.2a

ASSESSMENT CRITERIA — OTHER US AREAS

Exposure Category		Design Level Analysis (see Notes 1 and 2)	Ultimate Strength Analysis
Sig. Env. Impact	Manned, Non-Evac.	85% of lateral loading caused by 100-year environmental conditions (see Section 17.6.2b)	Reserve strength ratio (RSR) ≥ 1.6 (see Section 17.6.2b)
	Unmanned		
Insig. Env. Impact	Manned, Non-Evac.		
	Unmanned	50% of lateral loading caused by 100-year environmental conditions (see Section 17.6.2b)	RSR ≥ 0.8 (see Section 17.6.2b)

Table 17.5.2b

Notes: (1) Design Level Analysis not applicable for platforms with inadequate deck height.

(2) One-third increase in allowable stress is permitted for design level analysis (all categories)

Figure 2.2: Platform Assessment Process (API RP 2A - Section 17)

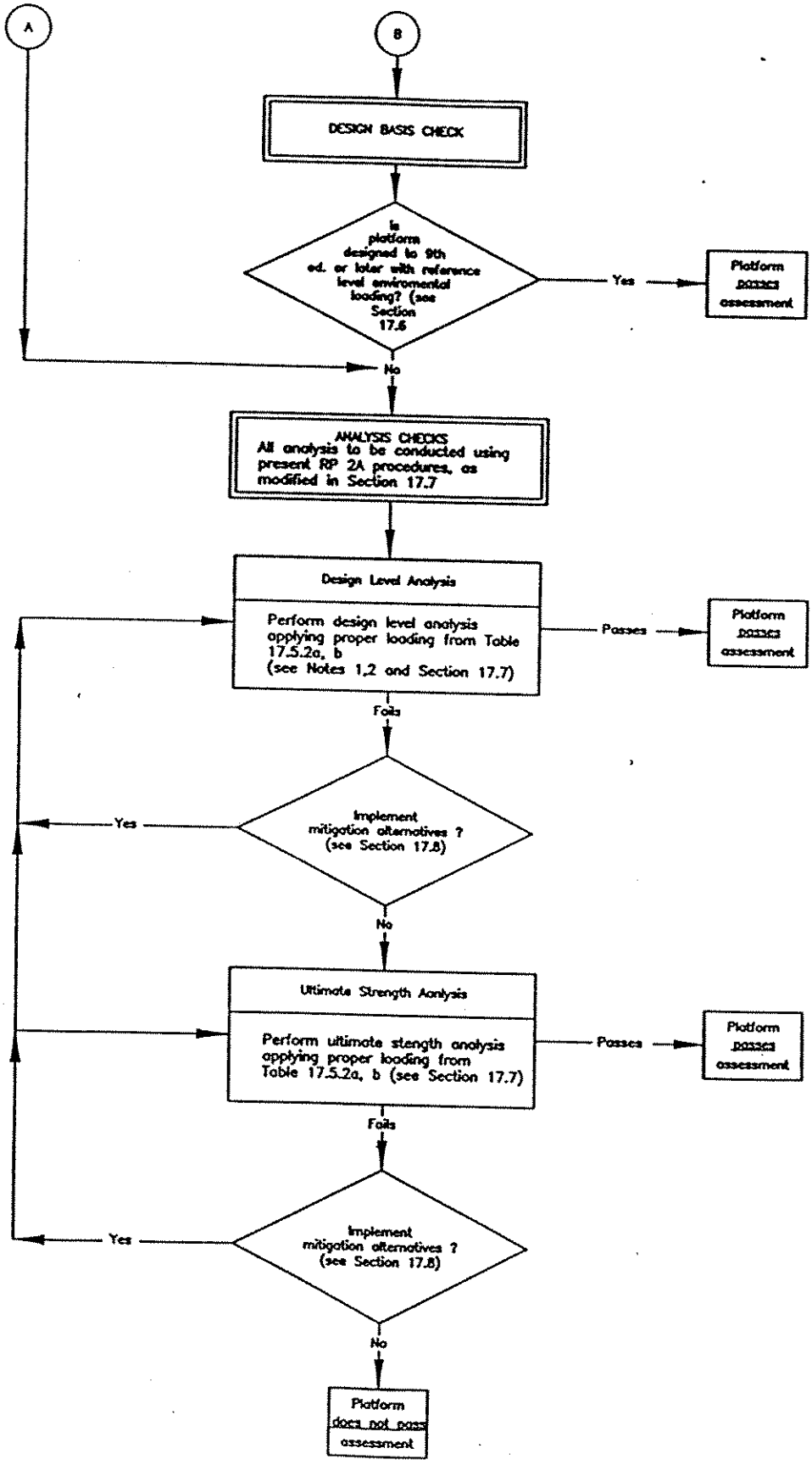

Figure 2.2 (Continue): Platform Assessment Process (API RP 2A - Section 17)

3. Aero- and Hydrodynamic Loadings

3.1 Introduction

The purpose of this part of the study was to develop a simple procedure that helps determining the loadings acting on a platform. Given the environmental conditions including wind speed at +30 ft elevation, wave height and the associated period, and current profile, Stokes 5th Order Wave Theory is utilized to estimate the water particle velocities and accelerations.

All of the structure elements are modeled as equivalent vertical cylinders that are located at the wave crest. Appurtenances (boat landings, risers) are modeled in a similar manner. Marine growth can be accounted for. For wave crest elevations that reach the lower decks, the horizontal hydrodynamic forces acting on the lower decks are computed based on the projected area of the portions of the structure that would be able to withstand the high pressures.

3.2 Loading Calculation Procedure

Wave, current, wind, and storm tide are considered. Aerodynamic and hydrodynamic loadings are calculated according to API RP 2A guidelines. The maximum wind force S_a acting on the exposed decks is based on the wind velocity pressure

$$S_a = \frac{\rho_a}{2} C_s A_d V_d^2 \tag{3.1}$$

where ρ_a is the mass density of air, C_s the wind velocity pressure (drag) coefficient, A_d is the effective projected area of the exposed decks, V_d the wind velocity at the deck elevation and for an appropriate time interval.

Wave horizontal velocities are based on Stokes 5th order theory. Using equations given by Skjelbreia and Hendrickson (1961) and Fenton (1985), a computer program was developed to determine the wave kinematics (Preston, 1994). Given the wave height H, period T and water depth d, the vertical profile of maximum horizontal velocities beneath the wave crest are estimated as

$$\frac{u}{c} = K_{ds} \sum_{n=1}^{5} n\phi'_n \cosh(nks) \tag{3.2}$$

where K_{ds} is a coefficient that recognizes the effects of directional spreading and wave irregularity on the Stokes wave theory based velocities. k is the wave number and s is the vertical coordinate counting positive upward from the sea floor. c is the wave celerity and given as

$$\frac{c^2}{gd} = \frac{\tanh(kd)}{kd}\left[1 + \lambda^2 C_1 + \lambda^4 C_2\right] \tag{3.3}$$

The crest elevation η is estimated as

$$k\eta = \sum_{n=1}^{5} \eta'_n \tag{3.4}$$

ϕ'_n and η'_n are given functions of λ and kd. C_n are known functions of kd only, given by Skjelbreia and Hendrickson (1961). The wave number k is obtained by implicitly solving the following equation given by Fenton(1985)

$$\frac{2\pi}{T(gk)^{0.5}} - C_0 - \left(\frac{kH}{2}\right)^2 C_2 - \left(\frac{kH}{2}\right)^4 C_4 = 0 \tag{3.5}$$

The parameter λ is then calculated using the equation given by Skjelbreia and Hendrickson(1961)

$$\frac{2\pi d}{gT^2} = \frac{d}{L}\tanh(kd)\left[1 + \lambda^2 C_1 + \lambda^4 C_2\right] \tag{3.6}$$

The specified variation of current velocities with depth is stretched to the wave crest and modified to recognize the effects of structure blockage on the currents. The total horizontal water velocities are taken as the sum of the wave horizontal velocities and the current velocities.

The maximum hydrodynamic force S_h acting on the portions of structure below the wave crest are based on the fluid velocity pressure

$$S_k = \frac{\rho_w}{2} C_d A_j U^2 \tag{3.7}$$

where ρ_w is the mass density of water, A_j the effective vertical projected area of the exposed structure element, and U the horizontal velocity of water at a particular point on the submerged portion of the structure element.

All of the structure elements are modeled as equivalent vertical cylinders that are located at the wave crest. Appurtenances (boat landings, risers) are modeled in a similar manner. For inclined members, the effective vertical projected area is determined by multiplying the product of member length and diameter by the cube of the cosine of its angle with the horizontal.

For wave crest elevations that reach the lower decks, the horizontal hydrodynamic forces acting on the lower decks are computed based on the projected area of the portions of the structure that would be able to withstand the high pressures. The fluid velocities and pressures are calculated in the same manner as for the other submerged portions of the structure with the exception of the definition of C_d. In recognition of rectangular shapes of the structural members in the decks a higher C_d is taken. This value is assumed to be developed at a depth equal to two velocity heads (U^2/g) below the wave crest. In recognition of the near wave surface flow distortion effects, C_d is assumed to vary linearly from its value at two velocity heads below the wave crest to zero at the wave crest (Fig. 3.1) (McDonald et. al., 1990, Bea, DesRoches, 1993).

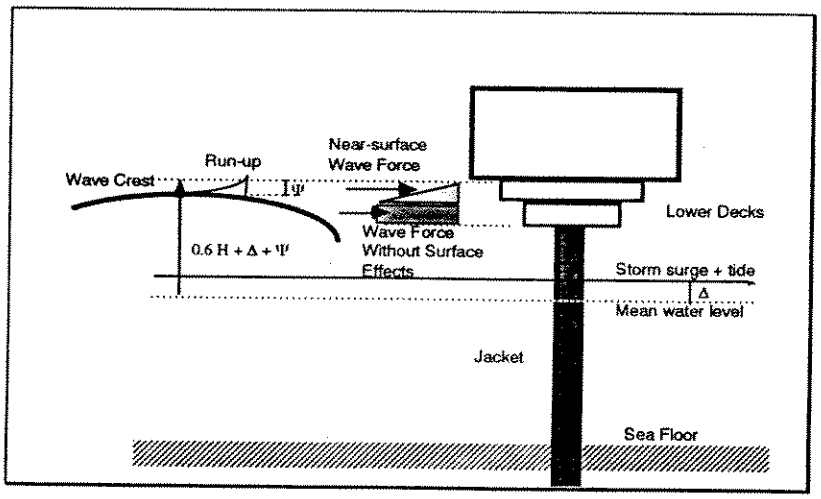

Figure 3.1: Wave Crest Forces Acting on the Platform Decks

3.3 Verification of Wave Loading Calculation Procedure

The procedure used to estimate the wave forces acting on a jacket structure is checked against computer output for four design wave cases calculated during a wave force study by Exxon and Shell (Bea, 1973).

Using ULSLEA, the wave force acting on a 3 ft diameter surface piercing cylinder was estimated. This was done using Stokes 5^{th} Order and Depth Stretched Linear Wave Theories. A drag coefficient of C_d=0.6 was used in all cases. The results were also compared to those gained by using Dean's Charts (Dean, 1973) that are developed based on 9^{th} Order Stream Function Theory. The results are summarized in figures 3.2 to 3.5.

Figure 3.2 shows the results for deep water conditions. Using Stokes V to model the wave kinematics results in an estimate of base shear that is in good agreement with results reported in Exxon-Shell wave force study. Surprising is the result gained by using Depth Stretched Linear Wave Theory, which gives a base shear that is almost 40% less than that given by Stokes V. Interestingly, this base shear is in good agreement with that gained using Dean's Charts. At this stage, the authors can not explain this disparity.

Figures 3.3 and 3.4 show the results for transitional water depths. Again, it can be seen that Stokes V results are in good agreement with those reported in Exxon-shell study. Depth Stretched Linear Wave Theory underpredicts the base shear by 40% to 50%. Dean's Charts result in a base shear that is about 20% to 30% less than that gained by using Stokes V.

Figure 3.5 shows the results for shallow water conditions. Stokes V base shear is about 10% to 15% larger than the base shear predicted by Exxon-Shell study and that gained by using Dean's Charts. Airy Wave based prediction is 80% less than Stokes V results.

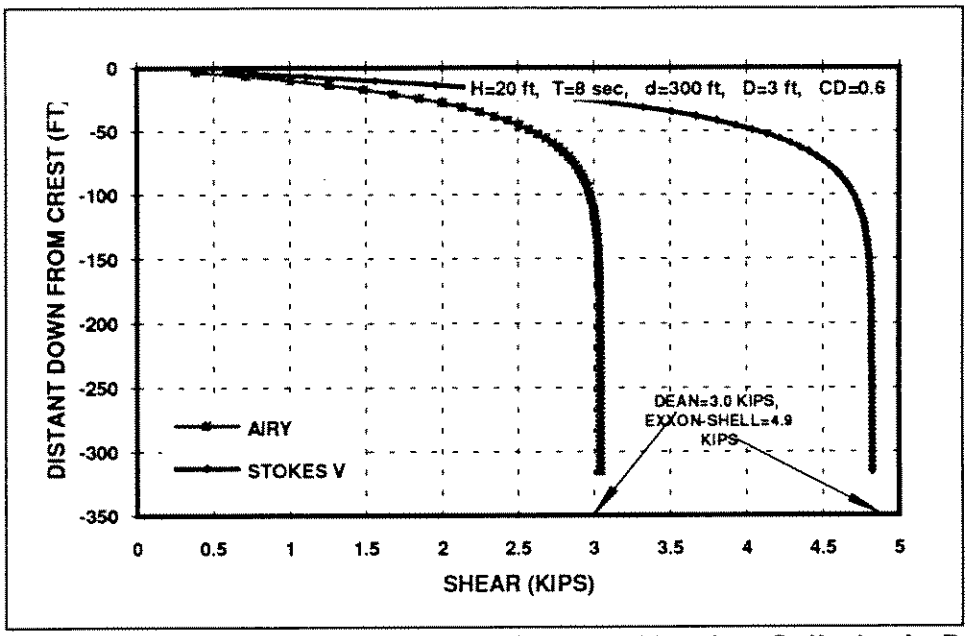

Figure 3.2: Wave Force on a Vertical Surface Piercing Cylinder in Deep Water

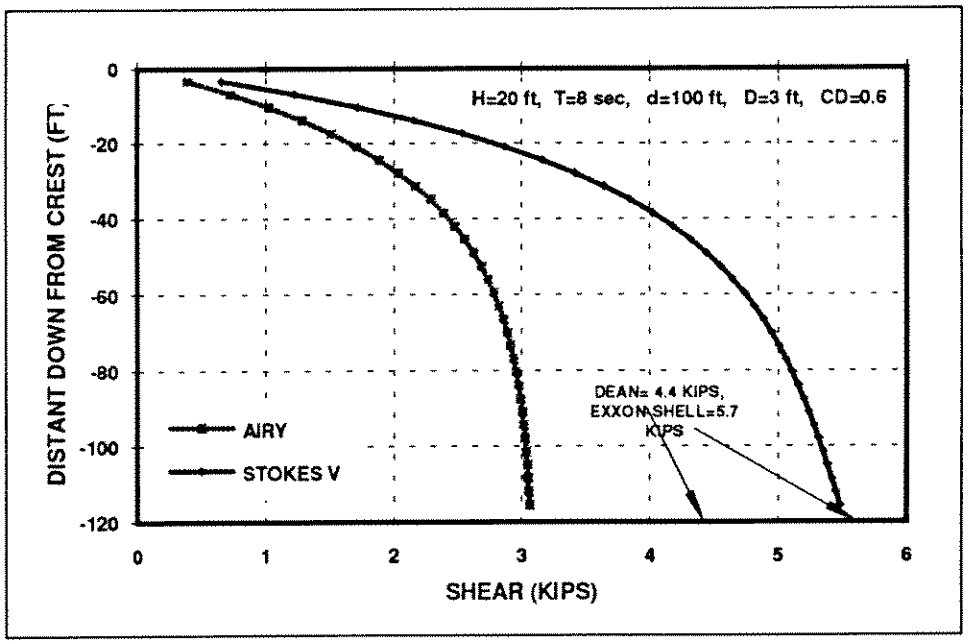

Figure 3.3: Wave Force on a Vertical Surface Piercing Cylinder in Transitional Water Depth

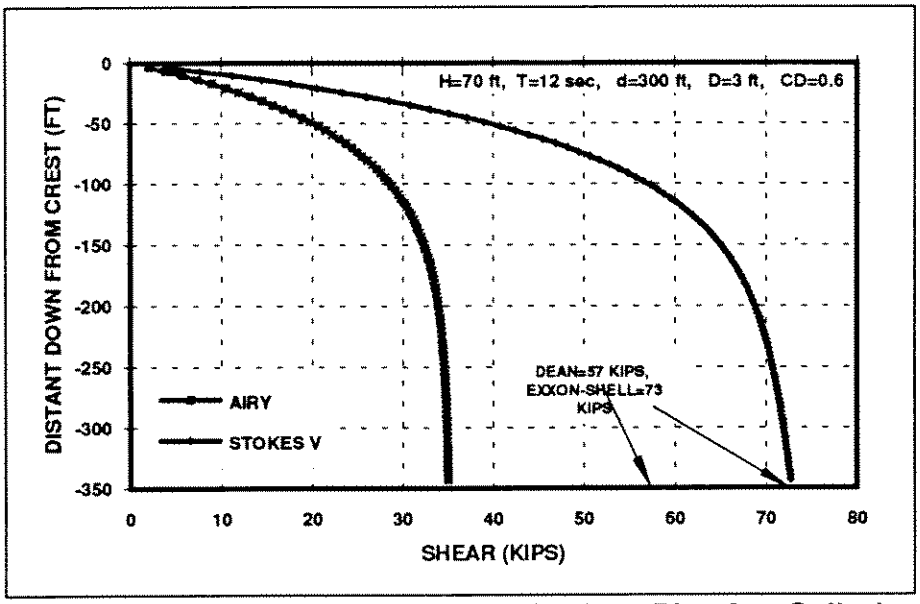

Figure 3.4: Wave Force on a Vertical Surface Piercing Cylinder in Transitional Water Depth

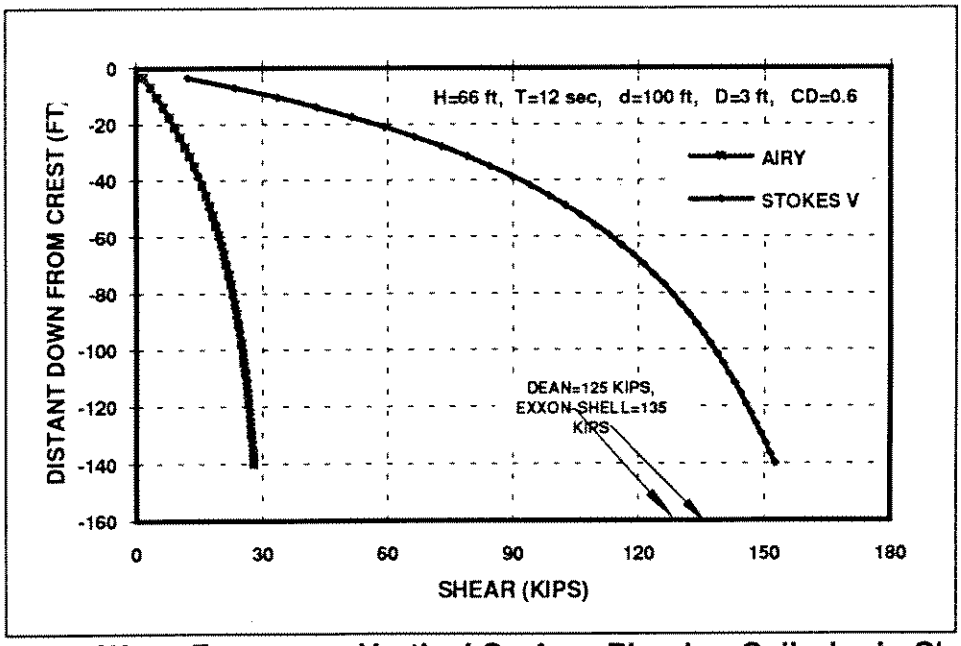

Figure 3.5: Wave Force on a Vertical Surface Piercing Cylinder in Shallow Water

3.3 Summary

This section describes a simple environmental loading model that is able to predict estimates of total lateral wind, wave and current loading acting on jacket-type offshore platforms.

The wave loading prediction model utilizes Stokes 5th Order Wave Theory, based on which a sub-routine has been developed that estimates the wave kinematics. The current velocity profile is added to the wave velocity profile. The hydrodynamic drag force acting on the structure's simplified model is estimated using the first term in the Morrisons (MJOS) equation.

The procedure has been verified with results reported in a wave force study performed by Exxon and Shell (Bea, 1973). Good agreement has been achieved for wave loading on a surface piercing cylinder in deep water and transitional water depth conditions. In shallow water conditions the procedure tends to overpredict the base shear by about 10%.

Verification studies have also been performed on platforms. The results are documented in Chapter 8 of this report and indicate an overprediction of total base shear of about 10% in average as compared to results gained using a sophisticated three dimensional wave loading calculation program (WAJAC, DNV, 1993).

4. Platform's Lateral Loading Capacity

4.1 Introduction

This Chapter describes the development of element and component capacity estimation procedures used to predict the ultimate lateral loading capacity of platform system.

Using the concept of plastic hinge theory, limit equilibrium is formulated by implementing principle of virtual work. This is the key to the simplified ultimate limit state analysis method. Where of importance, geometric and material nonlinearities are considered. This method is being increasingly used in plastic design of simple structures or structural elements (e.g. moment frames, continuous beams). Due to the impracticality of such analyses for more complicated structures, these methods have not found broad use in design or assessment of complex structures; all possible failure modes need be considered and evaluated to capture the "true" collapse mechanism and the associated ultimate lateral load.

Actual field experience and numerical results from three dimensional nonlinear analyses performed on a variety of template-type platforms indicate that in most cases certain failure modes govern the ultimate capacity of such platforms: plastic hinge formation in the deck legs and subsequent collapse of the deck portal, buckling of the main load carrying vertical diagonal braces in the jacket, lateral failure of the foundation piles due to plastic hinge formation in the piles and plastification of foundation soil, and pile pullout or pile plunging due to exceedance of axial pile and soil capacities.

Within the framework of a simplified analysis and based on experience, collapse mechanisms are assumed for the three primary components that comprise a template-type platform: the deck legs, the jacket, and the pile foundation. Based on the presumed failure modes, the principle of virtual work is utilized to estimate the ultimate lateral capacity for each component.

4.2 Deck Legs Capacity

The ultimate shear that can be resisted by an unbraced deck portal is estimated based on bending moment capacities of the tubular deck legs that support the upper decks.

A collapse mechanism in the deck bay would form by plastic yielding of the leg sections at the top and bottom of all of the deck legs. The interaction of bending moment and axial force (***M-P***) is taken into account. The maximum bending moment and axial force that can be developed in a tubular deck leg is limited by local buckling of leg cross-sections.

The vertical dead loads of the decks are assumed to be equally shared between the deck legs. The vertical live loads in the deck legs caused by the lateral overturning forces are computed and summed to define the axial loading in each deck leg.

Due to relatively large axial loads (weight of the decks and topside facilities) and large relative displacements (deck bay drift) at collapse, ***P-Δ*** effect play a role in reducing the lateral shear capacity and hence is taken into account.

To derive a realistic estimate of ***P-Δ*** effect with out leaving the framework of a simplified analysis, it is assumed that the deck is rigid. It is further assumed that plastic yielding of the sections at the bottom of the deck legs occur simultaneously, following the plastic yielding of the sections at the top of the legs and hence an estimate of plastic hinge rotations to calculate the deformations is unnecessary.

Finally, to estimate the deck bay drift at collapse Δ, the jacket is replaced by rotational springs at the bottom of each deck leg. The spring stiffness C_r is approximated by applying external moments, which are equal in magnitude and have the same direction, to the top of jacket legs at the uppermost jacket bay. Assuming rigid horizontals and fixed boundary conditions at the bottom of these jacket legs, the rotation of cross-sections at the top of the legs and hence the rotational stiffness C_r is determined

$$\frac{1}{C_r} = \frac{L_l}{K} - \frac{3C_s L_l^4}{4C_s L_l^3 K + 12K^2} \tag{4.1}$$

where C_s is a lateral stiffness coefficient and given as

$$C_s = \frac{1}{2}\sum_i \frac{\cos^2\alpha_i E_i A_i}{L_i} \tag{4.2}$$

summed over all diagonal braces within the uppermost jacket bay and

$$K = E\, I_1 \cos\beta \tag{4.3}$$

where I_1 denotes the moment of inertia of the jacket leg at the uppermost jacket bay. The deck bay drift can now be estimated as

$$\Delta = M_{cr} L_d \left(\frac{L_d}{6EI} + \frac{1}{C_r} \right) \tag{4.4}$$

The principle of virtual force is implemented to calculate the deck bay horizontal drift at collapse. Equilibrium is formulated using the principle of virtual displacement. Using the actual collapse mechanism as the virtually imposed displacement, the equilibrium equation for the lateral shear capacity of the unbraced deck portal is derived

$$P_u = \frac{1}{L_d}(2n M_u - Q\Delta) \tag{4.5}$$

and

$$\frac{M_u}{M_{cr}} - \cos\left(\frac{\pi}{2} \frac{Q/n}{P_{crl}} \right) = 0 \tag{4.6}$$

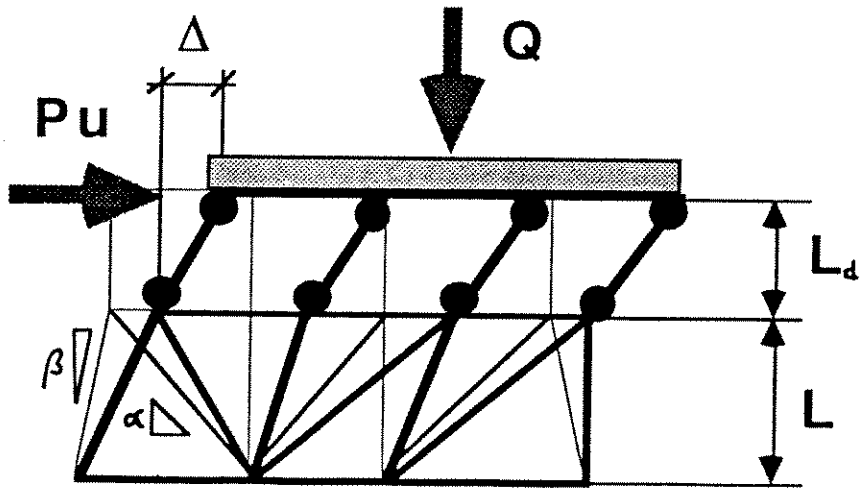

Fig. 4.1 : Deck Portal at Ultimate Lateral Load

4.3 Jacket Bay Capacity

The shear capacity of each of the bays of vertical bracing that comprise the jacket is estimated including the tensile and compressive capacity of the diagonal braces and the associated joint capacities. The capacity of a given brace is taken as the minimum of the capacity of the brace or the capacity of either its joints.

To derive a lower-bound capacity formulation, the notion of Most Likely To Fail (*MLTF*) element is introduced. *MLTF* element is defined as the member with the lowest capacity over stiffness ratio. The lower-bound lateral capacity of a jacket bay is estimated by adding the horizontal force components of all load carrying members in the given bay at the instant of first member failure. A linear multi-spring model is used to relate the forces and displacements of diagonal braces within a bay. The axial force in the jacket legs due to lateral overturning moment is estimated at each bay and its batter component is added to the lateral capacity.

$$P_{u,l} = P_{u,MLTF} + \sum_i \left(\frac{P_{u,MLTF}}{K_{MLTF}} \right) K_i + F_L \tag{4.7}$$

where $P_{u,l}$ denotes the lower bound shear capacity of a jacket bay, P_u is the horizontal component of axial force in a given diagonal brace, F_L is the batter component of leg forces, and K_i denotes the lateral stiffness of braces given by

$$K_i = \frac{L_i \cos^2 \alpha}{E_i A_i} \tag{4.8}$$

where L, E, A, and α denote the length, Young modulus, cross-sectional area, and the angle between the diagonal brace and the horizon respectively.

An upper-bound capacity is also formulated for each bay. After the *MLTF* member in compression reaches its axial capacity, it can not maintain the peak load and any further increase in lateral displacement will result in unloading of this member. Presuming that the load path remains intact (inter-connecting horizontals do not fail), a load redistribution follows and other members carry the loading of the lost members until the last brace reaches its peak capacity.

An empirical residual capacity modification factor α is introduced. Assuming elasto-perfectly plastic material behavior, α is equal to 1.0 for members in tension (neglecting strain hardening effects) and less than 1.0 for members in compression due to P-δ effects (generally in the range of 0.15 to 0.5). The upper-bound capacity of a given jacket bay, $P_{u,u}$, is estimated by adding the horizontal component of the residual strength of all of the braces within the bay

$$P_{u,u} = \sum_i P_{ui}\alpha_i + F_L \tag{4.9}$$

Within the frame work of a simplified analysis, the jacket has been treated as a trusswork. Plastic hinge formation in the jacket legs is not considered because this hinge development occurs at a lateral deformation that is much greater than is required to mobilize the axial capacities of the vertical diagonal braces. At the large lateral deformations required to mobilize the lateral shear capacities of the legs, the diagonal brace load capacities have decreased markedly due to column buckling or tensile rupture.

In general, the effect of bending moment along the jacket legs on the lateral capacity is neglected. This assumption is explained by the following example.

We impose a virtual displacement to the i^{th} jacket bay of a two dimensional jacket frame (Figure 4.2) and equate the external and internal work:

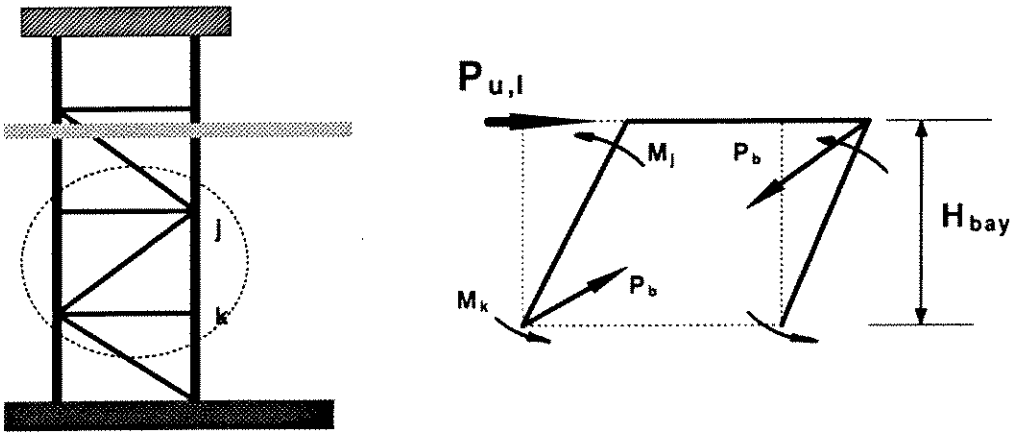

Fig. 4.2 : Lateral Capacity of a Jacket Bay

$$W^{(E)} = W^{(I)} \tag{4.10}$$

which leads to the following equation for the jacket bay capacity

$$P_{u,I} = P_{bh} + \frac{2(M_J + M_K)}{H_{bay}} \tag{4.11}$$

where P_{bh} denotes the horizontal component of brace axial force. Assuming that the bending moment in the jacket legs is negligible

$$M_J = M_K = 0 \tag{4.12}$$

the following simplified relationship results

$$P_{u,I} = P_{bh} \tag{4.13}$$

This assumption leads to estimates of lateral capacity of a jacket bay that are either conservative or unconservative depending on the actual bending moment distribution in the legs. However, the difference in capacities (estimated vs. actual) is negligible for all but the uppermost and lowest jacket bays. Due to frame action in the deck portal and rotational restraint of the legs at mud level, the jacket legs experience relatively large bending moments at these two bays. The bending moment in the legs at the lowest bay has the direction of a resisting moment and hence not considering it can only be conservative. In contrary, the shear force due to the large moment gradient at the uppermost jacket bay has the same direction as the global lateral loading and hence reduces the lateral capacity. If this effect is not taken into account, the lateral capacity will be over-estimated.

A simplified procedure is developed to account for the effect of shear force in the top jacket bay. We are interested in moment distribution along the legs at this bay due to frame action in the deck portal. Given the geometry of the deck portal and the load acting on deck areas, the moment distribution along the deck legs can be estimated.

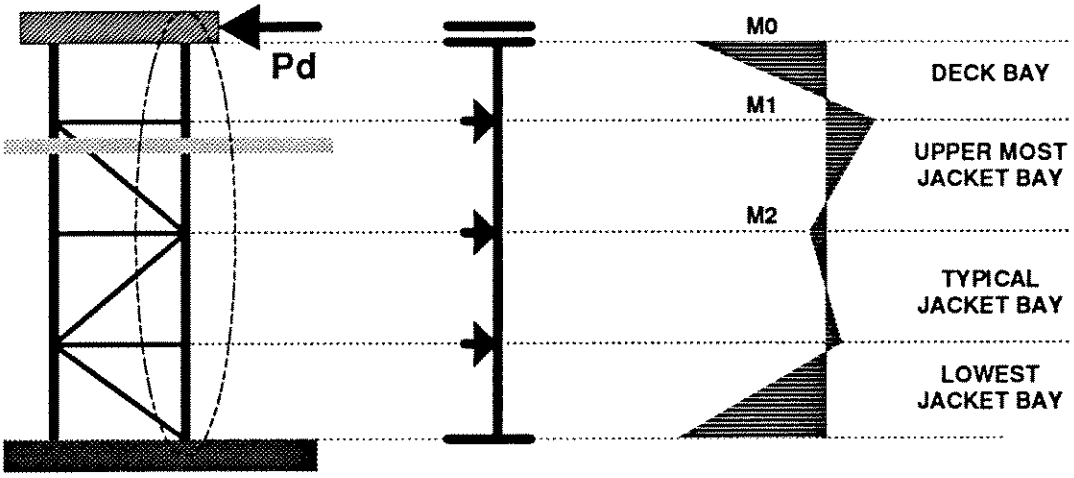

Fig. 4.3 : Moment Distribution in Jacket Legs

$$M_0 = \frac{\frac{P_d L_d^2}{2EI} + \frac{P_d L_d}{C_r}}{\frac{L_d}{EI} + \frac{1}{C_r}} \leq M_p \qquad (4.14)$$

$$M_1 = M_0 - P_d L_d \leq M_p \qquad (4.15)$$

Thinking of a jacket leg as a continuous beam which is supported by horizontal framings, the applied moment at the top of the leg rapidly decreases towards the bottom. Based on geometry of the structure, in particular jacket bay heights and the cross-sectional properties of the jacket leg (if non-prismatic), and in the limiting case of rigid supports, an upper-bound for the desired moment distribution is estimated. For equal spans, constant moment of inertia and limiting case of rigid supports the following relationship can be derived

$$|M_2| \leq 0.286 |M_1| \qquad (4.16)$$

Tubular Brace Capacity

The diagonal braces near the free surface are exposed to high combined bending moments and axial forces. The existing bending moment result in a reduction of the ultimate axial load capacity of the brace. At the ultimate state the large deflections result in inelastic strains. Generally an elastic-plastic

load deflection (P-δ) analysis should be performed to determine the ultimate strength of the brace.

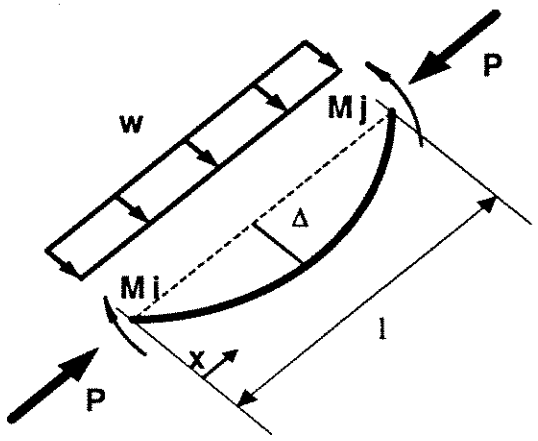

Fig. 4.4: Brace Element Under Compressive and Transverse Loading

The braces are treated as though there are no net hydrostatic pressures (e.g. flooded members). The governing differential equation of the beam-column can be given as

$$M_{xx} + \frac{P}{EI} M = -w - 8P \frac{\Delta_0}{l^2} \tag{4.18}$$

where M_{xx} stands for the second derivative of bending moment with regard to the coordinate x. The following substitutions

$$\xi = \frac{x}{l} \quad , \quad \varepsilon = l\sqrt{\frac{P}{EI}} \tag{4.19) , (4.20}$$

result in the transformed equation

$$M_{\xi\xi} + \varepsilon^2 M = -wl^2 - 8P\Delta_0 \tag{4.21}$$

which has the following closed-form solution

$$M(\xi)=\frac{\sin\varepsilon(1-\xi)}{\sin\varepsilon}M(\xi=0)+\frac{\sin\varepsilon\xi}{\sin\varepsilon}M(\xi=1)+\frac{1}{\varepsilon^2}\left(\frac{\cos\varepsilon(0.5-\xi)}{\cos\frac{\varepsilon}{2}}-1\right)\left(wl^2+8P\Delta_o\right) \tag{4.22}$$

Based on a three-hinge failure mode, the exact solution of the second order differential equation for the bending moment of a beam-column is implemented to formulate the equilibrium at collapse

$$M(\xi=0.5)=-M(\xi=0)=-M(\xi=1)=M_u \tag{4.23}$$

$$M_u=\left(\frac{1}{1+2\frac{\sin 0.5\varepsilon}{\sin\varepsilon}}\right)\frac{1}{\varepsilon^2}\left(\frac{1}{\cos\frac{\varepsilon}{2}}-1\right)\left(wl^2+8P_u\Delta_o\right) \tag{4.24}$$

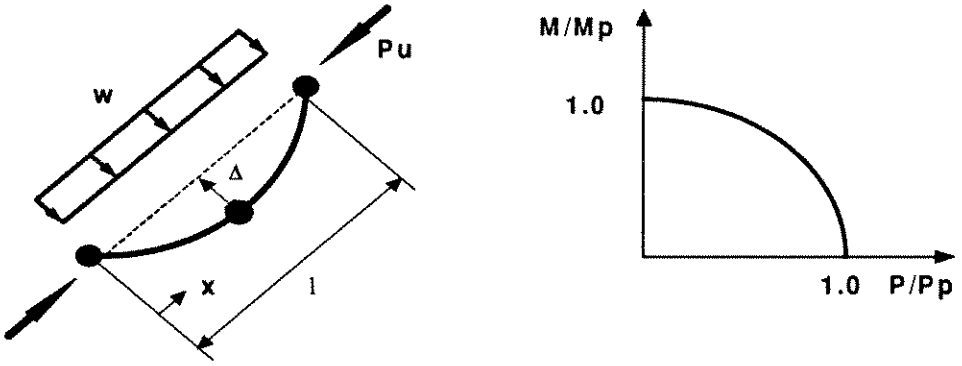

Fig. 4.5: Three Hinge Failure Mode for Diagonal Braces

Elasto-perfectly plastic material behavior is assumed. The ultimate compression capacity is reached when full plastification of the cross-sections at the member ends and mid-span occurs. It is further assumed that plastic hinges at member ends form first followed by plastic hinge formation at mid-span. ***M-P*** interaction condition for tubular cross-sections provides a second equation for the unknown ultimate moment M_u and axial force P_u in plastic hinges at collapse

$$\frac{M_u}{M_p} - \cos\left(\frac{\pi}{2}\frac{P_u}{P_p}\right) = 0 \tag{4.25}$$

The results have been verified with results from the nonlinear finite element program USFOS. Using the same initial out-of-straightness Δ_0 for both simplified and complex analyses, the axial compression capacity of several critical diagonal members of different structures has been estimated. The simplified method slightly over-predicts the axial capacity of compression members (less than 10%).

The initial out-of-straightness Δ_0 is used to calibrate the axial compression capacity of braces to the column buckling curves according to API RP-LRFD (API, 1993)

$$\Delta_0 = \frac{M_p \cos\left(\frac{\pi}{2}\frac{P_{cr}}{P_p}\right)}{\left(\frac{1}{1+2\frac{\sin 0.5\varepsilon}{\sin\varepsilon}}\right)\frac{1}{\varepsilon^2}\left(\frac{1}{\cos\frac{\varepsilon}{2}}-1\right)(8P_{cr})} \tag{4.26}$$

Using "appropriate" buckling length factors, the calibrated results are in close agreement with results from USFOS (Hellan et. al., 1994).

Tubular Joint Capacity

Tubular members are frequently used in offshore structures mainly because of their drag characteristics. The stress analysis of the circular tubular joints and the theoretical prediction of their ultimate strength has proven to be difficult. Various approaches to "elastic" stress analysis of different joint types and geometries can be found in the literature, ranging from shell theory, to thin-shell finite elements, to isoparametric finite elements. However these stress analyses do not address the ultimate strength, as tubular connections have a high plastic reserve strength beyond first yield. Hence empirical capacity equations based on test results have often been used to predict the joint ultimate strength. The following parameters have a significant influence on the capacity of a joint (P.W.Marshall, 1986):

- Chord yield strength (f_y)
- Chord radius to thickness ratio (γ)

- Type of load (axial tension, axial compression)
- Load pattern (type of joint : ***K, Y, T, DT, X***)
- Geometric parameters (diameter ratio, ratio of gap between braces in a ***K***-joint to brace diameter)
- Existing load in chord

Based on a reliable data base of 137 tests of tubular joints, Yura et. al. (1980) recommended one formula for both compressive and tensile ultimate capacity in the branch of a ***K***-joint. This formula is identical to that for ***T*** and ***Y*** joints except for the additional gap factor. The test capacity was taken as the first crack load. For simple tubular joints with no gussets, diaphragms, or stiffeners, the capacity equations given in Table 4.1 are used.

Joint Type	Tension	Compression
T , Y	$\frac{f_y T^2 (3.4 + 19\beta)}{\sin\theta}$	$\frac{f_y T^2 (3.4 + 19\beta)}{\sin\theta}$
DT , X	$\frac{f_y T^2 (3.4 + 19\beta)}{\sin\theta}$	$\frac{f_y T^2 (3.4 + 13\beta)}{\sin\theta} Q_\beta$
K	$\frac{f_y T^2 (3.4 + 19\beta)}{\sin\theta} Q_g$	$\frac{f_y T^2 (3.4 + 19\beta)}{\sin\theta} Q_g$

Table 4.1: Capacity Equations for Simple Tubular Joints

Q_β is a factor accounting for geometry and Q_g is a gap modifying factor and are estimated according to the following equations

$$Q_g = 1.8 - 0.1\frac{g}{T} \quad \text{for} \quad \gamma \le 20 \tag{4.27}$$

$$Q_g = 1.8 - 4\frac{g}{D} \quad \text{for} \quad \gamma > 20 \tag{4.28}$$

$$Q_\beta = \frac{0.3}{\beta(1 - 0.833\beta)} \quad \text{for} \quad \beta > 0.6 \tag{4.29}$$

$$Q_\beta = 1.0 \quad \text{for} \quad \beta \le 0.6 \tag{4.30}$$

g denotes the gap between branches of K-joints, $\beta = d/D$ and $\gamma = d/2T$. d, D, and T are the branch and chord diameter and thickness respectively.

4.4 Foundation Capacity

Pile Lateral Capacity

The pile shear capacity is based on an analysis similar to that of deck legs with the exception that the lateral support provided by the foundation soils and the batter shear component of the piles are included.

For cohesive soils, the distribution of lateral soil resistance along the pile per unit length, p_s, is assumed to be

$$p_s = 9 S_u D \tag{4.31}$$

where S_u is the effective undrained shear strength of the soil and D is the pile diameter. For a constant S_u over the pile length and for a given scour depth, X, the ultimate lateral force that can be developed at the pile top is estimated as (Tang, 1990)

$$P_{u,l} = 0.5\left\{-\left(27D^2S_u + 18S_uXD\right) + \left[\left(27D^2S_u + 18S_uXD\right)^2 + 144S_uDM_u\right]^{0.5}\right\} \tag{4.32}$$

M_u is the plastic moment capacity of the pile cross-section computed in the same manner as for the deck legs. In the case of linearly increasing shear strength with depth the ultimate lateral capacity of the pile, $P_{u,l}$, can be derived from the following equations

$$P_{u,l}\left(C + \xi\right) - 2M_o - \left(A + \eta\xi\right)\frac{C^2}{2} - \left(\frac{\eta}{2}\right)\frac{C^3}{3} = 0 \tag{4.33}$$

$$C = \frac{1}{\eta}\left[\left(-A + \eta\xi\right) + \sqrt{\left(A + \eta\xi\right)^2 + 2\eta P_{u,l}}\right] \tag{4.34}$$

where

$$\eta = \frac{B - A}{L_p} \tag{4.35}$$

$$\xi = 1.5D + X \tag{4.36}$$

$$A = 9 S_{u1} D \quad \text{and} \quad B = 9 S_{u2} D \tag{4.37), (4.38}$$

S_{u1} and S_{u2} denote the undrained shear strength at mudline and at the pile tip respectively.

For cohesionless soils, the distribution of lateral soil pressure along a pile at a depth, z, is assumed to be

$$p_s = 3\gamma z K_p \tag{4.39}$$

where

$$K_p = \tan^2\left(45 + \frac{\phi}{2}\right) \tag{4.40}$$

ϕ is the effective angle of internal friction of the soil and γ is the submerged unit weight of the soil. The ultimate lateral force that can be developed at the pile top with no scour is (Tang, 1990)

$$P_{u,1} = 2.382 M_p^{2/3} (\gamma D K_p)^{1/3} \tag{4.41}$$

For a scour depth equal to X, the ultimate lateral force is

$$P_{u,1} = \frac{2 M_p}{\left[X + 0.544\left(\frac{P_{u,1}}{\gamma D K_p}\right)\right]^{0.5}} \tag{4.42}$$

The horizontal batter component of the pile top axial loading is added to estimate the total lateral shear capacity of the piles. This component is computed based on axial loads carried by the piles due to storm force overturning moment (Bea, DesRoches 1993).

Pile Axial Capacity

The axial resistance capacity of a pile is based on the combined effects of a shear yield force acting on the lateral surface of the pile and a normal yield

force acting over the entire base end of the pile. Thus the ultimate axial capacity Q, is expressed as

$$Q = Q_s + Q_p = q\ A_p + f_{av} A_{sh} \tag{4.43}$$

Q_p denotes the ultimate end bearing and Q_s is the ultimate shaft capacity, q is the normal end yield force per unit of pile-end area acting on the area of pile tip A_p, and f_{av} denotes the ultimate average shear yield force per unit of lateral surface area of the pile acting on embedded area of pile shaft A_{sh}.

It is assumed that the pile is rigid and that shaft friction and end bearing forces are activated simultaneously. It is further assumed that the spacing of the piles is sufficiently great so that there is no interaction between the piles. In the case of compressive loading, the weight of the pile and the soil plug (for open-end piles) is deducted from the ultimate compressive loading capacity of the pile. For open-end piles, the end bearing capacity is assumed to be fully activated only when the shaft frictional capacity of the internal soil plug exceeds the full end bearing.

For cohesive soils with an undrained shear strength S_u, the ultimate bearing capacity is taken as the end bearing of a pile in clay

$$q = 9 S_u \tag{4.44}$$

The ultimate shaft friction is taken as

$$f_{av} = \alpha S_{u,av} \tag{4.45}$$

where α is the side resistance factor and a function of the average undrained shear strength $S_{u,av}$ as given in Table 4.2.

$S_{u,av}$ (ksf)	α
<0.5	1
0.5 - 1.5	1 - 0.5
>1.5	0.5

Table 4.2: Side Resistance Factor for Cohesive Soils

For cohesionless soils the ultimate bearing capacity of a deeply embedded pile is estimated as

$$q = N_q \sigma_v \tag{4.46}$$

N_q is a bearing capacity factor and a function of the friction angle of the soil Φ, and σ_v denotes the effective pressure at the pile tip. Since sand soils possess high permeability, the pore water quickly flows out of the soil mass and the effective stress is assumed equal to applied stress. The unit shaft resistance on pile increment is estimated as

$$f_i = k \sigma_{vi} \tan\delta \tag{4.47}$$

where k is an earth lateral pressure coefficient assumed to be 0.8 for both tension and compression loads, σ_{vi} denotes the effective overburden pressure at the given penetration, and δ denotes the friction angle between the soil and pile material and is taken as

$$\delta = \Phi - 5^{\circ} \tag{4.48}$$

The unit shaft resistance and the unit end bearing capacity can not indefinitely increase with the penetration. The ultimate axial capacity of piles in sand soils is estimated based on commonly used limiting values for N_q, q_{max} and f_{max} given by Focht and Kraft (1986), (Table 4.3).

Φ	N_q	q_{max}(ksf)	f_{max}(ksf)
20	8	40	1.0
25	12	60	1.4
30	20	100	1.7
35	40	200	2.0

Table 4.3: Frequently Used Values for Medium Dense Materials

After considering the weight of the pile and the soil plug (for open-end piles), the ultimate compressive loading capacity of the pile, Q_c, can be calculated as

$$Q_c = q\pi D_o^2/4 + (f_{av}\pi D_O - w_p)L_p \tag{4.49}$$

where

$$w_p = \gamma_{st}A_{st} + \gamma_s A_s = \gamma_{st}\pi(D_o^2 - D_i^2)/4 + \gamma_s \pi D_i^2/4 \tag{4.50}$$

The end bearing capacity can be fully activated only when the shaft frictional capacity of the internal soil plug exceeds the full end bearing (Focht and Kraft, 1986). This condition can be formulated as

$$q\pi D_i^2/4 < (f_{av}\pi D_i + w_s)L_p \tag{4.51}$$

The tensile capacity is similarly estimated as

$$Q_t = (f_{av}\pi D_o + w_p)L_p \tag{4.52}$$

5. Deterministic Failure Analysis

Utilizing the background that is developed in Chapters 3 and 4, the methodology behind a simplified "static" nonlinear analysis of platform systems is described in this Chapter.

The process is summarized in figures 5.1 and 5.2. The geometry of the platform is defined by specifying a minimum amount of data by the user. These include the effective deck areas, the proportion and topology of jacket legs, braces, and joints and of the foundation piles and conductors. The projected area characteristics of appurtenances such as boat landings, risers, and well conductors must also be specified. If marine fouling is present, the variation of the fouling thickness with depth may be specified by the user.

Specialized elements may be designated including grouted or ungrouted joints, braces, and legs. In addition, damaged or defective elements can be included. Dent depth and initial out-of-straightness are specified by user for braces with dents and global bending defects. User-defined element capacity reduction factors are introduced to account for other types of damage to joints, braces, and foundation (corrosion, fatigue cracks, etc.).

Steel elastic modulus, yield strength, and effective buckling length factor for vertical diagonal braces are specified by the user. Soil characteristics are specified as the depth variation of effective undrained shear strength (for cohesive soils) or the effective internal angle of friction (for cohessionless soils). Scour depth can be specified by the user.

Storm wind speed at the deck elevation, wave height and period, current velocity profile, and storm water depth are also defined by the user. These values are assumed to be colinear and to be the values that occur at the same time. Generally the load combination is chosen to be wind speed component and current component that occur at the same time and in the same principal direction as the expected maximum wave height. The wave period is generally taken to be expected period associated with the expected maximum wave height.

To calculate wind loadings acting on the exposed decks the user must specify the effective drag coefficient. Similarly, the user must specify the

hydrodynamic drag coefficients for smooth and marine fouled members. User specified coefficients can also be introduced to recognize the effects of wave directional spreading and current blockage.

Collapse mechanisms are assumed for the three primary components that comprise a template-type platform: the deck legs, the jacket, and the pile foundation (Chapter 4). Based on the presumed failure modes, the principle of virtual work is utilized to estimate the ultimate lateral capacity for each component and a profile of horizontal shear capacity of the platform is developed.

Storm intensity is based on the expected maximum wave height with wind speed and current velocities that have the same principal direction and occur at the same time as the maximum wave height (Chapter 3). Comparison of the storm shear profile with the platform shear capacity profile identifies the "weak link" in the platform system. The base shear or total lateral loading at which the capacity of this weak link is exceeded defines the static ultimate lateral capacity of the platform R_{us}. The static lateral loading capacity is corrected with a loading effects modifier, F_v, to recognize the interactive effects of transient wave loadings and nonlinear hysteretic platform response (Bea and Young, 1993)

$$R_u = R_{us} F_v \tag{5.1}$$

With these results, the Reserve Strength Ratio (RSR) can be determined as

$$RSR = \frac{R_u}{S_r} \tag{5.2}$$

S_r denotes the reference storm total maximum lateral loading.

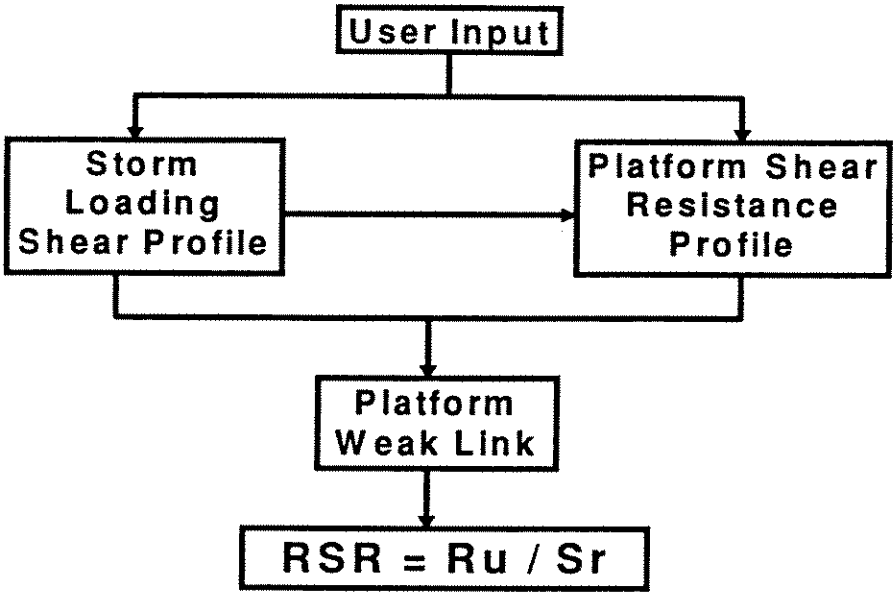

Figure 5.1: Deterministic Failure Analysis

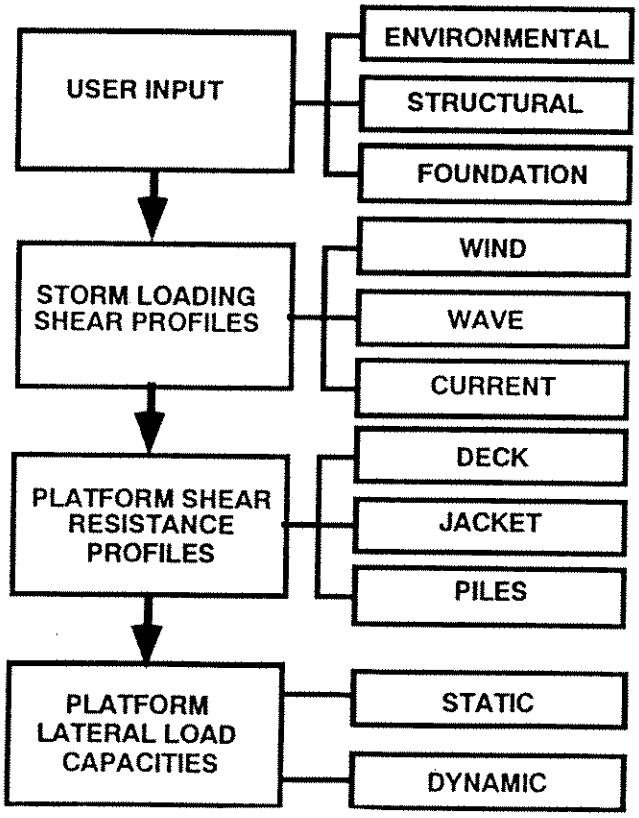

Figure 5.2: Deterministic Platform Loading and Capacity Analysis

6. Probabilistic Failure Analysis

6.1 Introduction

This chapter describes development of a simplified method to assess the structural reliability of conventional template-type offshore platforms. The objective is to identify the potential failure modes and weak links of the structure by taking into account the biases and uncertainties associated with loadings and capacities (Figure 6.1).

With this in mind, the maximum static force acting on a platform is treated as a function of random variables. Its statistical properties are derived considering the uncertainties associated with environmental conditions, structure conditions, kinematics, and force calculation procedures. The expected capacity of the structure and the uncertainty associated with it is also characterized. The simplified ultimate limit state (*ULS*) analysis procedures described in previous chapters are utilized to estimate an expected or best estimate capacity of the platform. The uncertainties associated with this capacity are estimated using a combination of series components and parallel elements. The series components are the superstructure (deck), the substructure (jacket), and the foundation. The capacity of the platform is reached when the capacity of anyone of these components is reached. Within each component there are parallel elements; deck legs, braces, joints, and piles. In order for a component to reach its *ULS* capacity, all of the parallel elements have to fail.

The proposed reliability analysis in this chapter is based on a First Order Second Moment (*FOSM*) approach. A study is made of the implications of the simplified *FOSM* method. In the case of an eight-leg drilling and production platform located in Gulf of Mexico (verification platform A), the results from *FOSM* reliability analysis are compared with those from first and second order reliability methods (*FORM* and *SORM*).

6.2 Loading and Capacity Formulations

Simplified loading and capacity equations have been developed in Chapters 3 and 4 of this report. Some of these equation are used in this section and are repeated for the sake of completeness.

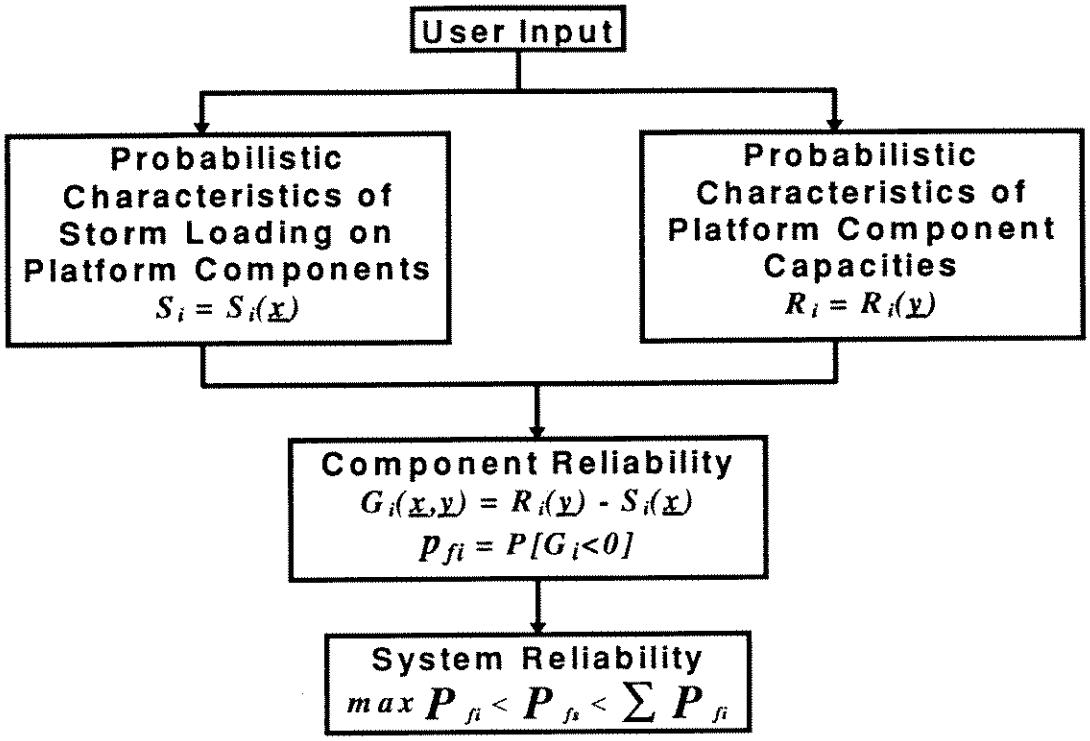

Figure 6.1: Probabilistic Failure Analysis

Storm Loadings

A combination of storm wind load and hydrodynamic wave and current loads is considered:

$$S = S_w + S_h \tag{6.1}$$

The wind load is given by:

$$S_w = K_w (V_{wd})^2 \tag{6.2}$$

where K_w is a structure dependent loading parameter, and V_{wd} is the wind speed that occurs at the same time as the maximum wave height. The total integrated drag force acting on a surface piercing vertical cylinder can be expressed as:

$$S_h = K_d K_u H^2 \tag{6.3}$$

K_u is an integration function that integrates the velocities along the cylinder and is a function of wave steepness and the wave theory used to estimate the velocities. K_d is a force coefficient and a function of mass density of water ρ, diameter of the cylinder D, and drag coefficient C_d. The mean forces acting on the elements are integrated and the shear force at each component level is calculated. These integrated shear forces define the means of the load variables S_D for deck, S_{Ji} for each jacket bay, and the base shear S_F for the foundation bay.

Deck Leg Shear Capacity

A mechanism in the deck leg bay would form when plastic hinges are developed at the top and bottom of all of the deck legs. Using this failure mode as a virtual displacement, virtual work principle can be utilized to estimate the deck leg shear resistance R_d:

and

$$R_d = \frac{1}{L_d}(2n M_u - Q\Delta) \tag{6.4}$$

where

$$\Delta = M_{cr} L_d \left(\frac{L_d}{6EI} + \frac{1}{C_r} \right) \tag{6.5}$$

$$\frac{M_u}{M_{cr}} - \cos\left(\frac{\pi}{2} \frac{Q/n}{P_{crl}} \right) = 0 \tag{6.6}$$

The moment capacity of the legs M_{cr} and the local buckling capacity P_{crl} are treated as random variables.

Jacket Bays Shear Capacity

Shear capacity in a given jacket bay is reached when the vertical diagonals are no longer capable of resisting the lateral load acting on the jacket bay. Tensile and compressive capacity of the diagonal braces, the associated joint capacities, and the batter component of axial forces in the legs due to overturning moment are included to estimate the jacket bay shear capacity. The capacity of a given brace is taken as the minimum of the capacity of the brace or the capacity of either its joints.

At this stage, it is assumed that the brace behavior governs the capacity of the joint-brace system. It is further assumed that interconnecting horizontal brace elements are rigid. Thus, the capacity of the n^{th} jacket bay R_{Jn} can be given as:

$$R_{J_n} = \sum_i R_i \alpha_i + F_L \tag{6.7}$$

where R_i is the horizontal resisting force of the brace element i. In the case of lower-bound capacity, α_i are deterministic factors accounting for geometry and relative member stiffness ($\alpha_i R_i$ = horizontal shear force of brace element i at the onset of first member failure). In the case of upper-bound capacity, α_i account for the post-yielding behavior of semi-brittle brace elements ($\alpha_i R_i$ = residual strength of brace element i), and F_L denotes the horizontal shear force in the jacket legs.

Foundation Capacity

Two basic types of failure mode in the foundation are considered: lateral and axial. The lateral failure mode of the piles is similar to that of the deck legs. In addition to moment resistance of the piles, the lateral support provided by foundation soils and the batter shear component of the piles are considered. The lateral and axial capacity equations for piles in sand and clay are given in Chapter 4 of this report.

6.3 Component and System Reliability

Based on a mean value first order second moment (*mvfosm*) approximation and using the load and capacity equations formulated earlier in this paper, the mean and standard deviation of loads and capacities can be estimated. Defining a safety margin as:

$$M = lnR - lnS \tag{6.8}$$

the probability of failure can be given by:

$$p_f = CDF(U) \tag{6.9}$$

where

$$U = \frac{(M - \mu_M)}{\sigma_M} \tag{6.10}$$

is a standard variate with zero mean and unit standard deviation. Presuming lognormal distribution for loads and capacities, the exact reliability index can be given as:

$$\beta = \frac{\mu_M}{\sigma_M} \tag{6.11}$$

where

$$\mu_M = ln\left(\frac{\mu_R}{\mu_S}\sqrt{\frac{1+V_S^2}{1+V_R^2}}\right) \tag{6.12}$$

$$\sigma_M^2 = ln\left(1+V_R^2\right) + ln\left(1+V_S^2\right) - 2\,ln\left(1+\rho_{RS}V_R V_S\right) \tag{6.13}$$

and

$$P_f = \Phi(-\beta) \tag{6.14}$$

where $\Phi(.)$ is the cumulative standard normal function. Please note that these equations and those derived for jointly normally distributed loads and capacities are the only known exact and closed form solutions of the probability of failure for non-trivial distributions of loads and capacities.

Unimodal bounds on probability of failure of a series system, p_{fs}, can be estimated by:

$$max\, P_{fi} < P_{fs} < \sum_i P_{fi} \tag{6.15}$$

where p_{fi} denotes the probability of failure of the i^{th} component.

Considering a platform as a series system, the structural reliability can be evaluated by using the formulations given earlier. The series components are the superstructure (deck), the substructure (jacket), and the foundation. The capacity of the platform is reached when the capacity of anyone of these

components is reached. Within each component there are parallel elements; deck legs, braces, joints, and piles. In order for a component to reach its ULS capacity, all of the parallel elements have to fail.

Using a first-order Taylor-series approximation around the mean point, the required means and standard deviations of loads and capacities can be computed. By specifying the means of input variables, the mean lateral load acting on components and the mean component capacities are estimated. The coefficient of variation of wave load is given as:

$$V_s = \sqrt{V_{K_1}^2 + V_{K_2}^2 + (2V_H)^2} \tag{6.16}$$

Since the dominating storm condition is the maximum wave height and its associated period, evaluation of the uncertainties in the wind forces does not play a major role and is not included.

Assuming perfect correlation between M_{cr} and P_{crl}, the standard deviation of deck legs capacity σ_{RD} can be given as:

$$\sigma_{RD}^2 = \sigma_{Mcr}^2 \left(\frac{\partial R_D}{\partial M_{cr}}\right)^2 + \sigma_{Pcrl}^2 \left(\frac{\partial R_D}{\partial P_{crl}}\right)^2 + 2\sigma_{Mcr}\sigma_{Pcrl}\left(\frac{\partial R_D}{\partial M_{cr}}\right)\left(\frac{\partial R_D}{\partial P_{crl}}\right) \tag{6.17}$$

where $\frac{\partial R_D}{\partial M_{cr}}$ and $\frac{\partial R_D}{\partial P_{crl}}$ are the partial derivatives of the deck legs shear capacity R_D with respect to moment and buckling capacities M_{cr} and P_{crl}.

Assuming perfect correlation among the brace capacities R_i, the standard deviation of the n^{th} jacket bay's shear capacity σ_{RJn}, can be given as:

$$\sigma_{RJn} = \sqrt{\sum_i (\alpha_i \sigma_{Ri})^2 + \sum_{i,j} \alpha_i \alpha_j \sigma_{Ri} \sigma_{Rj} + (B_{FL}\sigma_{FL})^2} \tag{6.18}$$

B_{FL} denotes the bias associated with axial leg forces. It should be noted that the diagonal brace capacities are negatively correlated with the lateral loading. This correlation is neglected at this stage.

Considering the uncertainties in soil and pile material properties, the uncertainty in foundation capacity can also be estimated.

6.4 Example Application

Located in the main pass area of the Gulf of Mexico, the 8-leg template type platform is installed in a water depth of approximately 271 feet (verification platform A, Figure A1). Designed and installed in 1968-70, the platform is exposed to high environmental loading developed by hurricanes passing through the Gulf.

Because of its dominance, only wave force is considered. According to oceanographic studies performed for the site, the 100 year return period wave height, H_{100}, is 70 feet. The uncertainties associated with wave height predictions are assumed and given in Table 6.1.

	σ_{lnH}	*Bias* (B_H)	σ_{lnBH}
H_{max}	**0.3**	**1.1**	**0.13**

Table 6.1: Wave Height Uncertainties

Considering these uncertainties result in a total bias of B_H=1.1 and a coefficient of variation of V_H = 0.34. Assuming lognormal and type I extreme value distributions, the probabilistic characteristics of the maximum wave height are given in Table 6.2. In latter case the distribution parameters are computed by tail-fitting.

$f_H(h)$	μ_H (*ft*)	σ_H (*ft*)
Lognormal	**34.5**	**11.7**
Type I largest	**34.0**	**11.4**

Table 6.2: Probabilistic Characteristics of the Maximum Wave Height

The variabilities of the force coefficients given by Bea (1990) are used to estimate the uncertainties associated with wave forces (Table 6.3).

	σ_{lnK}	*Bias* (B_k)	σ_{lnBk}
K_u	**0.1**	**0.41**	**0.47**
K_d	**0.1**	**1.67**	**0.23**

Table 6.3: Force Coefficient Uncertainties

Based on the background developed in the previous sections of this chapter, structural reliability of the example platform is studied for the two principal orthogonal directions. The mean loads acting on the structure and the mean capacities are calculated using the computer program ULSLEA. For each load direction, eight different failure modes are identified and analyzed; one in the superstructure, five in the substructure, and two foundation failure modes.

For bending moment capacity M_{cr}, local buckling capacity P_{crl}, and compressive capacity of diagonal braces P_{cr}, the mean-value curves given by Cox (1987) are utilized:

$$M_{cr} = M_p \left[1.113 \exp\left(\frac{-1.638 f_y D}{Et} \right) \right] \tag{6.19}$$

$$P_{crl} = P_y \left[1.79 - 0.25 \left(\frac{D}{t} \right)^{0.25} \right] \tag{6.20}$$

$$P_{cr} = P_y \left(1.03 - 0.24 \lambda^2 \right) \quad for \ 0 < \lambda < 1.7 \tag{6.21}$$

where

$$M_p = 1.3 Z f_y \tag{6.22}$$

$$P_y = A f_y \tag{6.23}$$

$$\lambda = \left(\frac{1}{\pi} \right) \left(\frac{KL}{r} \right) \sqrt{\frac{f_y}{E}} \tag{6.24}$$

For bending resistance, a combined c.o.v. of 0.106 is given. The c.o.v. for local buckling is 0.117. These coefficient of variations include the test

uncertainties, uncertainties in steel yield strength, and uncertainties associated with fabrication. These values are reported to be constant over the entire range of practical values of ***Et/fyD*** and ***D/t*** respectively. The uncertainties of column resistance over a practical range of λ are given in Table 4 (Cox, 1987).

λ	0.4	0.6	0.8	1.0	1.2	1.4
c.o.v.	0.099	0.100	0.106	0.119	0.150	0.212

Table 6.4: Column Resistance Uncertainties

In addition to uncertainties associated with test and fabrication, the uncertainties associated with yield stress f_y, elastic modulus E, and effective column length factor K are included in the column resistance uncertainty.

Due to lack of data regarding the pile capacity modeling uncertainty, the total uncertainties recommended by Tang and Gilbert (1990) are used, which are based on test results and implicitly include the model uncertainties (Table 6.5).

Lateral Capacity in:	Bias	c.o.v.
Clay	0.92	0.20
Sand	0.81	0.21

Table 6.5: Lateral Pile Capacity Uncertainties

The uncertainty associated with the batter component of the pile force is added to the total capacity uncertainty given for vertical piles. Available test data on axially loaded piles indicates a very wide range in capacity bias. The uncertainties associated with axial capacities of driven piles are given by Tang (1988) (Table 6.6).

Axial Pile Capacity in:	Bias	c.o.v.
Sand	0.9	0.47 - 0.56
Clay	1.3 - 3.7	0.32 - 0.53

Table 6.6: Axial Pile Capacity Uncertainties

To study the effect on *FOSM* results of different probability distributions of maximum wave height and nonlinear limit state functions, the computer

program CALREL (Der Kiureghian, et. al., 1989) was used to perform *FORM* and *SORM* analyses in addition to *FOSM* analysis (Appendix B).

In the case of lognormally distributed loads and capacities, the results from the simplified *FOSM* analysis and those from more sophisticated *FORM* and *SORM* are given in Tables 6.8 and 6.9. *FORM* and *SORM* analyses have also been performed assuming type I extreme value distribution for annual maximum wave height. Since the distribution parameters are computed by tail fitting, no significant changes in the reliability indices are observed.

The results indicate that the most probable failure mode in both loading cases involves the failure of the diagonals in the second jacket bay. The large uncertainties in storm loadings are due to uncertainties in force calculations and those associated with predicted wave heights. The partially large uncertainties in jacket bay capacities is mainly due to uncertainties associated with batter component of the leg forces. Based on the *FOSM* results, unimodal bounds on probability of platform failure are estimated for both loading directions and given in Table 6.7.

Loading	Lower Bound p_{fs}	Upper Bound p_{fs}
End -on	0.011	0.046
Broadside	0.013	0.042

Table 6.7: Unimodal Bounds on p_f

Some Notes and Remarks

The procedures and the case study presented in this chapter are based on simplifying assumptions including the following:

- Once the wave crest elevation exceeds the platform lower deck elevation, the load pattern changes significantly and the total forces acting on the platform increase much faster than before. This fact has not been accounted for. The problem can be solved by considering conditional probabilities.

- In the presented case study, deterministic values were assigned to brace capacity modification factors α, which were calibrated to give results consistent with those gained from a detailed nonlinear pushover analysis

of the studied platform. In a general case however, the α factor is taken to be a random variable. The uncertainty associated with this variable reflects the modeling uncertainty introduced by using simplifying assumptions regarding residual strength of compression braces and stiffness properties of inter-connecting horizontal braces.

- In the case of the studied platform the leg-pile annulus and the joints were grouted. This is why a connection failure mode was not included in the analysis. In a general case, the joints' capacity and the uncertainties associated with it needs to be considered.

- The diagonal brace capacities are negatively correlated with the lateral loading. This correlation is neglected at this stage of the research.

6.5 Summary

A simplified procedure is presented to perform structural reliability analysis of conventional, steel jacket, offshore platforms. This procedure can be used in the process of reassessment and requalification of older platforms, or it can be used in the preliminary design phase of a new platform. In both cases the reliability indices should be viewed as relative and not absolute measures. The analysis is based on a first order second moment approach. It is assumed that the loads and capacities are lognormally distributed.

A case study is performed and the structural reliability of an eight-leg offshore drilling and production platform located in Gulf of Mexico is studied. In addition to reliability indices for different failure modes, unimodal bounds for the system probability of failure is estimated. Using the computer program CALREL, first order and second order reliabilities are also computed. Two different distributions are selected for the maximum wave height; lognormal and type I largest value. In both cases the results are in good agreement with those from the simplified *FOSM* analysis.

BROADSIDE LOADING	LOAD (KIPS)	BIAS	C.O.V.	CAP (KIPS)	BIAS	C.O.V.	FOSM β	FOSM Pf	FORM β	SORM β
DECK LEGS	197	0.83	1.03	2606	1.00	0.11	3.64	1.34E-04	3.51	3.51
JACKET										
BAY1	544	0.83	1.03	2932	1.00	0.08	2.61	4.52E-03	2.48	2.48
BAY2	621	0.83	1.03	2621	1.00	0.24	2.22	1.32E-02	2.06	2.12
BAY3	638	0.83	1.03	4130	1.00	0.45	2.41	8.07E-03	2.41	2.47
BAY4	641	0.83	1.03	5702	1.00	0.49	2.67	3.85E-03	2.75	2.80
BAY5	643	0.83	1.03	6157	1.00	0.48	2.75	2.94E-03	2.84	2.90
FOUNDATION										
LATERAL	643	0.83	1.03	7700	0.81	0.56	2.69	3.58E-03	2.67	2.67
AXIAL	1035	0.83	1.03	4063	1.5	0.31	2.52	5.79E-03	2.49	2.49

Table 6.8: Component Reliabilities Based on FOSM, FORM and SORM Analyses, Broadside Loading

END-ON LOADING	LOAD (KIPS)	BIAS	C.O.V.	CAP (KIPS)	BIAS	C.O.V.	FOSM β	FOSM Pf	FORM β	SORM β
DECK LEGS	120	0.83	1.03	2606	1.00	0.11	4.22	1.20E-05	4.10	4.10
JACKET										
BAY1	424	0.83	1.03	1954	1.00	0.07	2.43	7.51E-03	2.29	2.29
BAY2	499	0.83	1.03	2046	1.00	0.10	2.28	1.13E-02	2.12	2.14
BAY3	515	0.83	1.03	2360	1.00	0.15	2.39	8.54E-03	2.25	2.28
BAY4	518	0.83	1.03	2538	1.00	0.20	2.43	7.62E-03	2.28	2.32
BAY5	520	0.83	1.03	2892	1.00	0.26	2.51	6.02E-03	2.38	2.43
FOUNDATION										
LATERAL	520	0.83	1.03	7200	0.81	0.53	2.88	1.96E-03	2.85	2.85
AXIAL	856	0.83	1.03	4063	1.5	0.31	2.74	3.12E-03	2.70	2.70

Table 6.9: Component Reliabilities Based on FOSM, FORM and SORM Analyses, End-on Loading

7. Damaged and Repaired Members

7.1 Introduction

A major problem associated with reassessment of an older platform is locating and evaluating the effects of defects and member damage on platform response to extreme loadings. Damage such as dents, global bending, corrosion, and fatigue cracked tubular members can significantly affect the ultimate strength of an offshore platform.

Given the physical properties of damage, an estimate of the ultimate and residual strength of the damaged members is necessary to perform a strength assessment of an offshore platform system. Recently, numerous investigators have devoted their attention to this subject and several theoretical approaches have been developed addressing different types of damage. Small and large scale experiments have been performed to verify the analytical capacity formulations and to gain better understanding of the ultimate and post ultimate behavior of damaged and repaired tubular members.

The objective of this research was first to perform a literature review and identify simplified methods to estimate the ultimate and residual capacity of damaged and repaired tubular members. This simplified residual capacity estimation methods are then used to predict the effects of member damage and repair on lateral capacity of platform system. The results of the simplified capacity estimation methods are compared with existing theoretical and experimental test results given in literature.

In the following, a literature review on the ultimate strength behavior of damaged and repaired tubular braces with dents, global out-of-straightness, and corrosion is summarized and discussed.

7.2 Dents and Global Bending Damage

Dent-damaged tubular bracing members have been analytically studied since late 70's. The analytical methods of strength prediction developed so far can be classified into three categories (Ricles, 1993):

a) Beam-column analysis (Ellinas, 1984; Chen, 1987; Ricles et al, 1992; Loh, 1993)

b) Numerical integration methods (Kim, 1992; Duan, 1993)
c) Nonlinear finite element methods

Beam-column analysis is based on formulation of equilibrium of the damaged member in its deformed shape. The P-Δ effects and the effects of out-of-straightness are considered in the equilibrium equations. The effect of dent depth is taken into account by modifying the cross-sectional properties.

Numerical integration methods use empirical moment-axial load-curvature relationships to iteratively solve the differential equation of axially loaded damaged member. The empirical M-P-Φ relationship is usually based on experimental test results or finite element studies of dented tubular segments.

Nonlinear FE analyses represent the most general and rigorous method of analysis. However, their accuracy and efficiency require evaluation and they are expensive and time consuming to perform.

Loh's Interaction Equations

Developed at Exxon, BCDENT is a general computer program that uses M-P-Φ approach to evaluate the full behavior of dented member. The behavior of the dent section is treated phenomenologically using a set of M-P-Φ expressions. Compared with the experimental results, BCDENT gives mean strength predictions for both dented and undented members.

Based on BCDENT- results, Loh (1993) presented a set of new unity check equations for evaluating the residual strength of dented tubular members. The unity check equations have been calibrated to the lower bound of all existing test data. The equations cover axial compression and tension loading, in combination with multidirectional bending with respect to dent orientation. When the dent depth approaches zero, the recommended equation is identical to API RP 2A equation for undamaged members.

Loh's equation for dent damaged members and those with global bending damage have been integrated in ULSLEA. These equations are listed at the end of this chapter.

Comparison Between Experimental and Predicted Capacities

Based on a comparison between the experimental ultimate capacities and the corresponding predicted capacities of dented tubulars using different methods of analysis, Ricles (1993) concludes that Ellinas' formulation, which is based on first yield in the dent saddle, is overly conservative. In general, it has been found that Ellinas' approach can be either conservative or unconservative depending on the dent depth, member slenderness, and out-of-straightness.

Ricles further concludes that DENTA (a computer program developed by Taby (1988)), Loh's interaction equation, numerical integration based on M-P-Φ relationships, and the nonlinear FEM are able to predict the residual capacity of the test members reasonably well.

Also, a joint industry project on testing and evaluation of damaged jacket braces was performed by PMB Engineering and Texas A&M University (1990). Twenty salvaged braces were tested and their strength behavior compared with results gained from analyses using finite element beam column models of damaged braces. It was found that in average the analyses would overpredict the capacities by 21%. The agreement in this case is not as good as that presented by other investigators. Use of new and artificially damaged braces in other investigations may explain this inconsistency. Generally corrosion is found to add large uncertainties to the properties of the entire member.

Some Observations and Conclusions

Based on experimental test results and parametric studies using different analytical methods, the following observations, which are relevant to our study, have been made and presented in the literature:

- The residual strength decreases significantly as the dent depth increases.
- For a given dent depth, the analyses show a decrease in residual strength for members with higher D/t ratio.
- The axial compression capacity decreases as the out-of-straightness increases, but the impact on ultimate moment is negligible.
- There is negligible conservatism in assuming a mid-length dent location for any practical dent within the middle-half section of members effective length.

- Accounting for strain hardening has only a small effect on the maximum predicted capacity.
- Lateral loadings, such as those caused by wave forces, can significantly affect dented brace capacity.
- The behavior of members with multiple forms of damage are generally dominated by one damage site.
- The most severe corrosion can occur on the inside surface of the member. A hole in the member would be the primary indication of this condition.
- Corrosion is found to add large uncertainties to the properties of the entire member.
- Ricles (1993) reports that DENTA (developed by Taby 1988), Loh's interaction equation, numerical integration based on M-P-Φ relationships, and the non-linear FEM are able to predict the residual capacity of the test members reasonably well.

7.3 Corrosion Damage

Marine environment is extremely corrosive. Although cathodic protection systems and protective coatings have been applied to prevent corrosion of steel members, in numerous cases corrosion damage of offshore platforms has been observed. Corrosion results in a reduced wall thickness of the steel member which can lead to premature local buckling at the corroded areas.

Ostapenko et. al. (1993) conducted experimental test on corroded tubulars from salvaged Gulf of Mexico platforms. Local buckling was reported at the most severely corroded area and an up to 50% reduction in capacity was observed. It was found that the patch with the most severe corrosion controls the local buckling of the member.

Ricles and Hebor (1994) performed and presented an analytical and experimental study on patch-corroded steel tubular members. They used the results of an experimental program to verify a non-linear finite element model. The calibrated FE model was then used to perform parametric studies and develop relationships between damaged member residual strength and corrosion patch geometry. Based on a multi-variable non-linear regression analysis, closed-form solution for patch-corroded tubular member strength were derived as a function of D/t ratio and corrosion patch geometry.

Excellent agreement is reported between the predicted and experimental capacities.

7.4 Residual Strength of Grout-Repaired Tubular Members

Given the loss of strength of a member due to damage has a significant impact on strength and reliability of the platform system, it is desirable to apply some measure of strengthening the damaged member. Internal full grouting or using grouted steel clamps are two economically attractive alternatives.

Experimental results have shown that grouting significantly increases the capacity of damaged tubular members and therefore is a viable mean of strengthening such members. In the past, practicing engineers have been applying existing analytical expressions for composite members to estimate the capacity of grout-filled damaged tubular members.

Parsanejad Method

Responding to the need for some sort of analytical expressions, Parsanejad (1987) presented a simple analytical expression for estimating the ultimate capacity of grout-filled damaged tubular members. The analysis is based on the following simplifying assumptions:

a) full interaction exists between grout and the damaged tube and
b) grout provides sufficient support to the tube wall in the damaged region to prevent premature local buckling.

The first yield collapse criterion is adopted by Parsanejad: it is assumed that the ultimate capacity of damaged tubular member is reached when the compressive stress in the steel tube at the dent equals the yield stress. The damaged member is treated as a beam column with uniform cross-sectional properties represented by the dented region. The total eccentricity is taken as the sum of eccentricities due to initial out-of-straightness, external load, and the distance between the original center of the tube and the centroid of the transformed cross section at the dent.

Comparing the analytical results with the limited experimental results existent at the time, Parsanejad reports good agreement: the analytical results present a close lower bound estimates of test results.

The equations developed for grout repaired tubulars by Parsanejad are integrated in ULSLEA and are listed at the end of this chapter.

Comparison between experimental and predicted capacities

Ricles et. al. (1993) performed experiments on thirteen large scale damaged and repaired tubular members with the following objectives:

a) Assessing the residual strength of dent damaged steel tubular bracing members under combined flexural and axial load and
b) determining the effectiveness of using internal complete grouting and grouted steel clamps to repair dent damaged members.

The residual strength of damaged unrepaired and grout repaired specimens were compared to the undamaged design strength according to WSD and LRFD formats respectively. Test results were also compared to results gained from modified Ellinas equation, computer program DENTA, and Parsanejad formulation. The following conclusions regarding grout-filled damaged tubular members are drawn by Ricles et al (1993):

- Internal grout and grouted steel clamp repairs of a 0.1D dent damaged brace are successful in reinstating the original undamaged member's strength by arresting dent growth inwards.
- The predicted strength of internally grout repaired members based on Parsanejad's method provided a close lower bound to experimental data.

Loh's Interaction Equations

Undamaged Cross Sectional Capacities

$$P_a = F_y A_o \qquad \text{for} \quad \frac{D}{t} \le 60 \tag{7.1}$$

$$P_a = F_y A_o \left[1.64 - 0.23 \left(\frac{D}{t} \right)^{0.25} \right] \qquad \text{for} \quad \frac{D}{t} \ge 60 \tag{7.2}$$

$$\frac{M_a}{M_p} = 1.0 \qquad \text{for} \quad 0 \le \frac{F_y D}{t} \le 1500(ksi) \tag{7.3}$$

$$\frac{M_a}{M_p} = 1.13 - 2.58 \frac{F_y D}{E t} \qquad \text{for} \quad 1500 \le \frac{F_y D}{t} \le 3000 \tag{7.4}$$

$$\frac{M_a}{M_p} = 0.94 - 0.76 \frac{F_y D}{E t} \qquad \text{for} \quad 3000 \le \frac{F_y D}{t} \le 300 F_y \tag{7.5}$$

$$M_p = F_y t (D - t)^2 \tag{7.6}$$

Dent-Section Properties

$$\frac{P_{ud}}{P_a} = \frac{A_d}{A_o} = exp\left(-0.08 \frac{dd}{t} \right) \ge 0.45 \tag{7.7}$$

$$\frac{M_{ud}}{M_a} = \frac{I_d}{I_o} = exp\left(-0.06 \frac{dd}{t} \right) \ge 0.55 \tag{7.8}$$

Strength Check

$$UC = \frac{P}{P_{ud}} + \sqrt{\left(\frac{M -}{M_{ud}} \right)^{\alpha} + \left(\frac{M^*}{M_u} \right)^2} \le 1.0 \tag{7.9}$$

$$UC = \frac{P}{P_{ud}} + \sqrt{\left(\frac{M +}{M_u} \right)^2 + \left(\frac{M^*}{M_u} \right)^2} \le 1.0 \tag{7.10}$$

Stability Check

$$UC = \frac{P}{P_{crd}} + \sqrt{\left(\frac{M_{-}}{\left(1-\frac{P}{P_{Ed}}\right) M_{ud}}\right)^{\alpha} + \left(\frac{M^{*}}{\left(1-\frac{P}{P_{E}}\right) M_{u}}\right)^{2}} \leq 1.0 \tag{7.11}$$

$$UC = \frac{P}{P_{crd}} + \sqrt{\left(\frac{M_{+}}{\left(1-\frac{P}{P_{Ed}}\right) M_{ud}}\right)^{2} + \left(\frac{M^{*}}{\left(1-\frac{P}{P_{E}}\right) M_{u}}\right)^{2}} \leq 1.0 \tag{7.12}$$

$$\alpha = 2 - 3\,dd / D \tag{7.13}$$

Critical Buckling Capacities

$$P_{crdo} = P_{ud}\left[1 - 0.25\lambda_{d}^{2}\right] \qquad \text{for} \quad \lambda_{ud} \leq \sqrt{2} \tag{7.14}$$

$$P_{crdo} = P_{ud}\frac{1}{\lambda_{d}^{2}} = P_{ED} \qquad \text{for} \quad \lambda_{ud} \geq \sqrt{2} \tag{7.15}$$

$$\frac{P_{crd}}{P_{crd\,0}} + \frac{P_{crd}\,\Delta Y}{\left(1 - \frac{P_{crd}}{P_{Ed}}\right) M_{ud}} = 1.0 \tag{7.16}$$

Parsanejad's Strength Equation for Grout-Filled Tubulars

Notations

A_g	area of grout at the dented section
A_s	area of steel
A_{tr}, A_{tr}^*	transformed areas at the dented and undented cross section
D	mid-thickness diameter
d	depth of denth
E_g	elastic modulus of grout
E_s	elastic modulus of steel
e	external eccentricity of load
e_g	distance between centroid of grout at the dented cross section to the centroid of undented cross section
e_s	distance between centroid of steel at the dented cross section to the centroid of undented cross section
e_t	$= e + \delta + e_{tr}$
e_{tr}	distance between centroid of the dented and undented transformed cross section
I_g	moment of inertia of grout at dented cross section
I_s	moment of inertia of steel at dented cross section
I_{tr}	transformed moment of inertia of dented cross section
k	nondimensionalized parameter = $A_{tr}\, e_t / Z_{tr}$
l	effective length of member
m	nondimensionalized parameter = A_{tr} / A_{tr}^*
n	elastic modular ratio = E_s / E_g
P_u	ultimate axial capacity
P_y	full yield capacity = $A_{tr}^* \sigma_y$
r_{tr}	transformed radious of gyration of dented section
t	thickness of tubular member
Z_{tr}	transformed section modulus with respect to the dented side
α	angle shown in fig.
δ	overall bending
λ	reduced slenderness parameter
σ_a	axial stress
σ_b	bending stress
σ_e	Euler buckling stress
σ_u	ultimate axial stress
σ_y	yield stress of steel

$$\left(\frac{\sigma_u}{\sigma_y}\right)^2 - \left(\frac{1+k}{\lambda^2} + m\right)\left(\frac{\sigma_u}{\sigma_y}\right) + \frac{m}{\lambda^2} = 0 \tag{7.17}$$

$$\lambda = \sqrt{\frac{\sigma_y}{\sigma_e}} = \frac{1}{\pi}\frac{l}{r_{tr}}\sqrt{\frac{\sigma_y}{E_s}} \tag{7.18}$$

$$k = \frac{A_{tr} e_t}{Z_{tr}} \tag{7.19}$$

$$m = \frac{A_{tr}}{A_{tr}^*} \tag{7.20}$$

Cross-Sectional Properties

$$A_{tr} = A_s + \frac{A_g}{n} \tag{7.21}$$

$$A_s = \pi D t \tag{7.22}$$

$$A_g = \frac{D^2}{4}(\pi - \alpha + \frac{1}{2}\sin 2\alpha) \tag{7.23}$$

$$n = \frac{E_s}{E_g} \tag{7.24}$$

$$\alpha = \cos^{-1}\left(1 - 2\frac{d}{D}\right) \tag{7.25}$$

$$e_{tr} = \frac{A_s e_s + \frac{A_g}{n} e_g}{A_{tr}} \tag{7.26}$$

$$e_s = \frac{D}{2\pi}(\sin\alpha - \alpha\cos\alpha) \tag{7.27}$$

$$e_g = \frac{(D \sin\alpha)^3}{12 A_g} \tag{7.28}$$

$$Z_{tr} = \frac{I_{tr}}{\frac{D}{2}} \cos\alpha + e_{tr} \tag{7.29}$$

$$r_{tr} = \sqrt{\frac{I_{tr}}{A_{tr}}} \tag{7.30}$$

$$I_{tr} = I_s + \frac{I_g}{n} + A_s (e_{tr} - e_s)^2 + \frac{A_g}{n}(e_g - e_{tr})^2 \approx I_s + \frac{I_g}{n} \tag{7.31}$$

$$I_s = \frac{D^3 t}{4}\left[\frac{\pi - \alpha}{2} - \frac{\sin 2\alpha}{4} + \alpha \cos^2\alpha - \frac{(\sin\alpha - \alpha\cos\alpha)^2}{\pi}\right] \tag{7.32}$$

$$I_g = \frac{D^4}{64}\left[\pi - \alpha + \frac{\sin 4\alpha}{4}\right] - \frac{D^4 \sin^6\alpha}{144 A_g} \tag{7.33}$$

$$A_{tr}^* = A_s + \frac{\pi D^2}{4n} \tag{7.34}$$

8. Verification Case Studies

8.1 Introduction

Thorough verification studies on five Gulf of Mexico (GOM) Platforms have been performed. The characteristics of these structures are summarized in the following sections. The verification cases include four eight-leg and one four-leg drilling and production platforms. The simplified estimates of total forces acting on the platforms during intense storms and predictions of ultimate member strength and platform capacity were verified with results from complex nonlinear analysis (Loch, Bea 1995).

In case of platform A, the results available from a detailed nonlinear push-over analysis (AIM platform analysis report) were used to verify the simplified analysis' results. In case of platforms B, C, D and E the nonlinear finite element computer program USFOS was utilized to perform the static push-over analyses. Wave and wind loads in the deck were manually calculated and applied as nodal loads. The hydrodynamic forces on jacket were generated using DNV's WAJAC wave load program. Stokes 5^{th} order wave theory was used and member loads were calculated based on Morrison's (MJOS) equation.

Simplified analyses were performed assuming elasto-perfectly plastic behavior for members in both tension and compression (a residual strength factor of $\alpha=1.0$) to estimate the upper-bound capacities of jacket bays.

8.2 Platform A

Platform A is an 8-leg structure located in the Main Pass area of the Gulf of Mexico in a water depth of 271 feet (Fig. A1). Designed and installed in 1968-70, the platform has been exposed to high environmental loading developed by hurricanes passing through the Gulf. The structure foundation consists of eight 42-inch piles which penetrate to a depth of 270 ft into medium sands overlaying stiff clays. The jacket legs are battered in two directions and the leg-pile annulus is grouted. The lower and upper decks are located at +46 ft and +63 ft respectively.

The detailed nonlinear analysis was performed using a 9th order stream function to compute wave crest elevations. A wave steepness of 1/12 was

used (wave period of 12.8 seconds for the 100-year wave). According to 1988 wave crest elevations, waves with return period greater than hundred years will result in deck inundation. Marine growth at the site was taken as 1 inch and considered for all members located between the waterline and -100 ft.

A three-dimensional platform computer model and a two-dimensional wave grid was used to compute the forces acting on the platform. The loading on each member throughout the platform is then summed to determine the platform's base shear. The process is repeated as the wave is moved through the structure in 24 increments to compute the maximum base shear. Wave forces are computed for two directions, end-on and broadside.

The Morrison's (MJOS) equation was used to compute the local forces on members. The drag coefficient was taken as C_d = 0.7 and the inertia coefficient was taken as C_m = 1.5. Wind forces were computed using the API RP2A formulation assuming a drag coefficient of C_s = 1.0 for clear decks, 1.5 for cluttered and 2.0 for blocked decks.

The wave begins to impact the deck at the 100-year return period condition. The additional forces due to deck inundation were manually calculated. The wave impact loads were computed using full impact area and a drag coefficient of C_d = 2.0. The remaining deck area not covered by the wave is exposed to the wind. This wind forces were calculated and added to the wave forces.

The *ULS* were determined for the platform's orthogonal directions using the nonlinear program SEASTAR. In the case of end-on loading, the wave in deck condition resulted in an ultimate capacity of 2,607 kips. Most of the member failures were due to compressive buckling of braces (Fig. A6). The analysis indicated a brittle strength behavior and little effective redundancy which is a typical result for *K*-braced platform systems. In the case of broadside loading with wave in the deck, the ultimate capacity was reported to be 2,935 kips (Fig. A3).

The same oceanographic conditions and hydrodynamic coefficients utilized in the detailed analysis were used to perform a simplified analysis. The maximum lateral forces are computed and plotted versus the return period. This is done for both broadside and end-on directions. Compared to the

results of detailed analysis, total lateral forces are over-predicted by up to 20% (Figs. A2 & A5). The principal difference is tracked to modeling assumptions in the simplified analysis; all of the platform elements are modeled as equivalent vertical cylinders that are concentrated at a single vertical position in the wave crest.

The shear capacity and storm shear are plotted versus platform elevation. In broadside loading direction, the simplified analysis predicted a failure mode in the second jacket bay at a total base shear of about 3,400 kips (Fig. A4). In end-on loading direction, the simplified analysis indicated a failure due to buckling of compression braces in the uppermost jacket bay at a lateral load of 2,900 kips (Fig. A7). These results are 10 to 15% higher than those gained from detailed nonlinear analyses. The principal difference lies in the nonlinear modeling of vertical diagonal braces which results in different buckling loads.

8.3 Platform B

Platform B is an eight-leg structure located in the Gulf of Mexico's South Timbalier region in a water depth of 118 ft (Fig. A8). The platform was designed using a design wave height of 55 ft. The cellar and main decks are located at +34 ft and +47 ft, respectively. The 39 in. jacket legs are battered in two directions and have no joint cans. The 36 in. piles are grouted inside the jacket legs.

Nonlinear push-over analysis results indicate that the platform is capable of resisting 3,850 kips in broadside loading (Fig. A11). The failure mechanism occurs in the uppermost jacket bay due to buckling of the compression braces. The analysis indicates a brittle strength behavior and no effective redundancy. The analysis showed the platform's end-on resistance capacity to be approximately 3,900 kips (Fig. A15). Failure begins in the uppermost jacket bay, where the four diagonal compression braces buckle almost simultaneously. The failure mechanism is completed when the horizontal struts in the upper jacket bay buckle in addition to compression braces.

The same oceanographic conditions, hydrodynamic coefficients, and wave theory (Stokes 5^{th} order) utilized in nonlinear push-over analysis were used to perform a simplified limit equilibrium analysis. Since the same procedure was used to estimate the wind and wave forces on the projected deck areas, they were essentially the same for both detailed and simplified analyses. In

broadside loading direction, the simplified force calculation procedures over-estimated the hydrodynamic loads on the jacket by 7% (Figs. A9 & A10). In end-on loading direction, the jacket loads were over-estimated by 15% (Figs. A13 & A14).

For each loading direction, the predicted performance of *MLTF* vertical diagonal brace has been verified. Using the same initial out-of-straightness for both simplified and complex analyses, the simplified column buckling formulation over-predicted the peak member load by 6% and 9% for end-on and broadside loading directions respectively. Using the calibrated format of simplified column buckling equations with a buckling length factor of K=0.65, the simplified analysis under-predicted the peak load by 7% and 1% for end-on and broadside loading directions respectively.

To study the effect of K-factor on predicted buckling load, a sensitivity analysis was performed. The calibrated buckling capacity formulation gave the "exact" result when buckling length factors of K=0.65 and 0.55 were used for *MLTF* members in compression for broadside and end-on loading directions respectively. Note that in the latter case, the brace is connected to jacket legs at both ends and is therefore stiffer. It is interesting to note that this result is in good agreement with those presented by Hellan, et al. (1994).

The platform shear capacity and storm shear profiles are plotted versus platform elevation. In case of broadside loading and using a buckling length factor of K=0.65 for braces in compression, the simplified analysis predicts a failure mode in the deck legs and uppermost jacket bay at a total base shear of about 3,600 kips, which is in good agreement with the results from non linear analysis (~ 6% under-prediction) (Figs. A11 & A12). In case of end-on loading with a buckling length factor of K=0.55 for compression braces, the simplified analysis predicts a collapse load of 3,100 kips (~ 20% under-prediction) due to failure of compression braces in the top jacket bay (Figs. A15 & A16).

8.4 Platform C

Platform C is a self contained four pile drilling and production platform (Fig. A17). It was installed in the Gulf of Mexico Ship Shoal region in a water depth of 157 ft in 1971. The platform has four decks at elevations +33 ft, +43 ft, +56 ft, and +71 ft. The jacket legs are battered in two directions and have

joint cans. The leg-pile annulus is ungrouted and the piles attached to the jacket with welded shimmed connections at the top of the jacket.

This platform has been the subject of extensive structural analyses. As an industry wide effort to assess the variability in predicted performance of offshore platforms in extreme storms, the ultimate capacity of this platform has been assessed by many investigators using a variety of nonlinear analysis software packages (Digre, et.al.,1995).

The force-displacement history for broadside loading is shown in figure A19. This curve indicates that platform fails at a total base shear of 1,673 kips. Since the foundation was shown to be the weak link in the platform, a fixed base analysis was also performed. This was accomplished by analyzing the platform while rigidly fixing the piles at the mudline.

If the foundation is assumed rigid or fixed, the braces in the second jacket bay become the weak link. Figure A20 indicates that compression braces at the second bay from mudline buckle at a total base shear of 3,440 kips. After the compression braces in the second jacket bay buckle the braces in the third jacket bay buckle and the jacket begins to "unzip".

Using the simplified approach for a reference wave height of 67 ft, a wave period of 14.3 sec and a uniform current velocity of 3.1 ft/sec, the total base shear for an orthogonal loading direction was estimated to be 3,050 kips (Fig. A18). Using a buckling length factor of 0.65 for compression braces, the limit equilibrium analysis indicated platform collapse at a base shear of 3,200 kips due to simultaneous failure of compression braces at three different jacket bays (Fig. A21). For this lateral loading, the mean axial pile capacity in compression was exceeded by approximately 30% (RSR=0.7). According to this "best estimate" result, a failure mode in foundation would govern the ultimate capacity of the platform.

These results are in good agreement with those gained from USFOS analysis. The comparison indicated that the simplified method over-estimated the current and wave loads in jacket by 17%. The ultimate capacity of the platform with dynamic pile capacities was under-predicted by 6%. The axial compression capacity of piles were over-estimated by 14%. After including the self-weight of the jacket to the axial pile loading, the pile capacities were in close agreement. Due to how the piles are installed and the potential

loadings carried by the mudline braces and mudmats, whether or not the dead loads are fully carried by the supporting piles is uncertain.

8.5 Platform D

Platform D is an eight pile drilling and production platform located in the Gulf of Mexico's South Timbalier region in 137 feet of water (Fig. A22). This region was subjected to 100 year wave loads during Hurricane Andrew (Vannan et al, 1994). The platform was designed and installed in 1964. Cellar and main deck elevations are at + 35 ft and +46 ft respectively. The jacket legs are battered at one to twelve in both broadside framing. The 30 in. piles extend approximately 180 ft below the mudline through firm to very stiff clay. A dense sand layer lies directly beneath the piles ends. The 30 in. deck legs are connected to the tops of the 30 in. piles. The 33 in. diameter legs are ungrouted but have thickened joint sections. The jacket bracing and horizontal framing are made of nominal 36 ksi steel with an average yield strength of 43 ksi.

The broadside wave was set to 56 ft while end-on wave was set at 60 ft. The drag coefficient, C_d, was taken to be 1.2 for both rough and smooth cylinders. The inertia coefficient, C_m, was taken to be 1.2 for rough cylinders and 1.6 for smooth cylinders respectively . A wave kinematics factor equal to 0.88 was used for both the deck and jacket loads. A current blockage factor of 0.80 for broadside loading and 0.70 for end-on loading was also included.

All members were given an initial imperfection of 0.003 of their length. Due to temporary problems in the analysis software and since the legs did have joint cans, the detailed analysis used rigid joints.

The non-linear soil springs were developed using section 6 of API RP 2A. These springs were then modified to account for dynamic loading effects and soil sample disturbance. In total, the strength of the axial springs was increased by approximately 1.5 and the strength of the lateral springs were increased by approximately 3.0. As with joint capacities, studies have shown that static soil capacities as derived by API RP 2A underestimate the true soil strength (Vannan et al, 1994).

The force-displacement curve for end-on loading is shown in figure A23. This curve indicates that the lowermost broadside braces buckle at a total

base shear of 2,697 kips. The force-displacement history indicates that there is some reserve strength in the end-on direction. ULSLEA is able to predict the collapse mechanism and the ultimate lateral loading capacity of 2,700 kips (Fig. A24).

The force-displacement curve for broadside loading is shown in figure A25. This curve indicates that platform fails at a total base shear of 4,475 kips. The maximum strength is controlled by buckling of the end-on braces in the third bay from the mudline. ULSLEA analysis for this loading direction also indicates a failure mechanism at the third jacket bay from mudline at a total base shear of 4,200 kips (Fig. A26).

8.6 Platform E

Platform E (PE) is also an eight pile drilling and production platform located in the Gulf of Mexico's South Timbalier region (Fig. A27). This platform was bridge-connected to Platform D (PD). The platform was designed with PD in 1964 and installed in 137 feet of water. PE is similar in geometry as PD except that PE is battered at one to ten in both broadside and end-on framing.

The same wave, wind and drag and inertia coefficients for PD were used for PE. However, PE has a much larger base shear for the same storm conditions due to its additional conductors.

Similar modeling assumptions were made for PE as were made for PD. All members were given an initial imperfection of 0.003 of their length, and the analysis used rigid joints. Also, as with PD, the soil springs were modified by the factors discussed previously.

The force-displacement curve for broadside loading is shown in figure A28. This curve indicates that platform reaches its maximum capacity at a total base shear of 4,709 kips. As with PD, the maximum strength is controlled by buckling of the end-on braces in the third bay from the mudline. This result is in good agreement with results developed using ULSLEA. For this loading direction, the simplified analysis indicates a collapse mechanism in the third jacket bay from mudline at a base shear of 4,400 kips (Fig. A29).

The force-displacement curve for end-on loading is shown in figure A30. This curve indicates that the lowermost broadside braces buckle at a total

base shear of 4,577 kips (Fig. A30). ULSLEA results for this loading direction shows failure due to simultaneous buckling of compression braces at the two lowest jacket bays. The simplified analysis indicates an ultimate lateral loading capacity of 4,450 kips (Fig. A31).

8.7 Summary

The results of the verification studies are summarized in Table A1. Defining a bias factor as the ratio of static ultimate lateral loading capacity of the platform predicted by USFOS/SEASTAR over that predicted by ULSLEA, a mean bias of B=1.02 has been achieved. This bias ranges from 0.85 to 1.26 (Table A1).

The reults of the verification study further indicate that the simplified loading calculation procedure over estimates the wave on jacket loads by 10% in average. This modeling bias is already integrated in ULSLEA so that the program gives a best estimate wave on jacket loading.

9. Summary, Conclusions & Future Research

In this study, simplified procedures are developed to assess the structural reliability of template-type offshore platforms under extreme storm conditions. The focus of the research was to develop simplified procedures to:

- determine best estimate aero- and hydrodynamic loadings and loading profiles acting on a given platform,
- determine the ultimate lateral loading capacity of various elements and components of the platform,
- evaluate the "static" ultimate limit state performance characteristics of platform system,
- take into account the uncertainties associated with loadings and capacities and assess the structural reliability of the platform, and finally
- account for damaged and repaired members in predicting the lateral loading capacity of platform system.

The next step was to verify the results gained from the simplified analyses with those gained from detailed nonlinear analyses of steel jacket-type offshore platforms and with actual field performance of such platforms during intense storms.

The results indicate that the simplified analyses can develop evaluations of both storm loadings on and ultimate lateral capacities of platforms that are good approximations of those derived from complex analyses. Defining a bias factor as the ratio of static ultimate lateral loading capacity of the platform predicted by USFOS over that predicted by ULSLEA, a mean bias of B=1.02 has been achieved. This bias ranges from 0.85 to 1.26 (Table A1).

Comparison of the estimated lateral load capacities with the estimated maximum loadings that these platforms have experienced and with observed performance characteristics of these platforms indicates that the analytical evaluations of both storm loadings and platform capacities are also in good agreement with the experience.

A computer program has been developed to perform the simplified analyses (ULSLEA) (Appendix C). High degrees of user-friendliness have been

employed in development of the soft ware to reduce the engineering effort, required expertise, likelihood of errors, costs and time associated with the analyses.

The use of the simplified analytical procedures to estimate reference storm lateral loading and platform capacities, and Reserve Strength Ratios are indicated to result in good estimates that can be used in the process of screening platforms that are being evaluated for extended service. In addition, the results from these analyses can be used to help verify results from complex analytical models that are intended to determine the ultimate limit state lateral loading capacities of platforms. In every verification case sited in this report, results from ULSLEA initially helped define major deficiencies and errors in either the complex analysis software or in the input to this software. Lastly, this approach can be applied as a preliminary design tool for design of new platforms.

Recommended Future Work

Potential research topics for future studies have been identified during the present research. These are listed and briefly discussed in the following:

- **Perform further verification and platform assessment studies**

The verification studies performed during this research included 5 Gulf of Mexico Platforms. Although the results are extremely encouraging, additional studies on platforms with a variety of bracing patterns and different configurations would help establish the probabilistic characteristics of the modeling bias and help increase the confidence in ULSLEA.

- **Investigate the effect of horizontal framing on load redistribution**

For the sake of simplicity in estimating the lateral capacity of jacket bays, it has been assumed in this study that the inter-connecting horizontal braces are rigid. In reality, however, these horizontal members have diameter and thickness close in size to those of vertical diagonal braces. The verification studies performed so far indicate that this assumption is reasonable in case of platforms with brittle strength behavior. In other words, the first member failure seems to be independent of the degree of rigidity of the inter-

connecting horizontals. The next step in refining the simplified capacity calculation techniques will be to investigate how the strength behavior of a redundant structure is affected by non-rigid horizontal framing.

- **Further refine foundation capacity model**

At present stage, ULSLEA includes a foundation capacity model that is based on one soil-layer. The next step in refining the procedure would be to include additional soil layers in the model. Development and verification of simplified procedures to account for soil sampling, testing, and cyclic-dynamic loading conditions is another potential research topic (Bea, 1987).

- **Further develop simplified reliability analysis procedures**

The basic approach to develop a simplified probabilistic failure analysis is documented in Chapter 6 of this report. The next step will be to further develop and refine these procedures and to integrate them in ULSLEA. Recently, sophisticated probability based nonlinear finite element analysis programs have been developed (Zhang and Der Kiureghian, 1995). These programs can be used to verify the validity of the simplified reliability analysis techniques.

- **Apply ULSLEA to design and proportioning of jacket structures**

One important application of ULSLEA is preliminary design and estimating of jackets. Case studies can be performed to realize and demonstrate the application of the simplified nonlinear analysis method in conceptual design and proportioning of jacket structures considering issues like robustness and damage tolerance. Subroutines can be developed to compute estimates of steel tonnage.

- **Develop a professional version of ULSLEA**

Based on a simultaneous development and verification/calibration approach, the present version of ULSLEA has been developed during the second year of this research. This version is a working example of a simplified nonlinear analysis computer program. Effort has been made to make the program

efficient and user friendly. The software runs on Excel 4.0. One reason for working with Excel was to provide compatibility with RMS (Requalification Management System), a parallel research project which had started a year prior to initiation of "Screening" project. ULSLEA is a major building block of RMS.

As for any other application software in its initial stages of development, ULSLEA has the potential to be further developed and include additional features that enhance the speed and user-friendliness of the program. It seems that the most efficient way to do so would be to rewrite ULSLEA in Visual Basic using Excel 5.0.

References

American Petroleum Institute (API), 1993. "Recommended Practice for Planning, Designing and Constructing Fixed Offshore Platforms - Load and Resistance Factor Design (RP 2A-LRFD)." First Edition, July, Washington, D.C.

American Petroleum Institute (API), 1994. "API RP 2A-WSD 20th Edition, Draft Section 17.0, Assessment of Existing Platforms," November, Houston, TX.

Bea, R.G. 1973. "Wave Forces, Comparison of Stokes Fifth and Stream Function Theories." Engineering Note No. 40, Environmental Mechanics, April.

Bea, R. G. and Young, C., 1993. "Loading and Capacity Effects on Platform Performance in Extreme Condition Storm Waves & Earthquakes." Proceedings Offshore Technology Conference, OTC No. 7140. Houston, TX.

Bea R. G., 1987. "Dynamic Response of Marine Foundations," Proceedings Ocean Structural Dynamics Symposium '84, Oregon State University, Corvallis, OR, Sept.

Bea, R.G. and Craig, M. J. K., 1993. "Developments in the Assessment and Requalification of Offshore Platforms," Proceedings Offshore Technology Conference, OTC 7138, Houston TX, May.

Bea, R. G., Loch, K., Young, P., 1995. "Evaluation of Capacities of Template-Type Gulf of Mexico Platforms." Proceedings 5th International Offshore and Polar Engineering Conference, ISOPE-95, The Hague, The Netherlands, June 11-16.

Bea, R. G. and Mortazavi, M., 1995. "Simplified Evaluation of the Capacities of Template-Type Offshore Platforms," Proceeding of 5th International Offshore and Polar Engineering Conference, The Hague, The Netherlands, June 11-16.

Bea, R. G., Mortazavi, M., Loch, K., Young, P., 1995. "Verification of A Simplified Method to Evaluate the Capacities of Template-Type Platforms." Proceedings Offshore Technology Conference, OTC 7780, Houston TX, May.

Bea, R. G., Mortazavi, M., Loch, K., Young, P., 1995. "Verification of A Second Generation Simplified Method to Evaluate the Storm Loadings on and Capacities of Steel Template-Type Platforms." Proceedings Energy and Environmental Expo 95, American Society of Mechanical Engineers, Houston, Texas, Jan.

Bea, R. G. and DesRoches, R., 1993. "Development and Verification of A Simplified Procedure to Estimate the Capacity of Template-Type Platforms." Proceedings 5th International Symposium Integrity of Offshore Structures, D. Faulkner et al., Emas Scientific Publications, pp. 129-148.

Bea, R. G., 1995. "Development and Verification of a Simplified Method to Evaluate Storm Loadings on and Capacities of Steel, Template-Type Platforms" Proceedings Energy and Environmental Expo 95, American Society of Mechanical Engineers, Houston, Texas, Jan.

Bea R.G., 1990, "Reliability Based Design Criteria for Coastal and Ocean Structures", published by The Institution of Engineers, Australia, 11 National Circuit, Barton, ACT, Australia.

Billington, C. J., Bolt, H. M., and Ward, J. K. 1993. "Reserve, Residual and Ultimate Strength Analysis of Offshore Structures: State of the Art Review." Proceedings Third International Offshore and Polar Engineering Conference, Singapore, June, pp. 125-133.

Cox J.W., 1987, "Tubular Member Strength Equations for LRFD". Final Report API PRAC Project 86-55.

Digre, K. A., Puskar, F. J., Irick, J. T., Krieger, W., 1995. "Modifications to and Applications of the Guidelines for Assessment of Existing Platforms Contained in Section 17 of API RP 2A". Proceedings Offshore Technology Conference, OTC 7779, Houston TX, May.

Det Norske Veritas, 1993. "WAJAC. Wave and Current Loads on Fixed Rigid Frame Structures." DNV SESAM AS. Version 5.4-02.

Ellinas C.P., 1984. "Ultimate Strength of Damaged Tubular Bracing Members." Journal of Structural Engineering, Vol. 110, No.2, February 1984.

Fenton, J.D., 1985. "A Fifth Order Stokes Theory for Steady Waves, "ASCE Journal of Waterway, Port, Coastal and Ocean Engineering, Vol. 111, No. 2, pp. 216-234.

Focht, J.A., and Kraft, L.M., 1986, "Axial Performance and Capacity of Piles, "Planning and Design of Fixed Offshore Platforms, McClelland, B., and Reifel, M.D., pp. 763-801.

Hellan, O., Moan, T., Drange, S.O., 1994, "Use of Nonlinear Pushover Analyses in Ultimate Limit State Design and Integrity Assessment of Jacket Structures, "Proceedings 7th International Conference on Behavior of Offshore Structures, Boss '94, Vol. 3, Structures, C. Chryssostomidis (Ed.) Elsevier Science Inc., New York, NY.

Imm, G. R., O'Connor, J.M., Light, J.M., and Stahl, B., 1994. "South Timbalier 161A: A Successful Application of Platform Requalification Technology." Proceedings Offshore Technology Conference, OTC 7471, Houston, Texas, May.

Kim W., Ostapenko A., "A Simplified Method to Determine The Ultimate Strength of Damaged Tubular Segment."

Liu, P. L., Lin, H. Z., Der Kiureghian, A., 1989. "CALREL User Manual." Report No.UCB/SEMM-89/18, Dept. of Civil Engineering, University of California at Berkeley.

Loh, J.T., 1993, "Ultimate Strength of Dented Tubular Steel Members," Proceedings, 3rd International Offshore and Polar Engineering Conference, Vol. 4, pp. 134-145.

Loch, K.J., Bea, R.G., 1995. "Determination of the Ultimate Limit States of Fixed Steel-Frame Offshore Platforms Using static Pushover Analyses." Report to U.S. Minerals Management Service and Joint Industry Project

Sponsors, Marine Technology Development Group, University of California at Berkeley, May.

Marshall, P.W., 1986. "Tubular Joint Design, " in Planning and Design of Fixed Offshore Platforms, McClelland, B., and Reifel, M.D., pp. 624-691.

McDonald, D. T., Bando, K., Bea, R. G., Sobey, R. J., 1990. " Near Surface Wave Forces on Horizontal Members and Decks of Offshore Platforms, Final Report," Coastal and Hydraulic Engineering, Dept. of Civil Engineering, University of California at Berkeley, Dec.

Mortazavi, M. and Bea R.G., 1994. "ULSLEA, Simplified Nonlinear Analysis for Offshore Structures." Report to Joint Industry-Government Sponsored Project, Marine Technology Development Group, Dept. of Civil Engineering, University of California at Berkeley, June.

Nordal H. et al. 1988. "A System Reliability Case Study of an Eight-leg Jacket Platform", Report No. RMS-3, Department of Civil Engineering, Stanford University.

Ostapenko A. Wood B., Chowdhury A., Hebor M., 1993. "Residual Strength of Damaged and Deteriorated Tubular Members in Offshore Structures," ATLSS Report No. 93-03, Lehigh University, Betlehem, PA.

PMB Engineering Inc., 1994. "Benchmark Analysis, Trial Application of the API-RP 2A-WSD Draft Section 17," Report to Minerals Management Service and Trials JIP Participants, San Francisco, CA., Dec.

Petrauskas, C., Botelho, D. L. R., Krieger, W. F., and Griffin, J. J., 1994. "A Reliability Model for Offshore Platforms and its Application to ST 151 H and K Platforms During Hurricane Andrew (1992)," Proceedings of the Behavior of Offshore Structure Systems, Boss '94, Massachusetts Institute of Technology.

Parsanejad S., 1987. "Strength of Grout-Filled Damaged Tubular Members," Journal of Structural Engineering, ASCE, Vol. 113, No. 3, March 1987.

Petrauskas, C., Heideman, J. C., and Berek, E. P., 1993. "Extreme Wave Force Calculation Procedure for 20th Edition of API RP 2A." Proceedings Offshore Technology Conference, OTC 7153, Houston, TX.

Preston, D.,1994, "An Assessment of the Environmental Loads on the Ocean Motion International Platform," MS Thesis, Department of Naval Architecture and Offshore Engineering, University of California, Berkeley, USA.

Ricles J.M., Bruin W.M., Sooi T.K., 1992. "Residual Strength and Repair of Dent-Damaged Tubulars and the Implication on Offshore Platform Assessment and Requalification."

Ricles J.M., Lamport W.P., Gillum T.E., 1992. "Residual Strength of Damaged Offshore Tubular Bracing," Proceedings Offshore Technology Conference, OTC 6938, Houston TX, May.

Ricles J.M., Gillum T.E., Lamport W.P., 1993. "Grout Repair of Dent-Damaged Steel Tubular bracing," Proceedings Offshore Technology Conference, OTC 7151, Houston TX, May.

Ricles J.M., Hebor M.F., 1994. "Residual Strength and Epoxy-based Grout Repair of Corroded Offshore Tubulars," Boss 94.

Skjelbreia, L., and Hendrickson J., 1961, "Fifth Order Gravity Wave Theory, "Proceedings, 7th Conference of Coastal Engineering, pp. 184-196.

Sintef, 1994. "USFOS. A Computer Program for Progressive Collapse Analysis of Steel Offshore Structures," Publication N-7034, Trondheim, Norway. Revised Version 6.0.

Tang W.H. and Gilbert R.B., 1990, "Offshore Lateral Pile Design Reliability," Research Report for Project PRAC 87-29 sponsored by the American Petroleum Institute.

Tang W.H., 1988, "Offshore Axial Pile Design Reliability", Research Report for Phase 1 of the Project PRAC 86-29B sponsored by the American Petroleum Institute.

Vannan, M.T., Thompson, H. M., Griffin, J. J., Gelpi, S. L., 1994. "An Automated Procedure for Platform Strength Assessment," Proceedings of the Offshore Technology Conference, OTC 7474, Houston, TX.

Yura, J. A., Zettlemoyer, N., Edwards, F. E., 1980. "Ultimate Capacity Equations for Tubular Joints." Proceedings Offshore Technology Conference, OTC 3690, Houston TX, May.

Zhang, Y., Der Kiureghian, A., 1995. "Finite Element Reliability Analysis of Limit Load," Proceedings ICASP-7, July, Paris, France.

Appendix A Detailed Results of Verification Case Studies

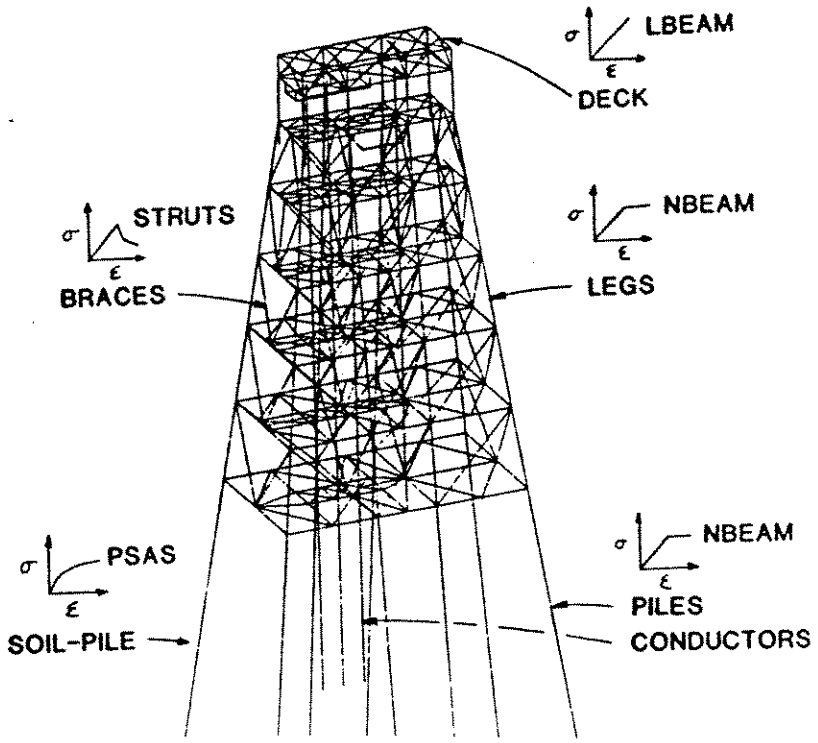

Figure A1 : Platform A

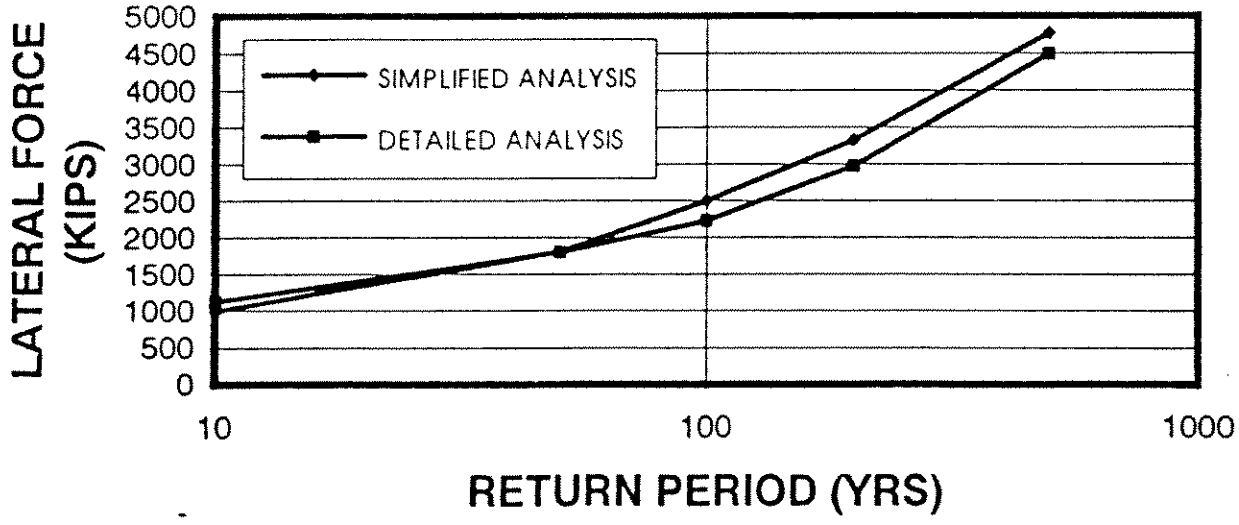

Figure A2 : Platform "A" Broadside Loading

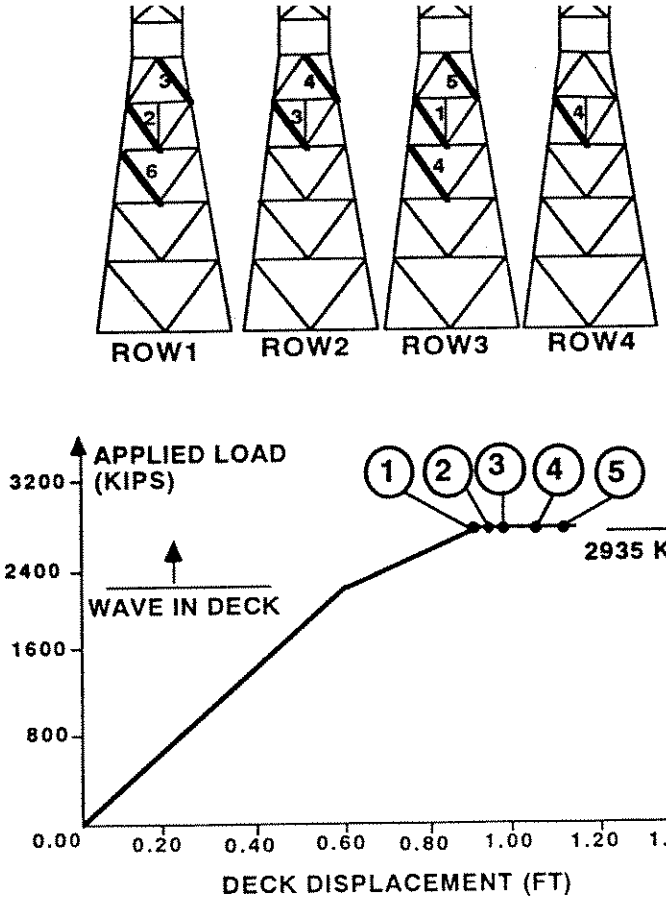

Figure A3 : Platform "A" Broadside Capacity (SEASTAR)

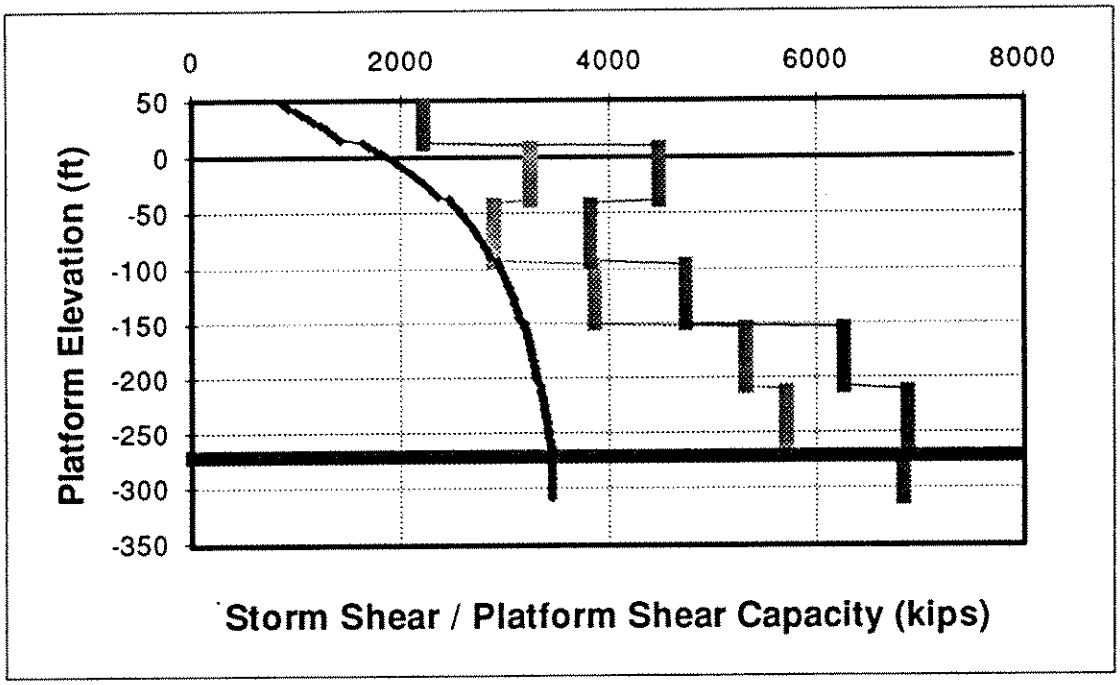

Figure A4 : Platform "A" Broadside Shear Capacity (ULSLEA)

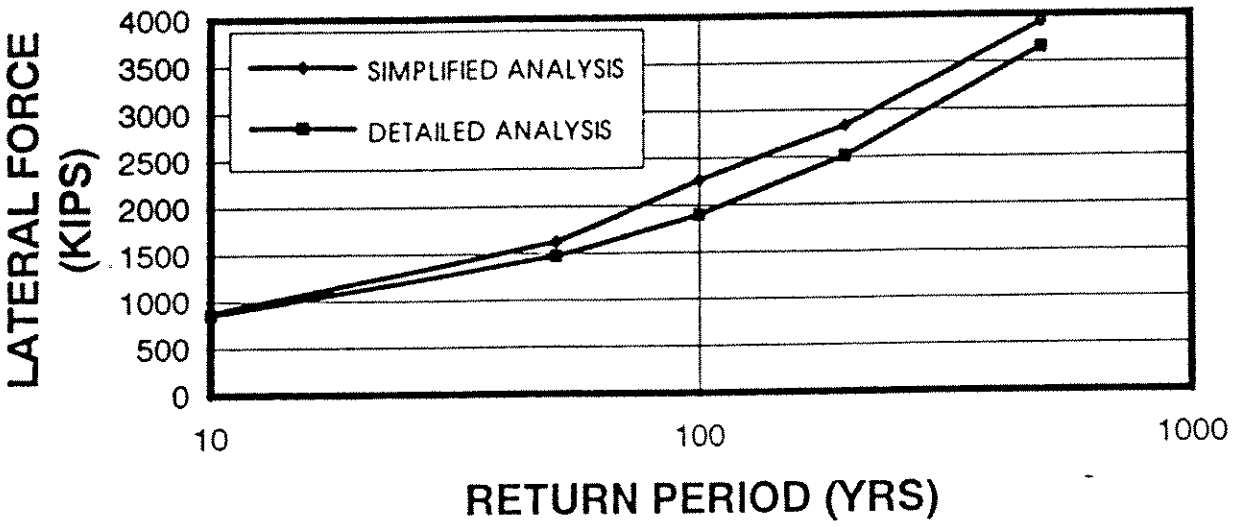

Figure A5 : Platform "A" End-on Loading

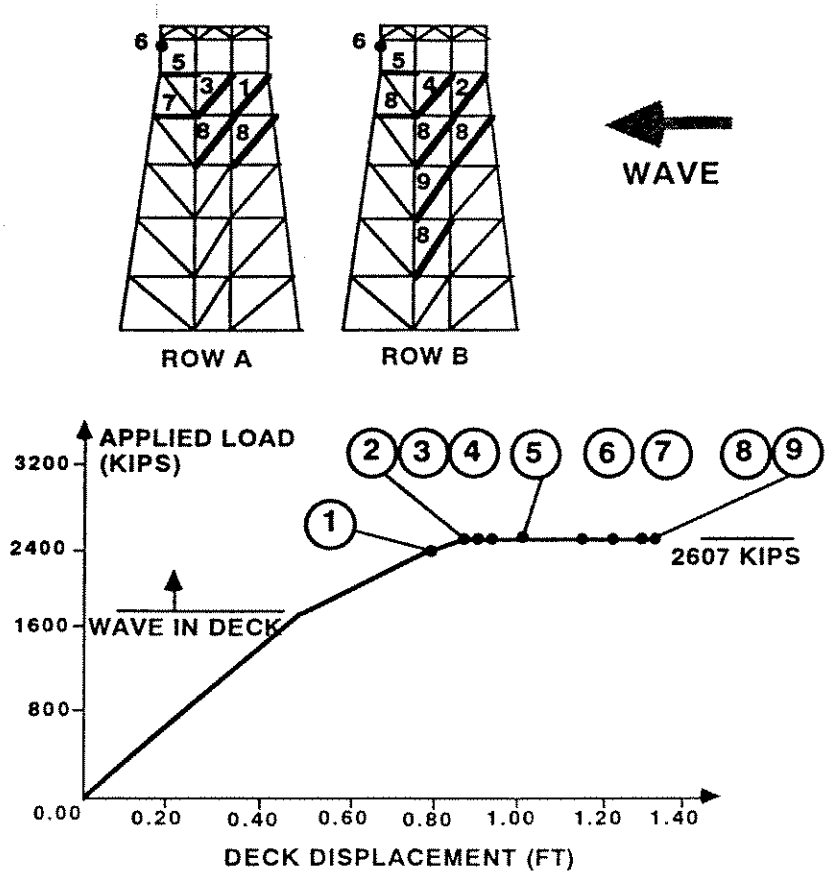

Figure A6 : Platform "A" End-on Capacity (SEASTAR)

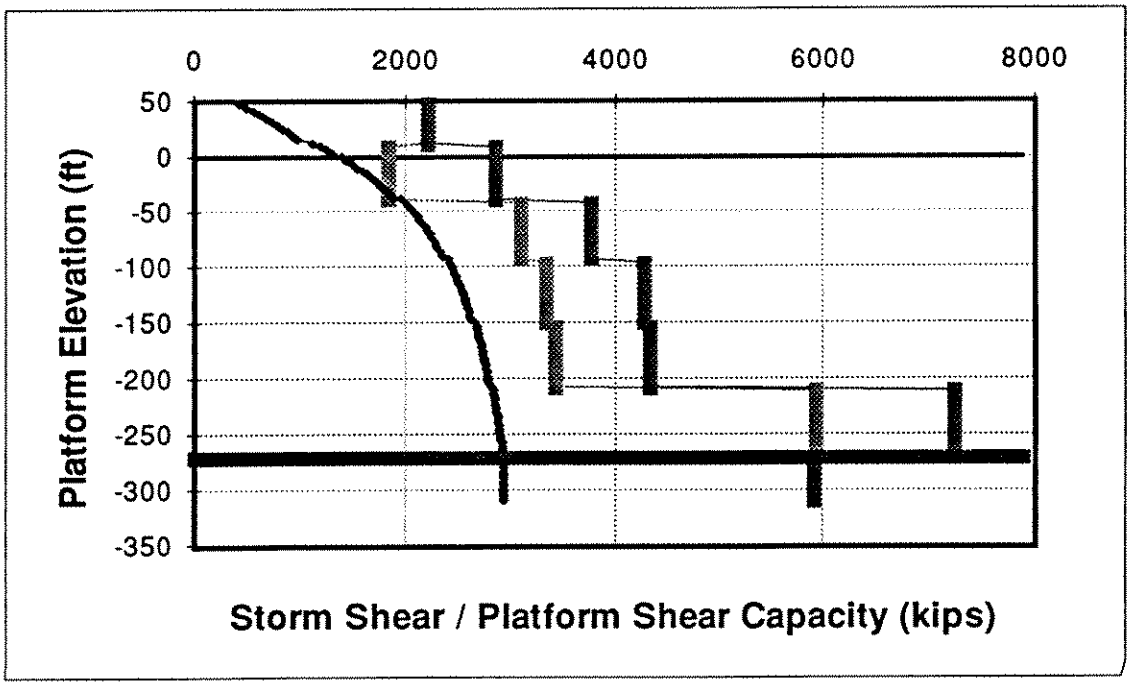

Figure A7 : Platform "A" End-on Shear Capacity (ULSLEA)

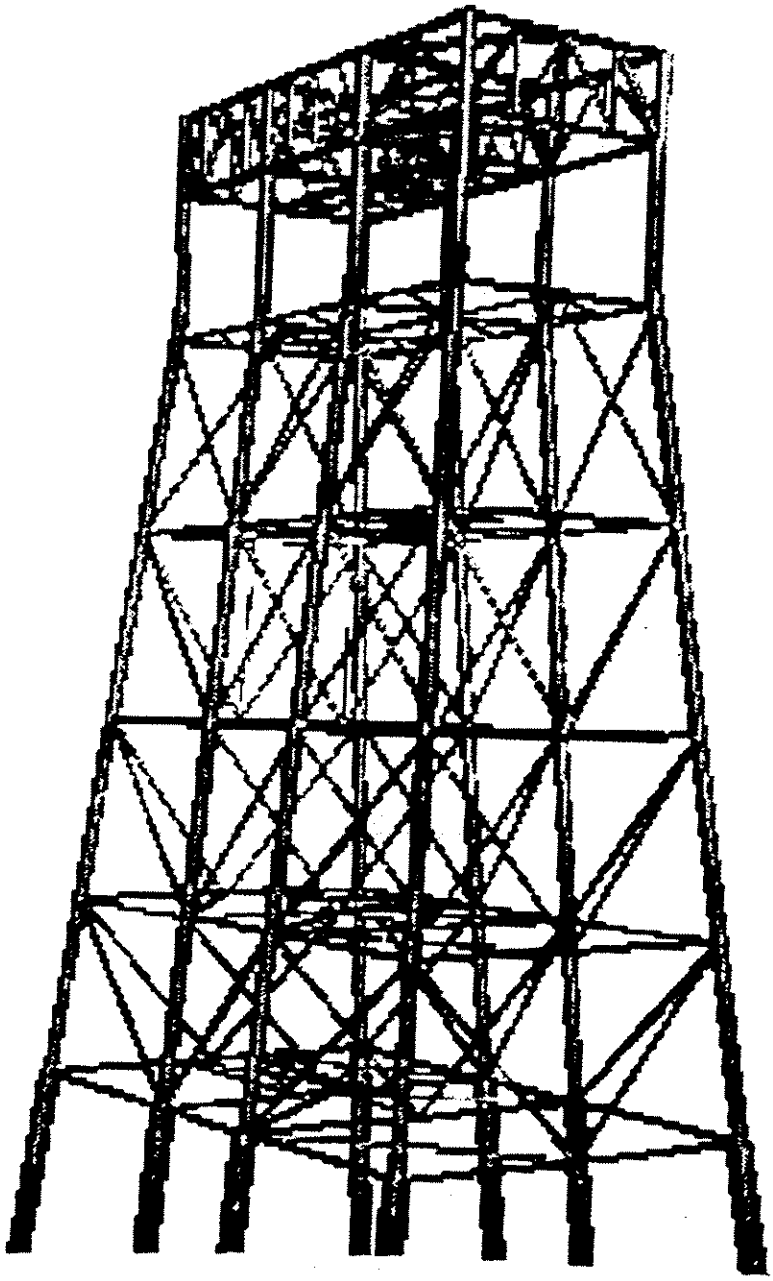

Figure A8 : Platform "B"

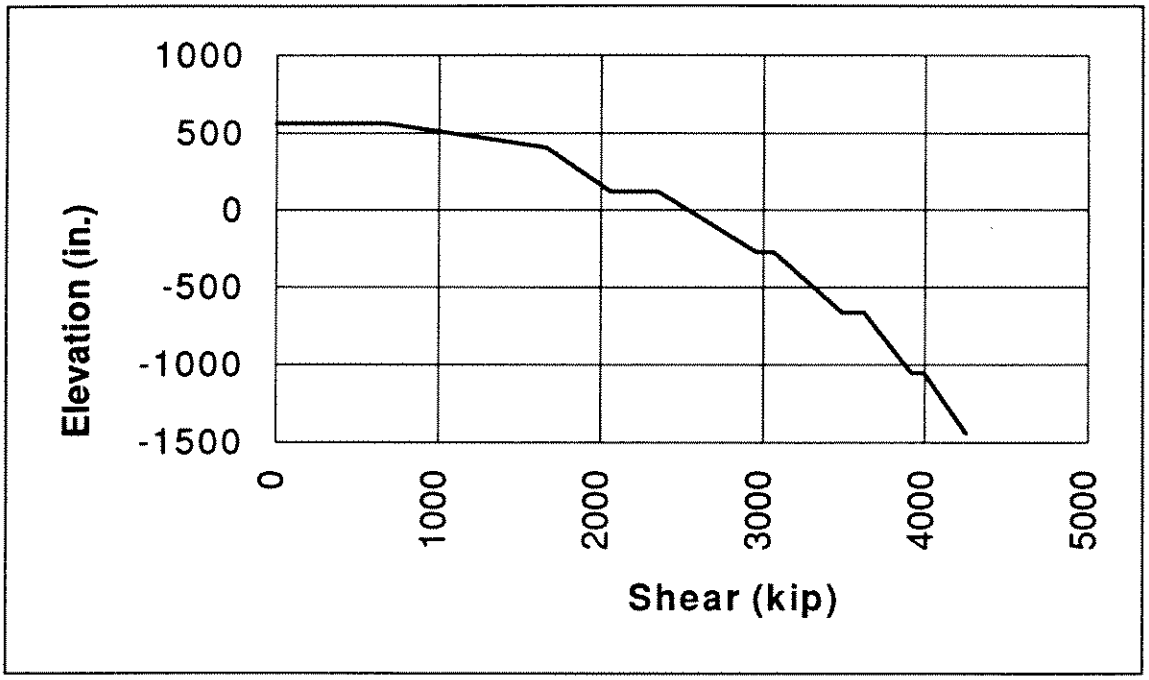

Figure A9 : Platform "B" Broadside Shear Profile (WAJAC) (Loch, 1995)

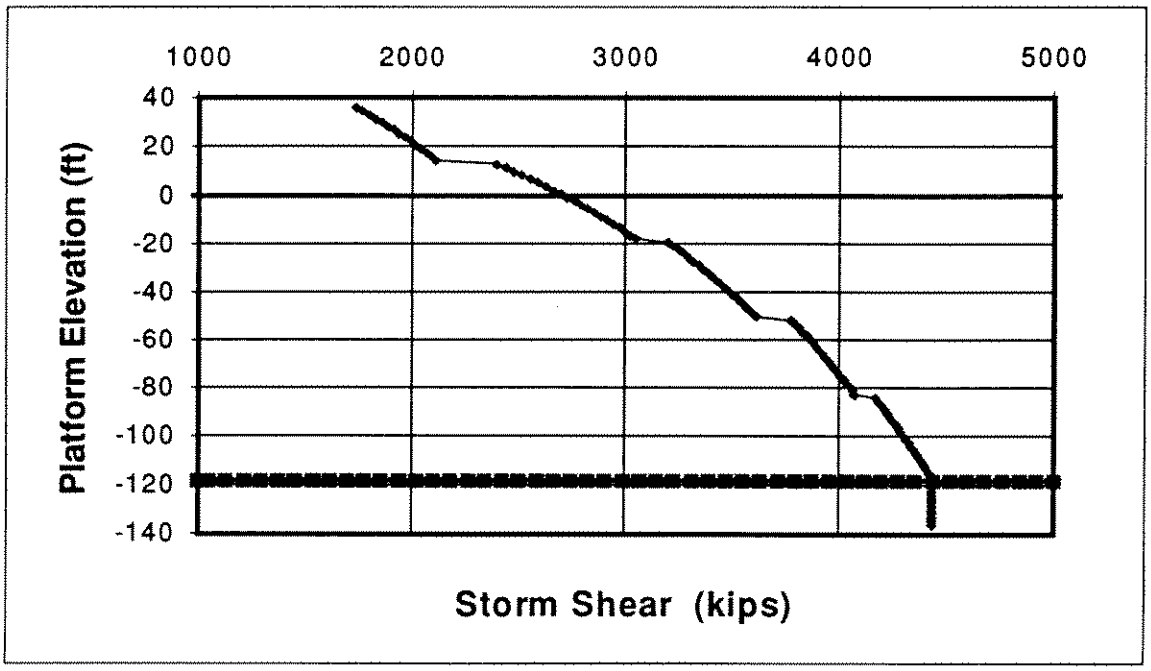

Figure A10 :Platform "B" Broadside Reference Storm Shear Profile (ULSLEA)

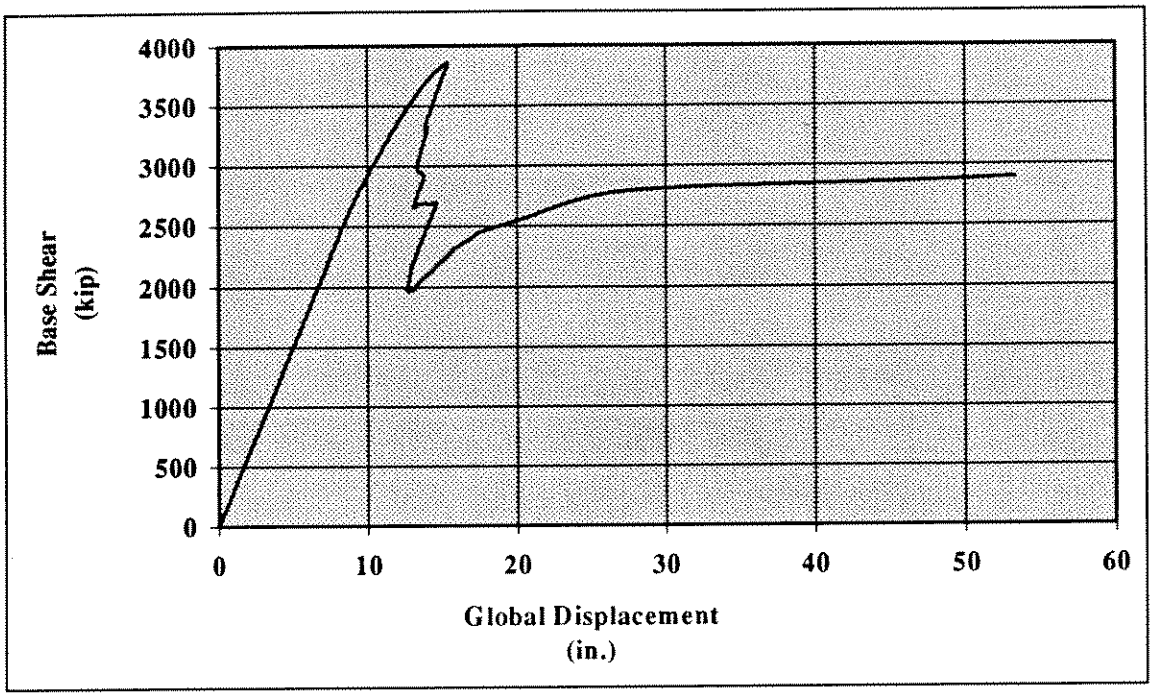

Figure A11 : Platform "B" Broadside Force-Displacement History (USFOS) (Loch, 1995)

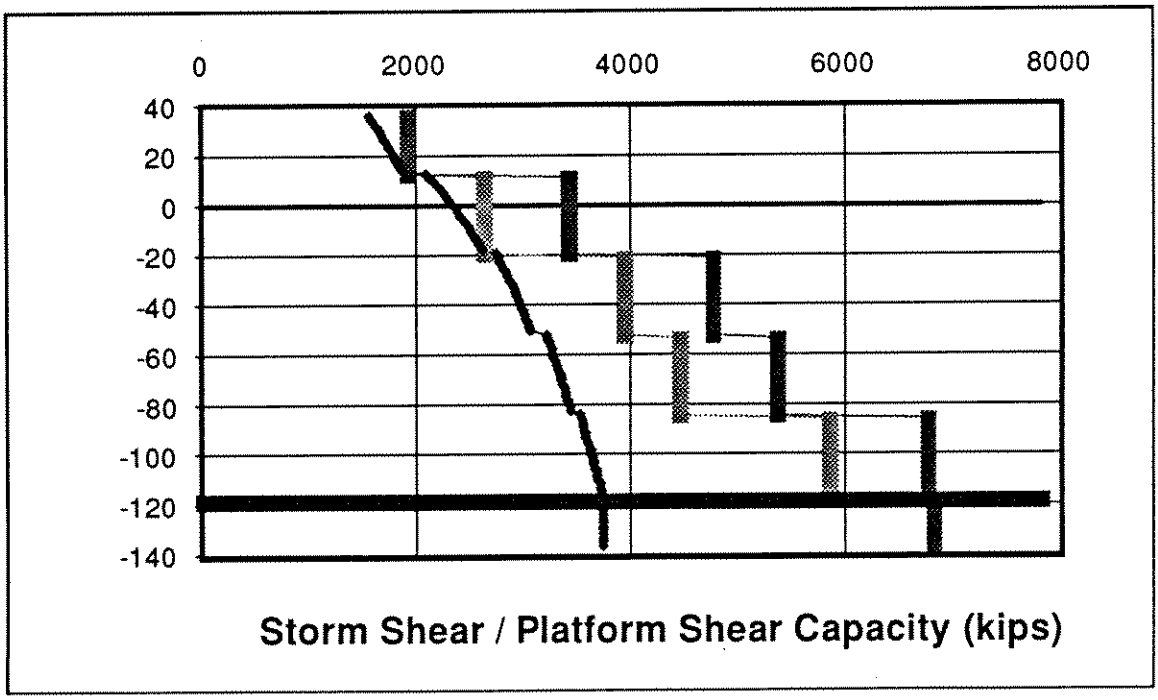

Figure A12 : Platform "B" Broadside Shear Capacity (ULSLEA)

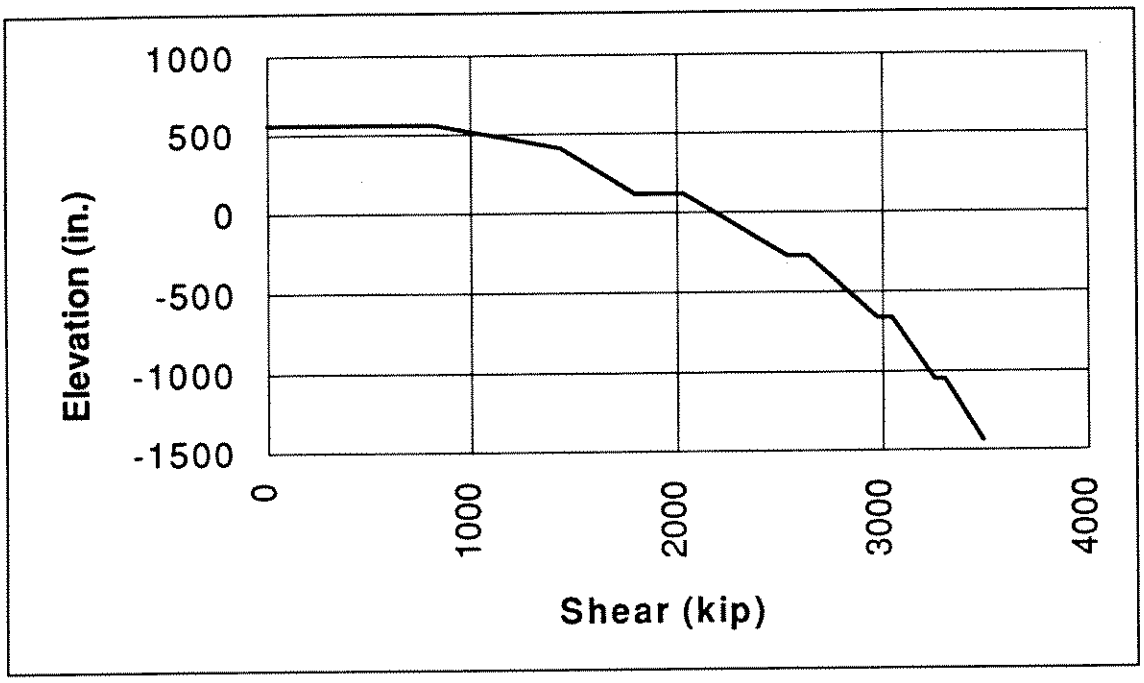

Figure A13 : Platform "B" End-On Shear Profile (USFOS) (Loch, 1995)

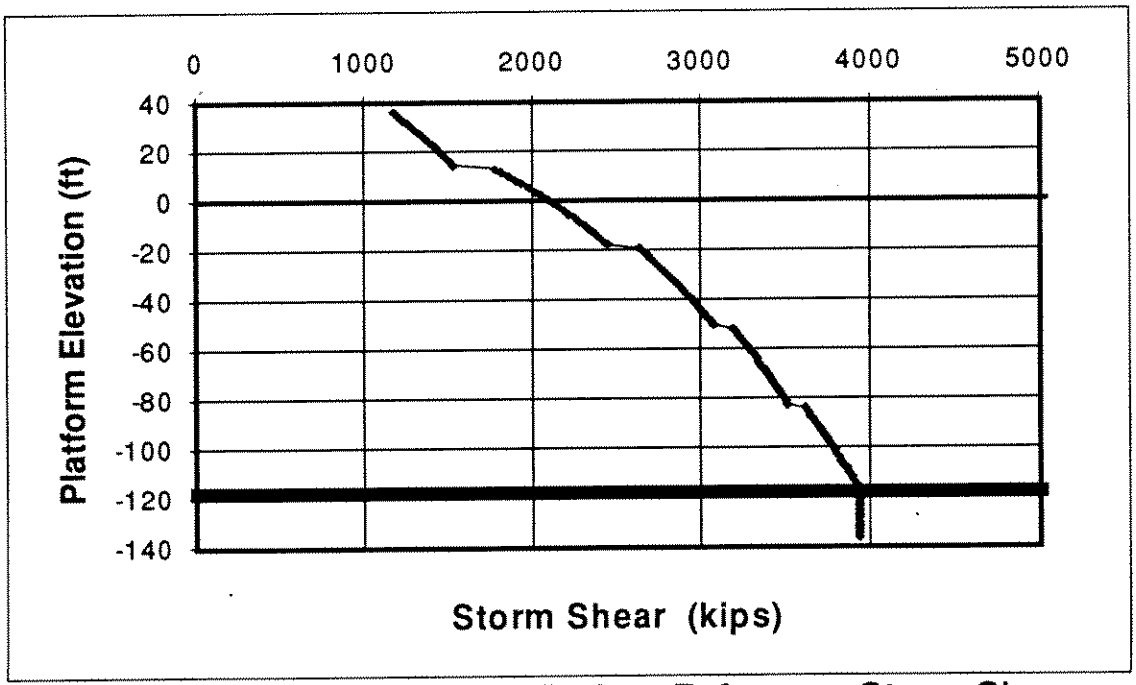

Figure A14 : Platform "B" End-on Reference Storm Shear (ULSLEA)

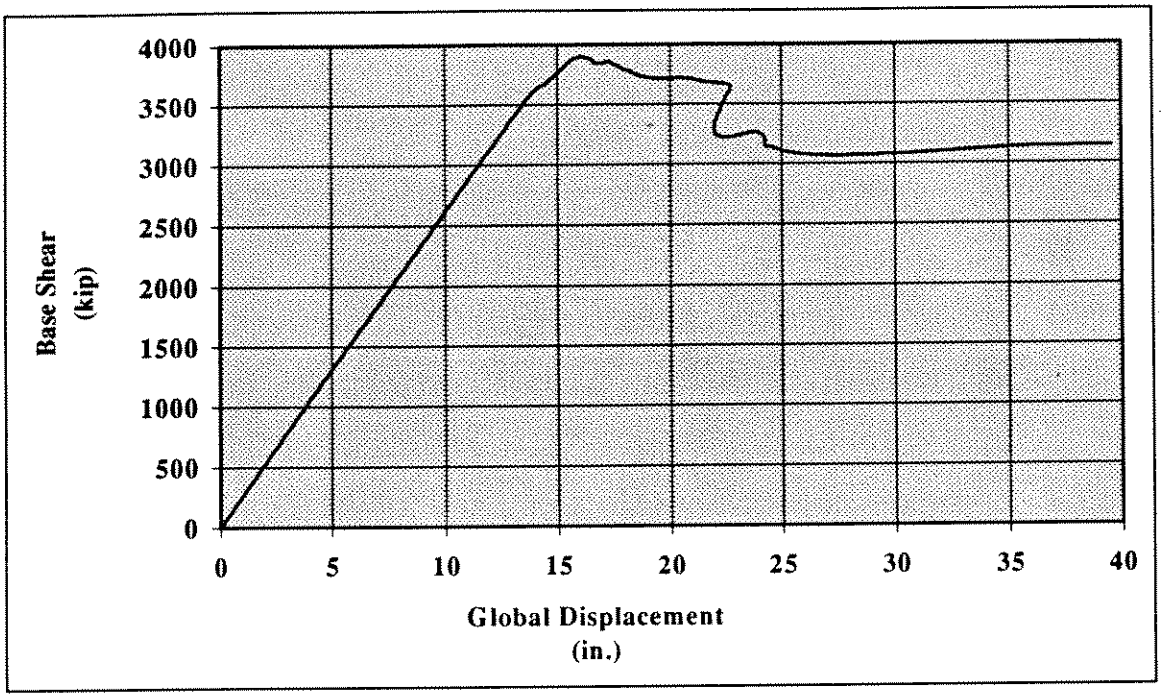

Figure A15 : Platform "B" End-On Force-Displacement History (USFOS) (Loch, 1995)

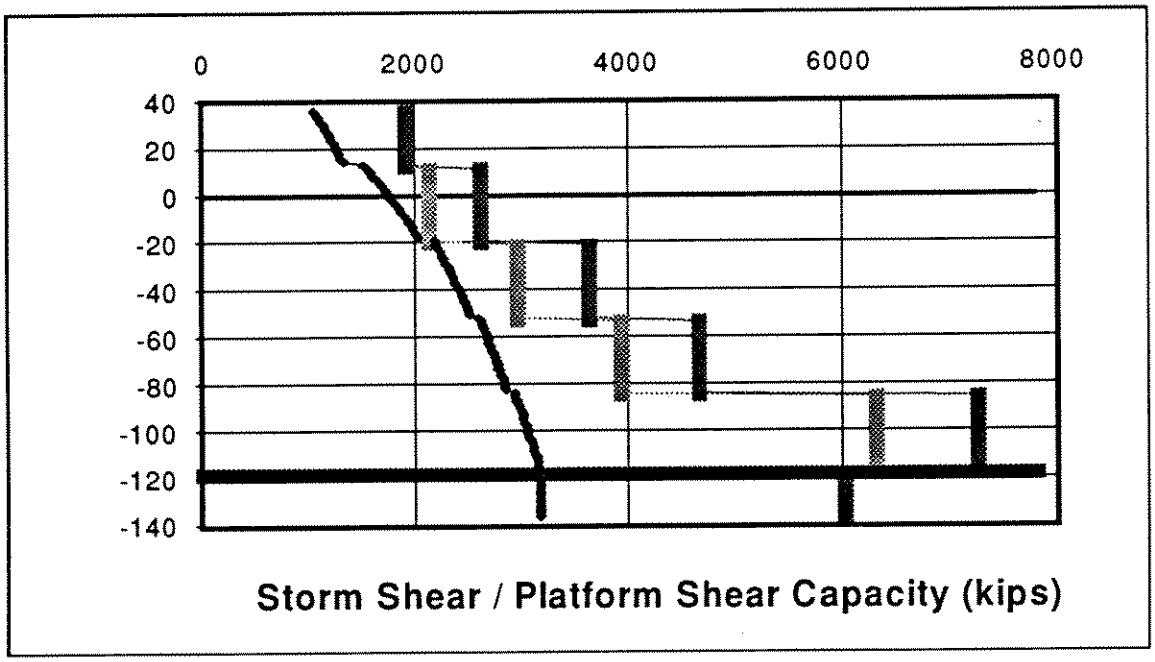

Figure A16 : Platform "B" End-on Shear Capacity (ULSLEA)

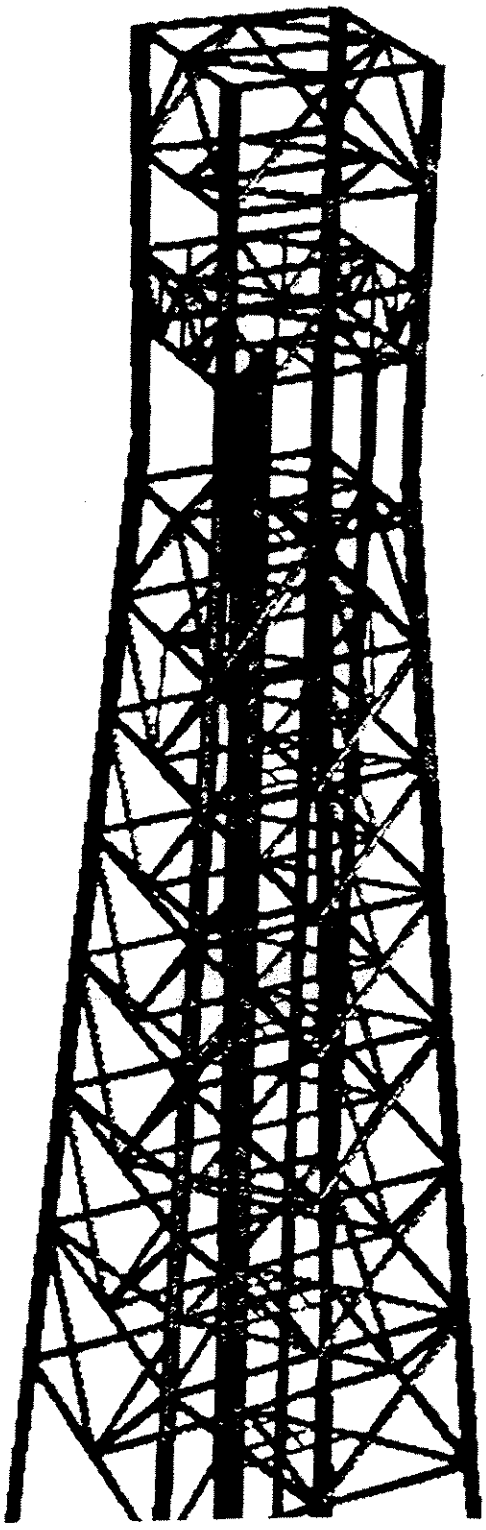

Figure A17 : Platform "C"

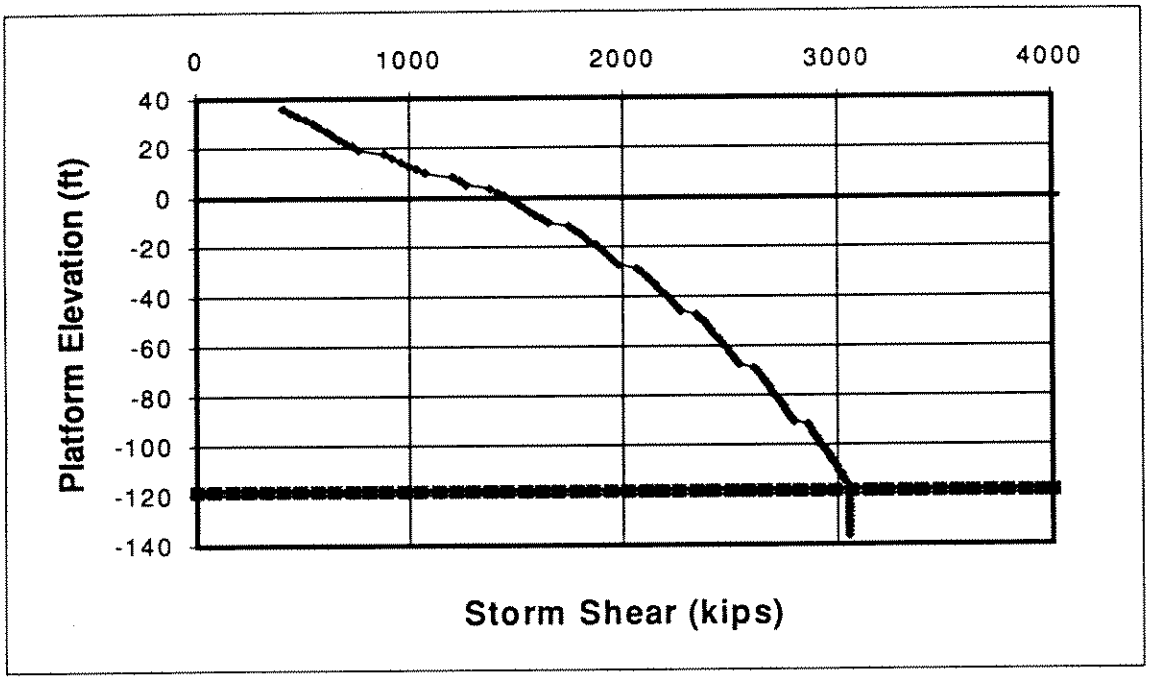

Figure A18 : Platform "C" Reference Storm Shear (ULSLEA)

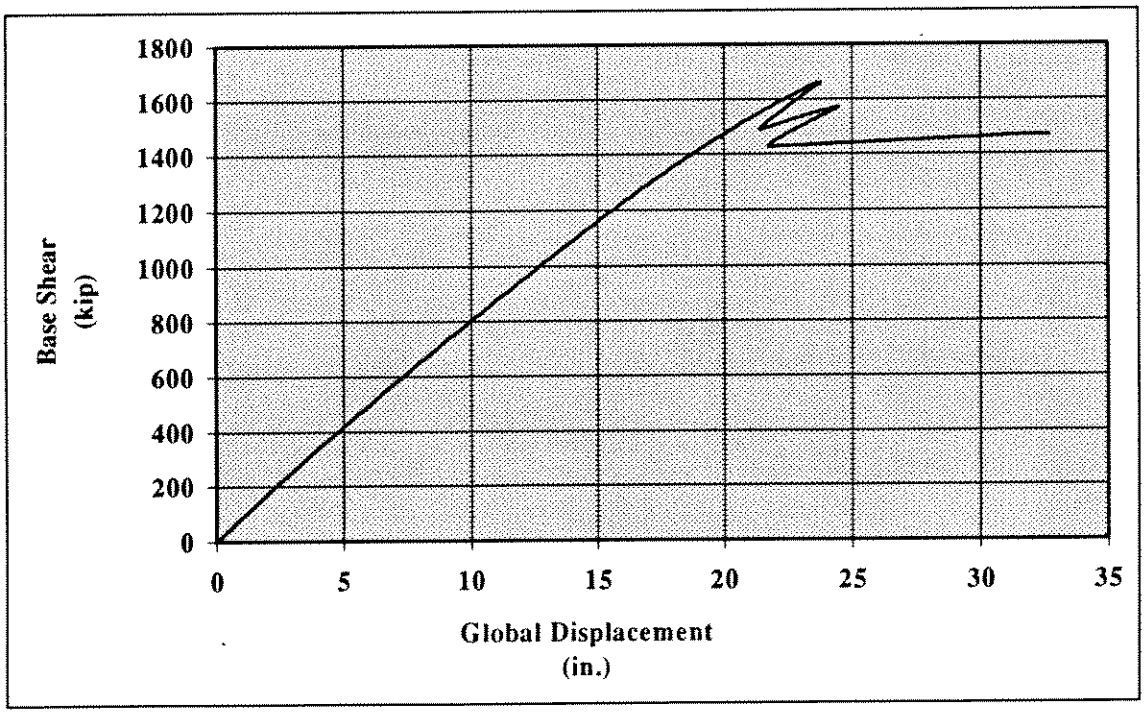

Figure A19 : Platform "C" Force-Displacement History (USFOS) (Loch, 1995)

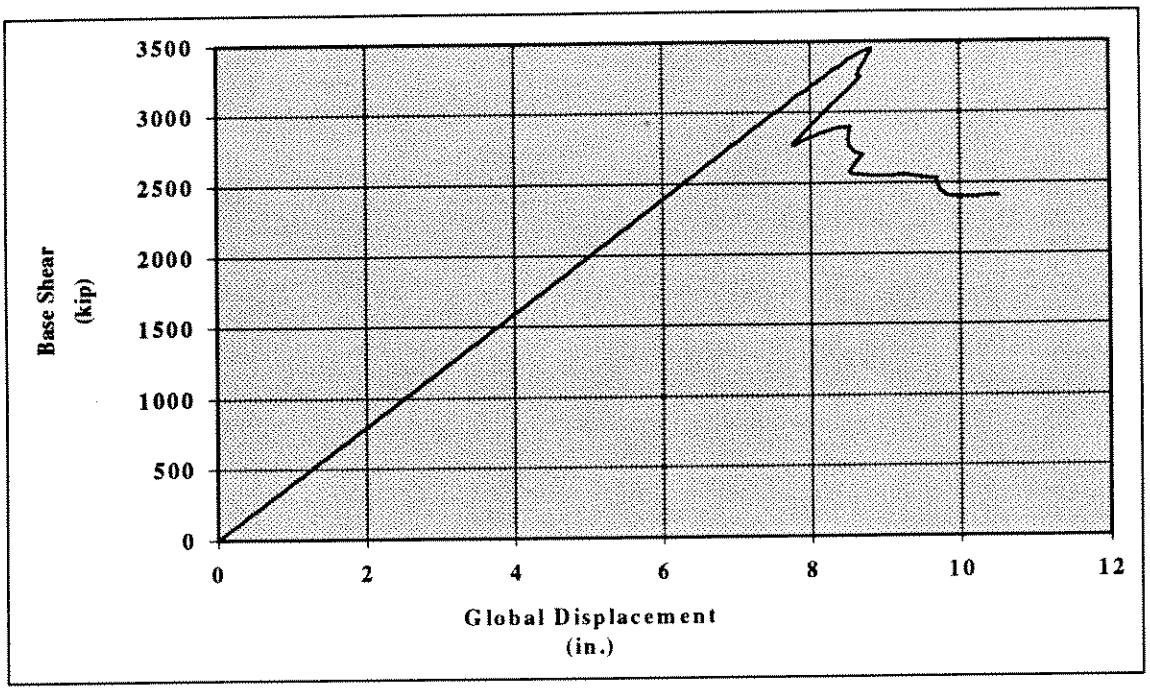

Figure A20 : Platform "C" Fixed Base Force Displacement History (USFOS) (Loch, 1995)

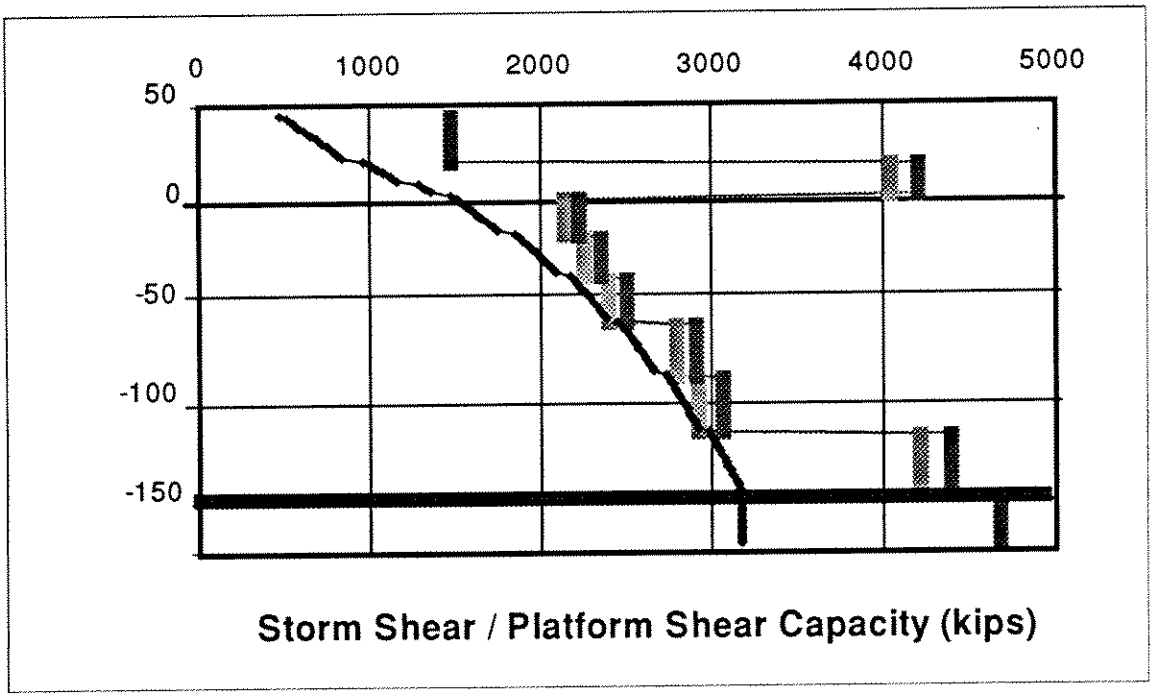

Figure A21: Platform "C" Fixed Base Shear Capacity (ULSLEA)

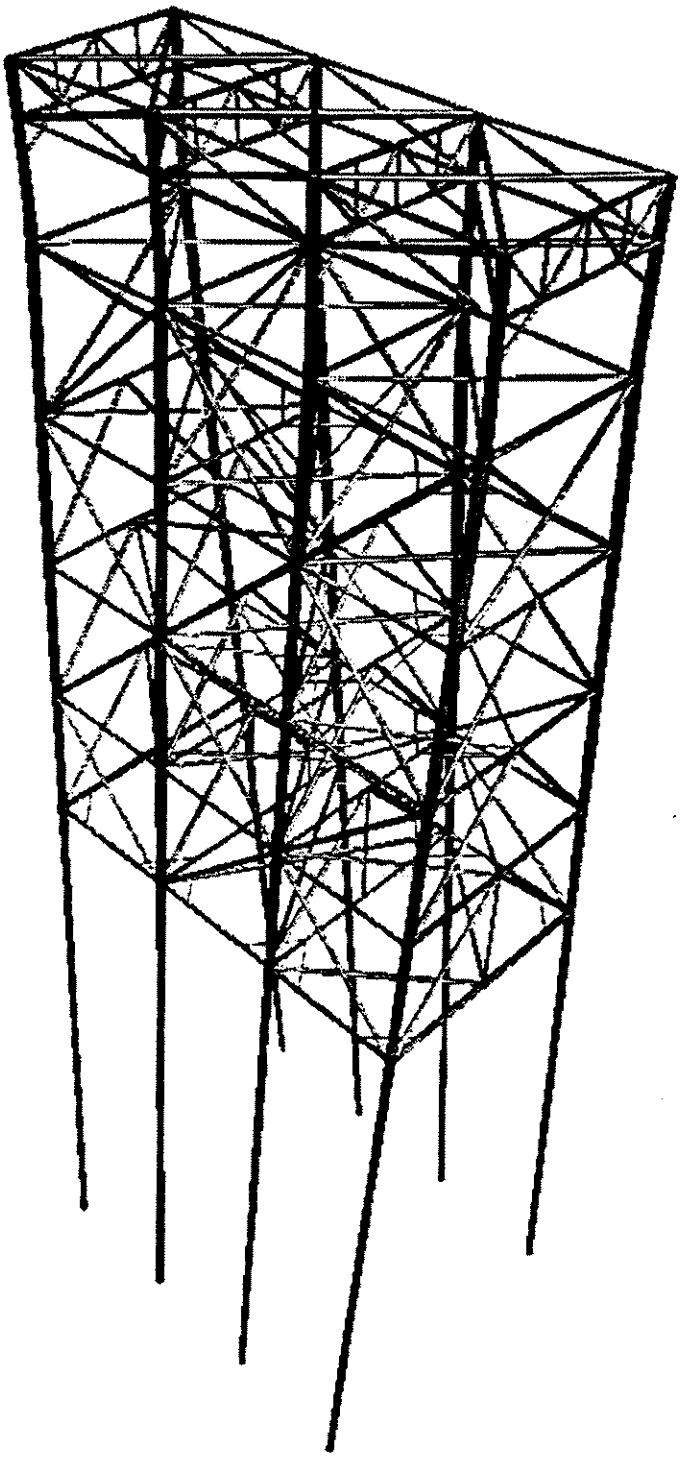

Figure A22: Platform "D"

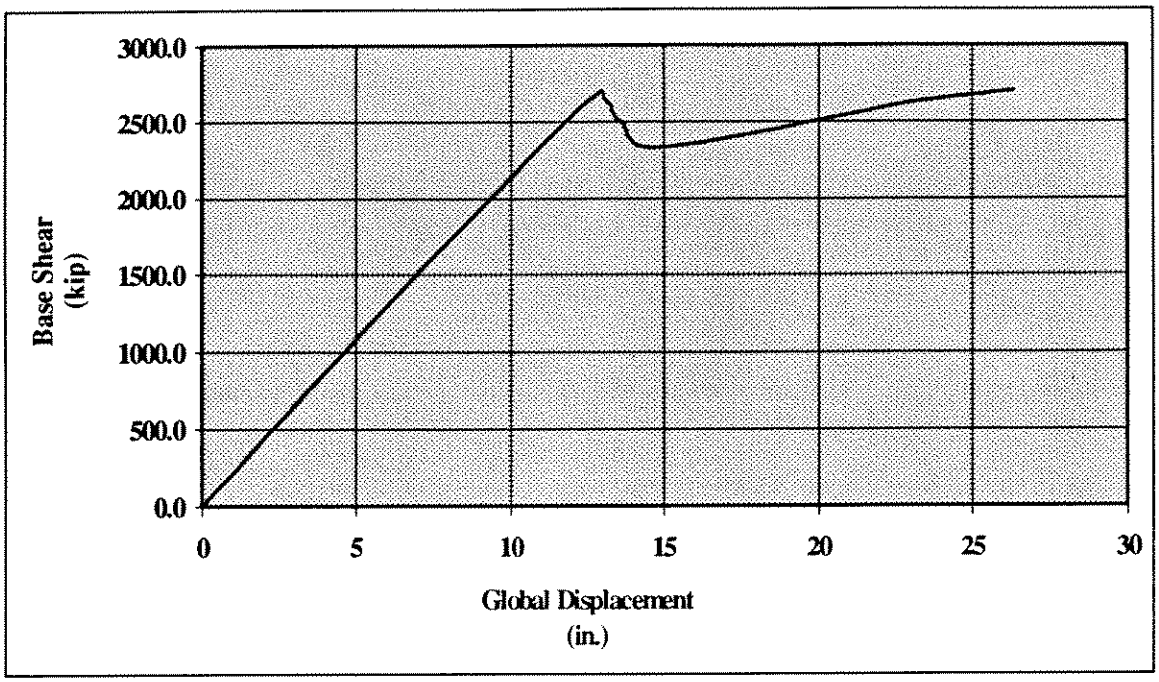

Figure A23 : Platform "D" End-on Loading Force-Displacement History (USFOS) (Loch, 1995)

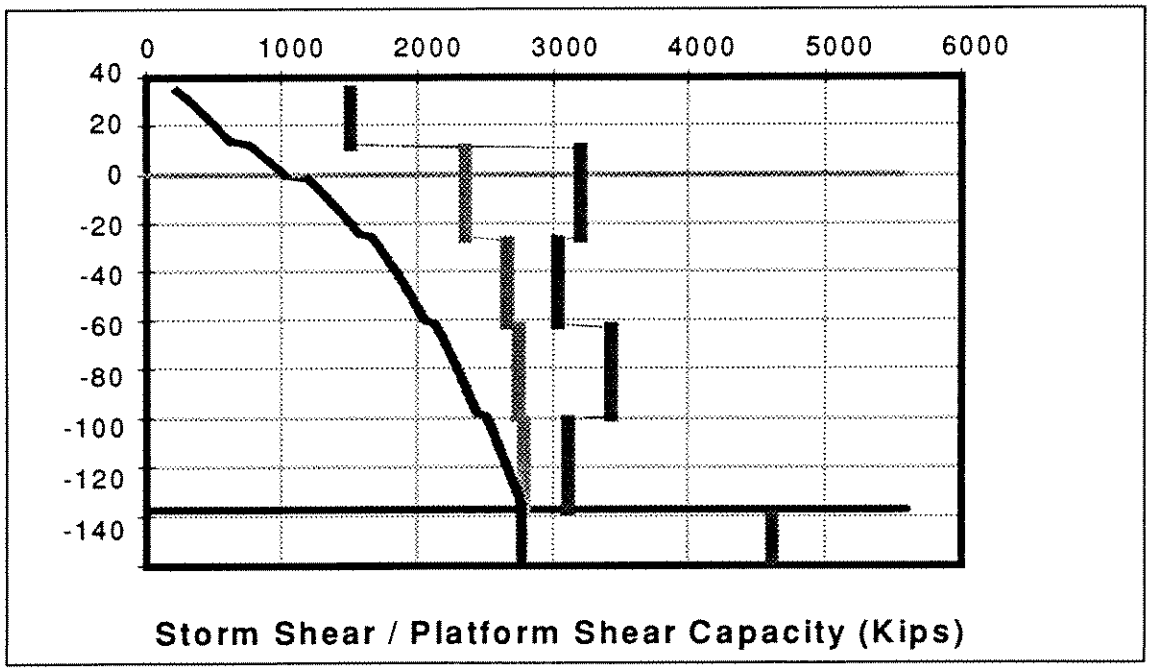

Figure A24 : Platform "D" End-on Loading (ULSLEA)

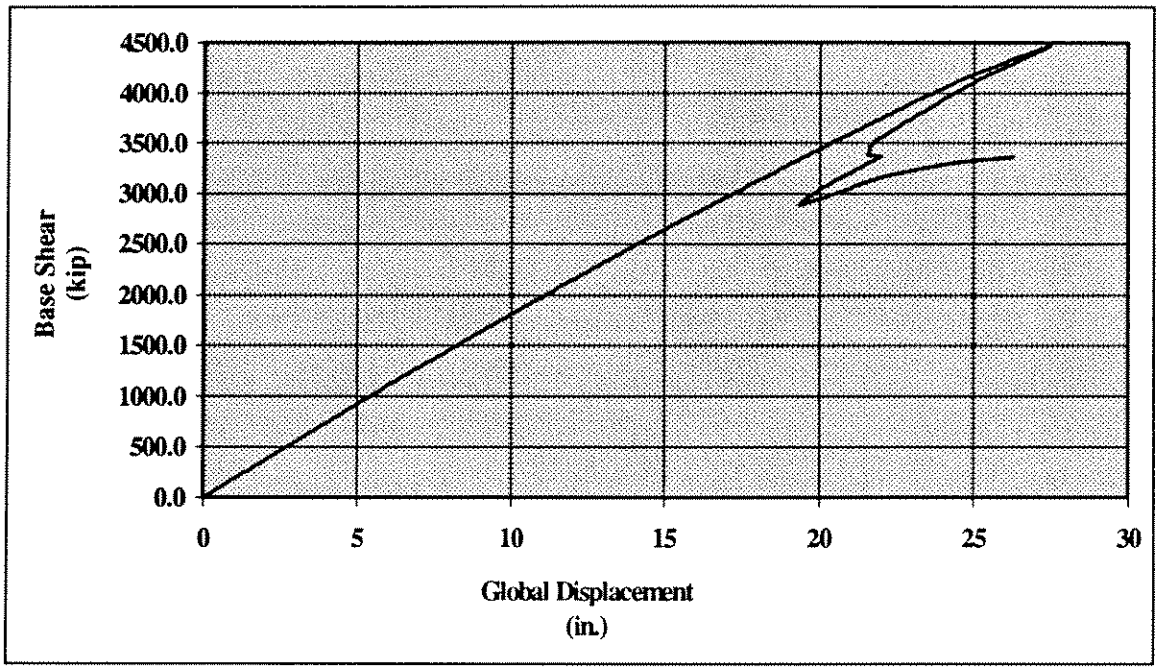

Figure A25 : Platform "D" Broadside Loading Force-Displacement History (USFOS) (Loch, 1995)

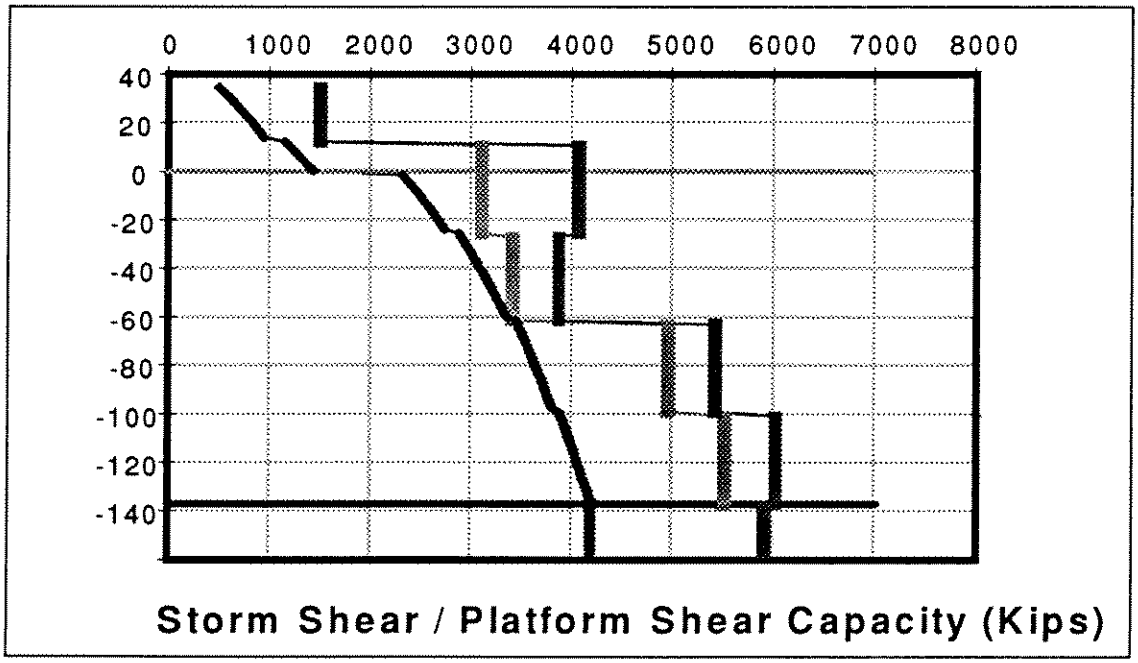

Figure A26 : Platform "D" Broadside Loading (ULSLEA)

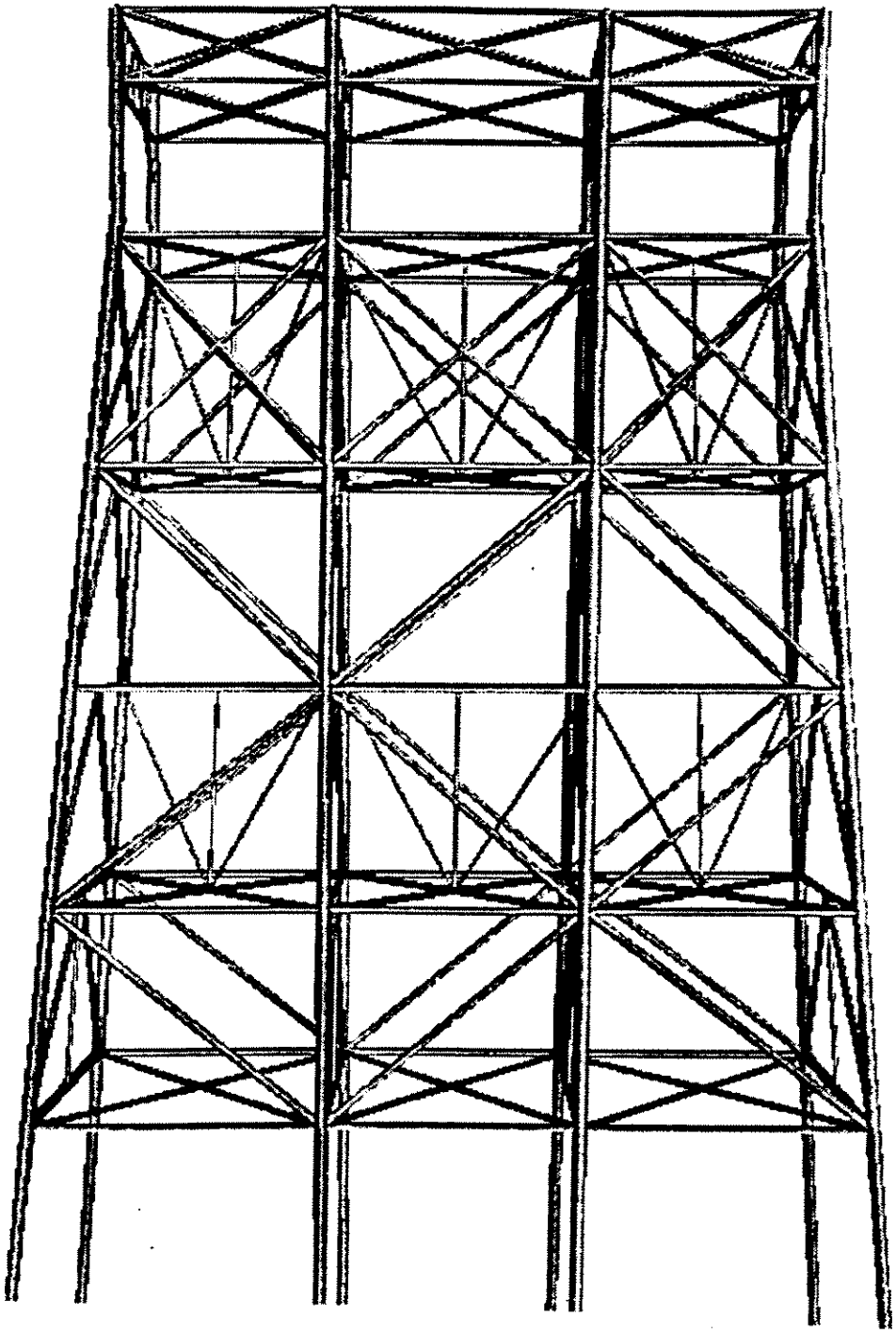

Figure A27 : Platform "E"

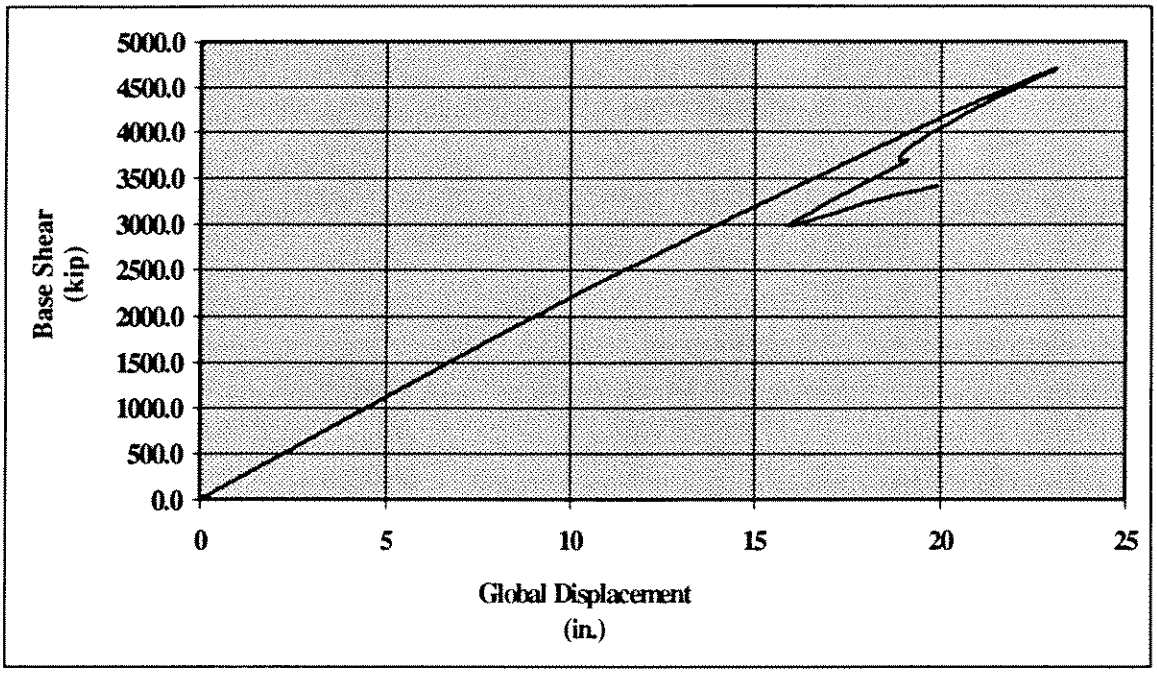

Figure A28 : Platform "E" Broadside Loading Force-Displacement History (USFOS) (Loch, 1995)

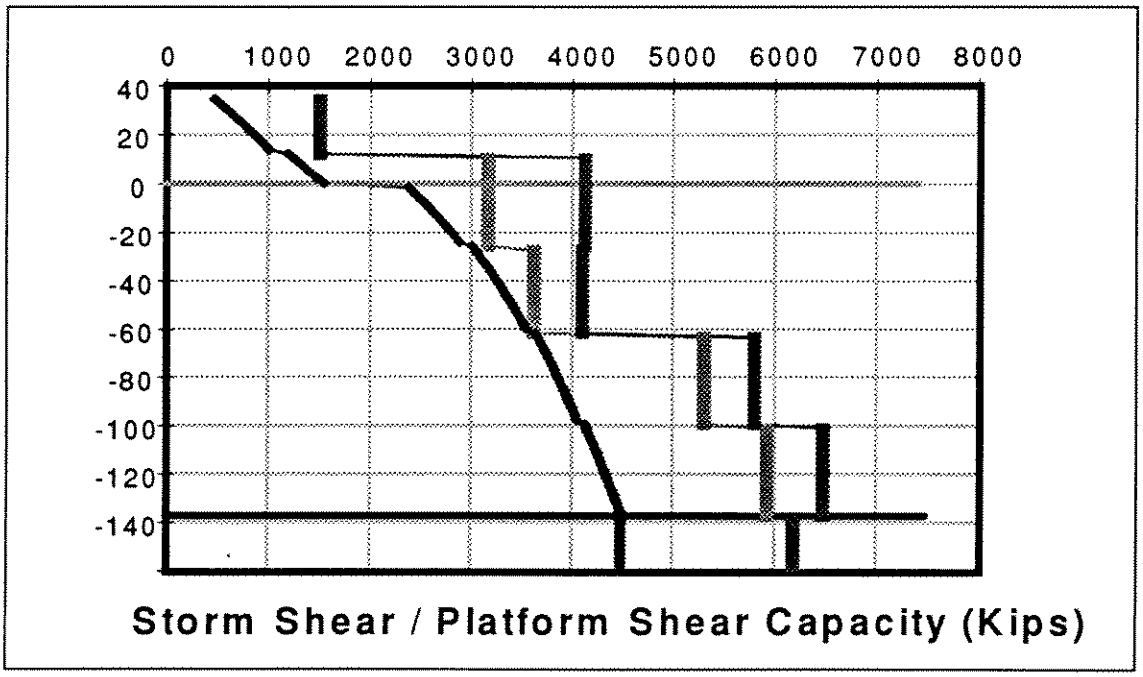

Figure A29 : Platform "E" Broadside Loading (ULSLEA)

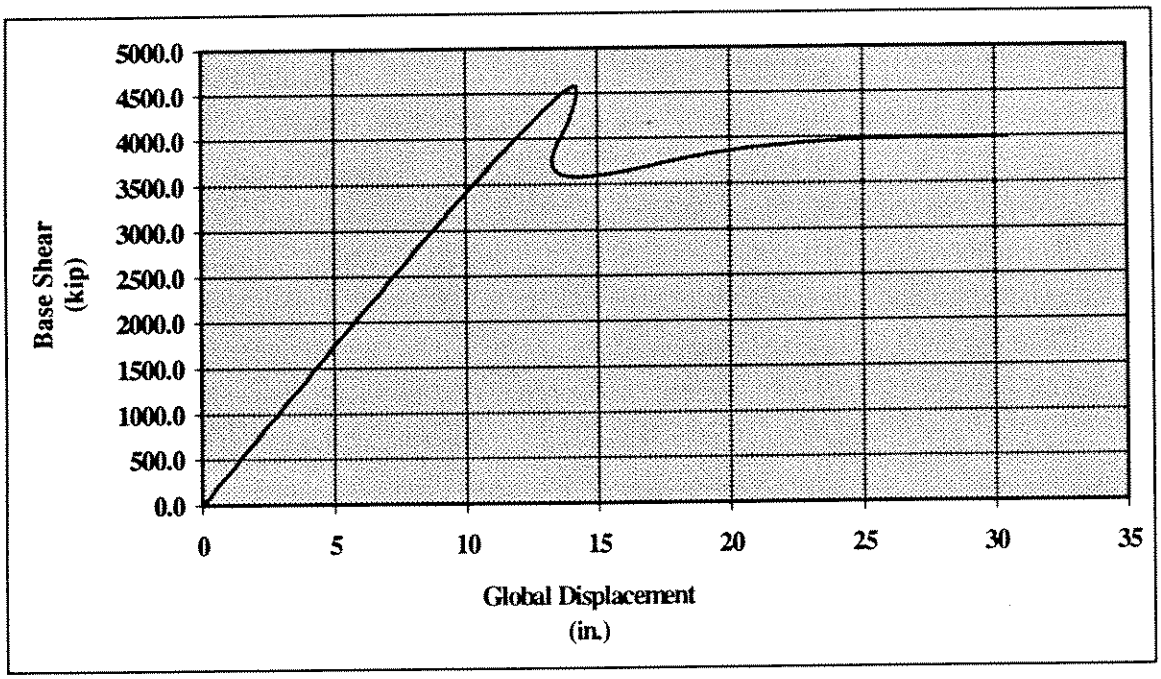

Figure A30 : Platform "E" End-on Loading Force-Displacement History (USFOS) (Loch, 1995)

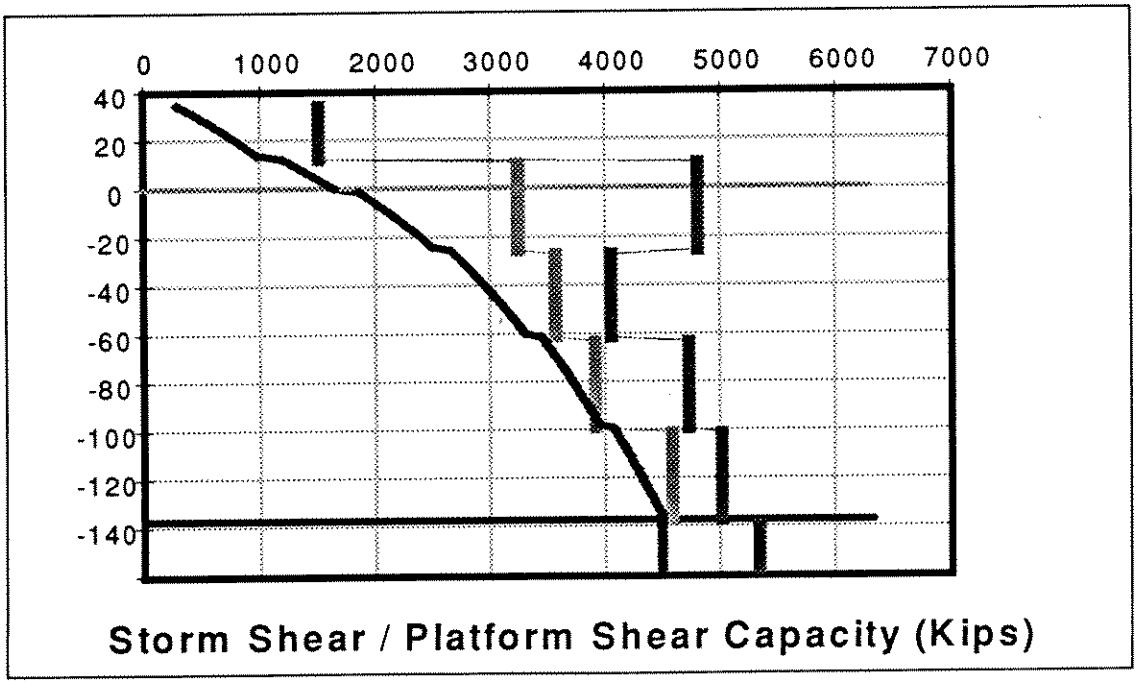

Figure A31 : Platform "E" End-on Loading

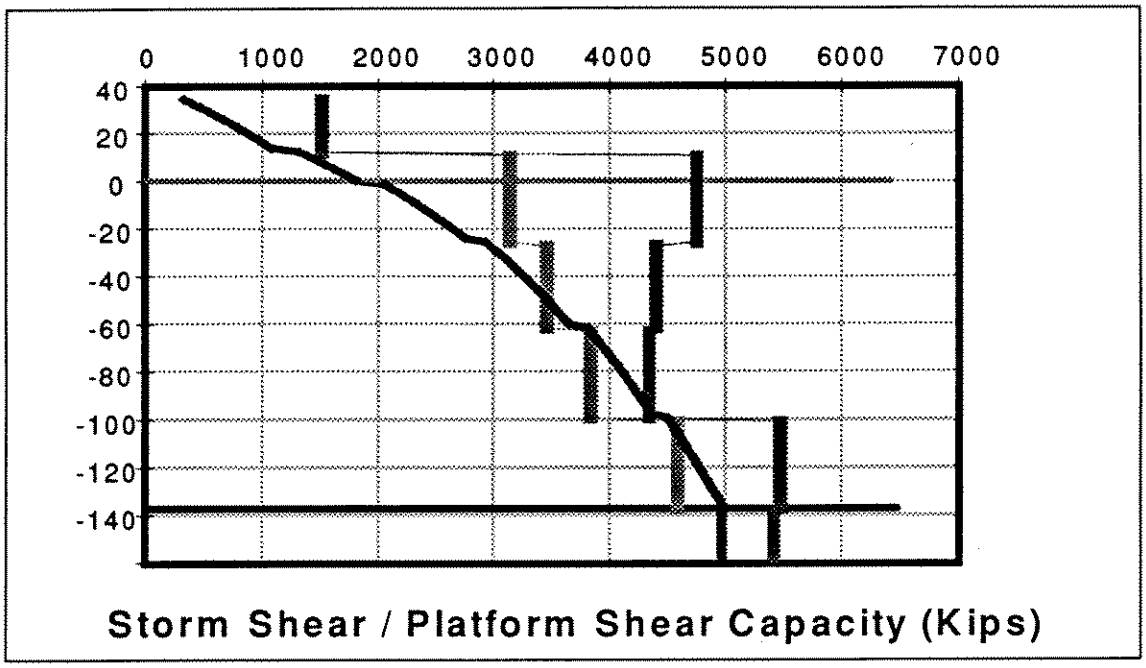

Figure A32 : Platform "E" End-on Loading 2

Platform	Configuration	Wave Direction	ULSLEA		USFOS / SEASTAR		Ratio of USFOS/ULSLEA Base Shears
			Failure Mode	Base Shear (kips)	Failure Mode	Base Shear (kips)	
A	8 leg double battered K-braced	End-on Broadside	1st jacket bay 2nd jacket bay	2,900 3,400	1st jacket bay 2nd jacket bay	2,600 2,900	0.90 0.85
B	8 leg double battered K-braced	End-on Broadside	1st jacket bay 1st jacket bay	3,100 3,700	1st jacket bay 1st jacket bay	3,900 3,900	1.26 1.05
C	4 leg double battered K-braced	End-on End-on	4th , 5th and 6th jacket bays Foundation	3,200 1,900 (1,700)	5th and 6th jacket bays Foundation	3,400 1,700	1.06 0.90 (1.00)*
D	8 leg single battered K-braced	End-on Broadside	4th jacket bay 2nd jacket bay	2,800 4,200	4th jacket bay 2nd jacket bay	2,700 4,500	0.96 1.07
E	8leg double battered K-braced	End-on Broadside	3rd and 4th jacket bays 3rd jacket bay	4,500 4,500	4th jacket bay 3rd jacket bay	4,400 4,700	0.98 1.04

*) Including the platform selfweight

Table A1 : Comparison of USFOS and ULSLEA / SEASTAR Results

Appendix B CALREL Input & Output Files

****

University of California
Department of Civil Engineering

CAL-RELiability program
Developed by
P.-L. Liu, H.-Z. Lin and A. Der Kiureghian

Last Revision: December 1990

****

INPUT - LIMIT STATE FUNCTIONS

DECK LEGS

```
      subroutine ugfun(g,x,tp,ig)
      implicit real*8 (a-h,o-z)
      dimension x(1),tp(1)
      go to(10) ig
   10 g = x(1)*cos(tp(1)/x(2))*tp(2)-tp(3)*x(3)*(tp(4)*x(4))**2-tp(5)
      return
      end
```

JACKET END-ON LOADING

```
      subroutine ugfun(g,x,tp,ig)
      implicit real*8 (a-h,o-z)
      dimension x(1),tp(1)
      go to(10) ig
   10 g =tp(1)*x(1)+tp(2)*x(2)+tp(3)*x(3)-tp(4)*x(4)*(tp(5)*x(5))**2
     *+x(6)
      return
      end
```

JACKET BROADSIDE LOADING

```
      subroutine ugfun(g,x,tp,ig)
      implicit real*8 (a-h,o-z)
      dimension x(1),tp(1)
      go to(10) ig
   10 g =x(1)-tp(1)*x(2)*(tp(2)*x(3))**2+tp(3)
      return
      end
```

FOUNDATION

```
      subroutine ugfun(g,x,tp,ig)
      implicit real*8 (a-h,o-z)
      dimension x(1),tp(1)
      go to(10) ig
   10 g =tp(1)*x(1)-tp(2)*x(2)*(tp(3)*x(3)**2)
      return
      end
```

DECK LEGS - END-ON LOADING

var	ids	mean	st. dev.	param1	param2	param3	param4	init. pt
x1	2	6.31E+03	6.68E+02	8.74E+00	1.06E-01			6.31E+03
x2	2	6.68E+03	7.82E+02	8.80E+00	1.17E-01			6.68E+03
x3	2	1.00E-01	5.80E-02	-2.45E+00	5.38E-01			1.00E-01
x4	2	3.45E+01	1.16E+01	3.49E+00	3.27E-01			3.45E+01

deterministic parameters in limit-state function:

tp (1) = 1.197E+03
tp (2) = 4.200E-01
tp (3) = 7.000E-01
tp (4) = 1.100E+00
tp (5) = 1.000E+00

>>>> FIRST-ORDER RELIABILITY ANALYSIS <<<<

iteration number .....iter= 7
value of limit-state function..g(x)=-3.016E-05
reliability index .....beta= 4.0956
probability .....Pf1= 2.106E-05

var	design point		sensitivity vectors			
	x*	u*	alpha	gamma	delta	eta
x1	5.944E+03	-5.067E-01	-.1237	-.1237	.1320	-.0753
x2	6.623E+03	-1.847E-02	-.0045	-.0045	.0046	-.0006
x3	3.474E-01	2.582E+00	.6304	.6304	-.0304	-1.1184
x4	9.133E+01	3.138E+00	.7663	.7663	-.1004	-2.0428

>>>> SECOND-ORDER RELIABILITY ANALYSIS -- POINT FITTING <<<<

coordinates and ave. main curvatures of fitting points in rotated space

axis	u'i	u'n	G(u)	a'+i	u'i	u'n	G(u)	a'-i
1	3.000	4.096	7.414E-08	-4.689E-06	-3.000	4.096	6.022E-08	-5.780E-06
2	3.000	4.092	1.774E-03	-8.501E-04	-3.000	4.089	4.470E-03	-1.371E-03
3	3.000	4.096	1.215E-11	-7.068E-08	-3.000	4.096	1.156E-11	-7.208E-08

	improved Breitung	Tvedt's EI
generalized reliability index betag =	**4.0950**	**4.0950**
probability Pf2 =	**2.111E-05**	**2.111E-05**

JACKET BAY 1 - END-ON LOADING

var	ids	mean	st. dev.	param1	param2	param3	param4	init. pt
x1	2	1.15E+03	1.73E+02	7.04E+00	1.49E-01			1.15E+03
x2	2	1.07E+03	1.60E+02	6.96E+00	1.49E-01			1.07E+03
x3	2	1.62E+03	1.30E+02	7.39E+00	8.01E-02			1.62E+03
x4	2	3.56E-01	2.06E-01	-1.18E+00	5.37E-01			3.56E-01
x5	2	3.45E+01	1.16E+01	3.49E+00	3.27E-01			3.45E+01

deterministic parameters in limit-state function:

tp (1) = 1.500E-01
tp (2) = 1.500E-01
tp (3) = 1.000E+00
tp (4) = 7.000E-01
tp (5) = 1.100E+00
tp (6) = 1.000E+00

>>>> FIRST-ORDER RELIABILITY ANALYSIS <<<<

iteration number .....iter= 8
value of limit-state function..g(x)=-9.461E-07
reliability index .....beta= 2.2855
probability .....Pf1= 1.114E-02

var	design point		sensitivity vectors			
	x*	u*	alpha	gamma	delta	eta
x1	1.134E+03	-3.554E-02	-.0155	-.0155	.0161	-.0028
x2	1.049E+03	-3.288E-02	-.0144	-.0144	.0149	-.0026
x3	1.593E+03	-1.786E-01	-.0781	-.0781	.0799	-.0201
x4	6.701E-01	1.446E+00	.6325	.6325	-.3923	-.4989
x5	5.818E+01	1.761E+00	.7703	.7703	-.4394	-1.0471

>>>> SECOND-ORDER RELIABILITY ANALYSIS -- POINT FITTING <<<<

type of integration scheme used .....itg= 2
itg=1 .....improved Breitung formula
itg=2 .....improved Breitung formula
.....& Tvedt's exact integral
max. number of iterations for each fitting point ..inp= 4

limit-state function 1

---

coordinates and ave. main curvatures of fitting points in rotated space

axis	u'i	u'n	G(u)	a'+i	u'i	u'n	G(u)	a'-i
1	2.279	2.292	-1.459E-06	2.322E-03	-2.281	2.291	-1.961E-06	1.927E-03
2	2.280	2.291	-1.318E-06	2.169E-03	-2.281	2.290	-1.672E-06	1.794E-03
3	2.283	2.288	-4.686E-08	1.024E-03	-2.283	2.288	-1.786E-06	1.110E-03
4	2.286	2.286	-1.372E-12	1.802E-06	-2.286	2.286	-1.212E-12	1.808E-06

	improved Breitung	Tvedt's EI
generalized reliability index betag =	**2.2881**	**2.2881**
probability Pf2 =	**1.107E-02**	**1.107E-02**

JACKET BAY 2 - END-ON LOADING

var	ids	mean	st. dev.	param1	param2	param3	param4	init. pt
x1	2	1.21E+03	1.81E+02	7.09E+00	1.49E-01			1.21E+03
x2	2	1.25E+03	1.87E+02	7.12E+00	1.49E-01			1.25E+03
x3	2	1.51E+03	1.21E+02	7.32E+00	8.01E-02			1.51E+03
x4	2	4.20E-01	2.40E-01	-1.01E+00	5.32E-01			4.20E-01
x5	2	3.45E+01	1.16E+01	3.49E+00	3.27E-01			3.45E+01

x6 2 1.70E+02 1.70E+02 4.79E+00 8.33E-01 1.70E+02

deterministic parameters in limit-state function:
tp (1) = 1.500E-01
tp (2) = 1.500E-01
tp (3) = 1.000E+00
tp (4) = 7.000E-01
tp (5) = 1.100E+00

>>>> FIRST-ORDER RELIABILITY ANALYSIS <<<<

iteration number .....iter= 7
value of limit-state function..g(x)=-8.777E-06
reliability index .....beta= 2.1190
probability .....Pf1= 1.705E-02

var	design point		sensitivity vectors			
	x*	u*	alpha	gamma	delta	eta
x1	1.189E+03	-3.397E-02	-.0160	-.0160	.0166	-.0029
x2	1.228E+03	-3.509E-02	-.0166	-.0166	.0171	-.0030
x3	1.485E+03	-1.521E-01	-.0718	-.0718	.0732	-.0166
x4	7.395E-01	1.330E+00	.6277	.6277	-.4253	-.4366
x5	5.589E+01	1.638E+00	.7729	.7729	-.4711	-.9605
x6	1.091E+02	-1.162E-01	-.0548	-.0548	.1034	-.0375

>>>> SECOND-ORDER RELIABILITY ANALYSIS -- POINT FITTING <<<<

type of integration scheme used .....itg= 2
itg=1 .....improved Breitung formula
itg=2 .....improved Breitung formula
.....& Tvedt's exact integral
max. number of iterations for each fitting point ..inp= 4

limit-state function 1

---

coordinates and ave. main curvatures of fitting points in rotated space

axis	u'i	u'n	G(u)	a'+i	u'i	u'n	G(u)	a'-i
1	2.107	2.131	-3.399E-06	5.489E-03	-2.105	2.133	-3.837E-06	6.214E-03
2	2.107	2.131	-3.212E-06	5.323E-03	-2.106	2.132	-3.504E-06	5.872E-03
3	2.079	2.158	-2.352E-05	1.825E-02	-2.039	2.196	-1.152E-05	3.690E-02
4	2.085	2.152	-5.008E-08	1.528E-02	-2.099	2.139	-4.931E-05	9.162E-03
5	2.119	2.119	-2.683E-09	1.593E-04	-2.119	2.119	-4.043E-09	1.500E-04

	improved Breitung	Tvedt's EI
generalized reliability index betag =	**2.1439**	**2.1441**
probability Pf2 =	**1.602E-02**	**1.601E-02**

JACKET BAY 3 - END-ON LOADING

var	ids	mean	st. dev.	param1	param2	param3	param4	init. pt
x1	2	1.28E+03	1.81E+02	7.14E+00	1.41E-01			1.28E+03
x2	2	1.25E+03	1.87E+02	7.12E+00	1.49E-01			1.25E+03
x3	2	1.66E+03	1.21E+02	7.41E+00	7.30E-02			1.66E+03
x4	2	4.33E-01	2.40E-01	-9.71E-01	5.18E-01			4.33E-01
x5	2	3.45E+01	1.16E+01	3.49E+00	3.27E-01			3.45E+01
x6	2	3.26E+02	3.26E+02	5.44E+00	8.33E-01			3.26E+02

deterministic parameters in limit-state function:
tp (1) = 1.500E-01
tp (2) = 1.500E-01
tp (3) = 1.000E+00
tp (4) = 7.000E-01
tp (5) = 1.100E+00

>>>> FIRST-ORDER RELIABILITY ANALYSIS <<<<

iteration number .....iter= 7
value of limit-state function..g(x)= 8.082E-06
reliability index .....beta= 2.2419
probability .....Pf1= 1.248E-02

var	design point		sensitivity vectors			
	x*	u*	alpha	gamma	delta	eta
x1	1.258E+03	-3.229E-02	-.0144	-.0144	.0148	-.0025
x2	1.228E+03	-3.329E-02	-.0148	-.0148	.0153	-.0027
x3	1.633E+03	-1.446E-01	-.0645	-.0645	.0656	-.0140
x4	7.744E-01	1.382E+00	.6164	.6164	-.4010	-.4674
x5	5.794E+01	1.748E+00	.7795	.7795	-.4478	-1.0500
x6	1.956E+02	-1.974E-01	-.0881	-.0881	.1712	-.0654

>>>> SECOND-ORDER RELIABILITY ANALYSIS -- POINT FITTING <<<<

type of integration scheme used .....itg= 2
itg=1 .....improved Breitung formula
itg=2 .....improved Breitung formula
.....& Tvedt's exact integral
max. number of iterations for each fitting point ..inp= 4

limit-state function 1

---

coordinates and ave. main curvatures of fitting points in rotated space

axis	u'i	u'n	G(u)	a'+i	u'i	u'n	G(u)	a'-i
1	2.232	2.252	-3.886E-06	3.927E-03	-2.232	2.252	-3.441E-06	3.879E-03
2	2.232	2.252	-4.284E-06	4.146E-03	-2.232	2.252	-3.708E-06	4.041E-03
3	2.193	2.290	-5.534E-05	2.007E-02	-2.157	2.324	-2.416E-05	3.520E-02
4	2.122	2.356	-1.171E-06	5.069E-02	-2.179	2.303	-5.560E-04	2.572E-02
5	2.240	2.244	-1.060E-07	7.520E-04	-2.240	2.244	-1.845E-07	6.793E-04

	improved Breitung	Tvedt's EI
generalized reliability index betag =	**2.2774**	**2.2778**
probability Pf2 =	**1.138E-02**	**1.137E-02**

JACKET BAY 4 - END-ON LOADING

var	ids	mean	st. dev.	param1	param2	param3	param4	init. pt
x1	2	1.21E+03	1.81E+02	7.09E+00	1.49E-01			1.21E+03
x2	2	1.14E+03	1.71E+02	7.03E+00	1.49E-01			1.14E+03
x3	2	1.70E+03	1.36E+02	7.44E+00	7.98E-02			1.70E+03
x4	2	4.35E-01	2.50E-01	-9.75E-01	5.34E-01			4.35E-01
x5	2	3.45E+01	1.16E+01	3.49E+00	3.27E-01			3.45E+01
x6	2	4.84E+02	4.84E+02	5.84E+00	8.33E-01			4.84E+02

deterministic parameters in limit-state function:
tp (1) = 1.500E-01
tp (2) = 1.500E-01
tp (3) = 1.000E+00
tp (4) = 7.000E-01
tp (5) = 1.100E+00

>>>> FIRST-ORDER RELIABILITY ANALYSIS <<<<

iteration number .....iter= 9
value of limit-state function..g(x)= 1.083E-06
reliability index .....beta= 2.2768
probability .....Pf1= 1.140E-02

var	design point		sensitivity vectors			
	x*	u*	alpha	gamma	delta	eta
x1	1.189E+03	-3.089E-02	-.0136	-.0136	.0140	-.0024
x2	1.122E+03	-2.919E-02	-.0128	-.0128	.0132	-.0023
x3	1.676E+03	-1.554E-01	-.0682	-.0682	.0696	-.0160
x4	8.080E-01	1.426E+00	.6264	.6264	-.3945	-.4861
x5	5.793E+01	1.747E+00	.7675	.7675	-.4410	-1.0335
x6	2.744E+02	-2.655E-01	-.1166	-.1166	.2324	-.0924

>>>> SECOND-ORDER RELIABILITY ANALYSIS -- POINT FITTING <<<<

coordinates and ave. main curvatures of fitting points in rotated space

axis	u'i	u'n	G(u)	a'+i	u'i	u'n	G(u)	a'-i
1	2.268	2.286	-4.140E-06	3.442E-03	-2.269	2.285	-3.156E-06	3.165E-03
2	2.269	2.285	-3.555E-06	3.175E-03	-2.269	2.284	-2.675E-06	2.887E-03
3	2.222	2.331	-8.461E-05	2.185E-02	-2.190	2.360	-3.043E-05	3.477E-02
4	2.103	2.439	-1.129E-04	7.323E-02	-2.182	2.368	-1.486E-03	3.819E-02
5	2.273	2.281	-4.979E-07	1.600E-03	-2.273	2.280	-1.215E-06	1.418E-03

		improved Breitung	Tvedt's EI
generalized reliability index betag =		**2.3198**	**2.3203**
probability	**Pf2 =**	**1.018E-02**	**1.016E-02**

JACKET BAY 5 - END-ON LOADING

var	ids	mean	st. dev.	param1	param2	param3	param4	init. pt
x1	2	1.19E+03	1.78E+02	7.07E+00	1.49E-01			1.19E+03
x2	2	1.12E+03	1.68E+02	7.01E+00	1.49E-01			1.12E+03
x3	2	1.80E+03	1.44E+02	7.49E+00	7.98E-02			1.80E+03
x4	2	4.37E-01	2.53E-01	-9.72E-01	5.38E-01			4.37E-01
x5	2	3.45E+01	1.16E+01	3.49E+00	3.27E-01			3.45E+01
x6	2	7.44E+02	7.44E+02	6.27E+00	8.33E-01			7.44E+02

deterministic parameters in limit-state function:
tp (1) = 1.500E-01
tp (2) = 1.500E-01
tp (3) = 1.000E+00
tp (4) = 7.000E-01
tp (5) = 1.100E+00

>>>> FIRST-ORDER RELIABILITY ANALYSIS <<<<

iteration number .....iter= 9
value of limit-state function..g(x)= 4.783E-06
reliability index .....beta= 2.3814
probability .....Pf1= 8.623E-03

var	design point		sensitivity vectors			
	x*	u*	alpha	gamma	delta	eta
x1	1.167E+03	-2.895E-02	-.0122	-.0122	.0125	-.0021
x2	1.102E+03	-2.733E-02	-.0115	-.0115	.0118	-.0020
x3	1.774E+03	-1.567E-01	-.0658	-.0658	.0671	-.0155
x4	8.429E-01	1.491E+00	.6260	.6260	-.3741	-.5181
x5	5.923E+01	1.815E+00	.7621	.7621	-.4215	-1.0750
x6	3.900E+02	-3.595E-01	-.1510	-.1510	.3111	-.1298

>>>> SECOND-ORDER RELIABILITY ANALYSIS -- POINT FITTING <<<<

coordinates and ave. main curvatures of fitting points in rotated space

axis	u'i	u'n	G(u)	a'+i	u'i	u'n	G(u)	a'-i
1	2.374	2.389	-5.010E-06	2.805E-03	-2.375	2.388	-3.397E-06	2.446E-03
2	2.374	2.389	-4.338E-06	2.602E-03	-2.375	2.388	-2.926E-06	2.254E-03
3	2.326	2.435	-1.387E-04	1.992E-02	-2.304	2.456	-5.407E-05	2.828E-02
4	2.132	2.607	-1.233E-03	9.919E-02	-2.238	2.517	-3.895E-03	5.410E-02
5	2.372	2.391	-2.431E-06	3.329E-03	-2.373	2.390	-1.016E-05	2.890E-03

		improved Breitung	Tvedt's EI
generalized reliability index betag =		**2.4312**	**2.4319**
probability	**Pf2 =**	**7.524E-03**	**7.509E-03**

FOUNDATION (LATERAL) - END-ON LOADING

var	ids	mean	st. dev.	param1	param2	param3	param4	init. pt
x1	2	7.20E+03	3.82E+03	8.76E+00	4.98E-01			7.20E+03
x2	2	4.37E-01	2.54E-01	-9.73E-01	5.39E-01			4.37E-01
x3	2	3.45E+01	1.16E+01	3.49E+00	3.27E-01			3.45E+01

deterministic parameters in limit-state function:
tp (1) = 8.100E-01
tp (2) = 7.000E-01
tp (3) = 1.100E+00

>>>> FIRST-ORDER RELIABILITY ANALYSIS <<<<

iteration number .....iter= 10
value of limit-state function..g(x)=-1.013E-08
reliability index .....beta= 2.8547
probability .....Pf1= 2.154E-03

var	design point		sensitivity vectors			
	x*	u*	alpha	gamma	delta	eta
x1	3.101E+03	-1.444E+00	-.5060	-.5060	1.0003	-.8704
x2	8.795E-01	1.566E+00	.5486	.5486	-.3070	-.4887
x3	6.090E+01	1.900E+00	.6656	.6656	-.3500	-.9927

>>>> SECOND-ORDER RELIABILITY ANALYSIS -- POINT FITTING <<<<

coordinates and ave. main curvatures of fitting points in rotated space

axis	u'i	u'n	G(u)	a'+i	u'i	u'n	G(u)	a'-i
1	2.855	2.855	2.802E-09	-2.736E-13	-2.855	2.855	1.666E-09	-1.561E-12
2	2.855	2.855	4.581E-09	-8.648E-13	-2.855	2.855	2.001E-09	-9.700E-13

		improved Breitung	Tvedt's EI
generalized reliability index	**betag =**	**2.8547**	**2.8547**
probability	**Pf2 =**	**2.154E-03**	**2.154E-03**

FOUNDATION (AXIAL) - END-ON LOADING

var	ids	mean	st. dev.	param1	param2	param3	param4	init. pt
x1	2	4.06E+03	1.26E+03	8.26E+00	3.03E-01			4.06E+03
x2	2	7.20E-01	4.20E-01	-4.75E-01	5.41E-01			7.20E-01
x3	2	3.45E+01	1.16E+01	3.49E+00	3.27E-01			3.45E+01

deterministic parameters in limit-state function:
tp (1) = 1.500E+00

tp (2) = 7.000E-01
tp (3) = 1.100E+00

>>>> FIRST-ORDER RELIABILITY ANALYSIS <<<<

---

iteration number .....iter= 8
value of limit-state function..g(x)= 7.839E-07
reliability index .....beta= 2.6956
probability .....Pf1= 3.513E-03

var	design point		sensitivity vectors			
	x*	u*	alpha	gamma	delta	eta
x1	2.949E+03	-9.059E-01	-.3360	-.3360	.4643	-.3881
x2	1.493E+00	1.618E+00	.6002	.6002	-.3202	-.5601
x3	6.204E+01	1.957E+00	.7259	.7259	-.3686	-1.1216

>>>> SECOND-ORDER RELIABILITY ANALYSIS -- POINT FITTING <<<<

coordinates and ave. main curvatures of fitting points in rotated space

axis	u'i	u'n	G(u)	a'+i	u'i	u'n	G(u)	a'-i
1	2.696	2.696	-3.426E-08	1.319E-11	-2.696	2.696	1.178E-07	9.164E-11
2	2.696	2.696	1.528E-08	4.389E-11	-2.696	2.696	7.024E-08	6.354E-11

		improved Breitung	Tvedt's EI
generalized reliability index betag =		**2.6956**	**2.6956**
probability	**Pf2 =**	**3.513E-03**	**3.513E-03**

DECK LEGS - BROADSIDE LOADING

var	ids	mean	st. dev.	param1	param2	param3	param4	init. pt
x1	2	6.31E+03	6.68E+02	8.74E+00	1.06E-01			6.31E+03
x2	2	6.68E+03	7.82E+02	8.80E+00	1.17E-01			6.68E+03
x3	2	1.65E-01	9.60E-02	-1.95E+00	5.40E-01			1.65E-01
x4	2	3.45E+01	1.16E+01	3.49E+00	3.27E-01			3.45E+01

deterministic parameters in limit-state function:
tp (1) = 1.197E+03
tp (2) = 4.200E-01
tp (3) = 7.000E-01
tp (4) = 1.100E+00
tp (5) = 1.000E+00

>>>> FIRST-ORDER RELIABILITY ANALYSIS <<<<

iteration number .....iter= 6
value of limit-state function..g(x)= 1.582E-05
reliability index .....beta= 3.5064
probability .....Pf1= 2.271E-04

var	design point		sensitivity vectors			
	x*	u*	alpha	gamma	delta	eta

x1	5.990E+03	-4.334E-01	-.1236	-.1236	.1310	-.0662
x2	6.626E+03	-1.579E-02	-.0045	-.0045	.0046	-.0006
x3	4.714E-01	2.214E+00	.6315	.6315	-.1469	-.9171
x4	7.871E+01	2.684E+00	.7655	.7655	-.2112	-1.7108

>>>> SECOND-ORDER RELIABILITY ANALYSIS -- POINT FITTING <<<<

coordinates and ave. main curvatures of fitting points in rotated space

axis	u'i	u'n	G(u)	a'+i	u'i	u'n	G(u)	a'-i
1	3.000	3.506	1.246E-07	-4.645E-06	-3.000	3.506	1.012E-07	-5.722E-06
2	3.000	3.503	3.034E-03	-8.486E-04	-3.000	3.500	7.652E-03	-1.369E-03
3	3.000	3.506	1.954E-11	-6.569E-08	-3.000	3.506	1.886E-11	-6.675E-08

	improved Breitung	Tvedt's EI
generalized reliability index betag =	**3.5059**	**3.5059**
probability Pf2 =	**2.276E-04**	**2.276E-04**

JACKET BAY 1 - BROADSIDE LOADING

var	ids	mean	st. dev.	param1	param2	param3	param4	init. pt
x1	2	2.93E+03	2.35E+02	7.98E+00	8.00E-02			2.93E+03
x2	2	4.57E-01	2.60E-01	-9.23E-01	5.30E-01			4.57E-01
x3	2	3.45E+01	1.16E+01	3.49E+00	3.27E-01			3.45E+01

deterministic parameters in limit-state function:
tp (1) = 7.000E-01
tp (2) = 1.100E+00
tp (3) = 0.000E+00

>>>> FIRST-ORDER RELIABILITY ANALYSIS <<<<

iteration number .....iter= 8
value of limit-state function..g(x)=-4.631E-06
reliability index .....beta= 2.4769
probability .....Pf1= 6.627E-03

var	design point		sensitivity vectors			
	x*	u*	alpha	gamma	delta	eta
x1	2.868E+03	-2.344E-01	-.0946	-.0946	.0971	-.0297
x2	9.030E-01	1.551E+00	.6261	.6261	-.3554	-.5577
x3	6.124E+01	1.917E+00	.7739	.7739	-.4028	-1.1668

>>>> SECOND-ORDER RELIABILITY ANALYSIS -- POINT FITTING <<<<

coordinates and ave. main curvatures of fitting points in rotated space

axis	u'i	u'n	G(u)	a'+i	u'i	u'n	G(u)	a'-i
1	2.477	2.477	2.713E-06	-3.212E-10	-2.477	2.477	2.731E-06	-4.792E-10
2	2.477	2.477	2.776E-06	-3.942E-10	-2.477	2.477	2.776E-06	-4.062E-10

	improved Breitung	Tvedt's EI
generalized reliability index betag =	**2.4769**	**2.4769**
probability Pf2 =	**6.627E-03**	**6.627E-03**

JACKET BAY 2 - BROADSIDE LOADING

var	ids	mean	st. dev.	param1	param2	param3	param4	init. pt
x1	2	2.02E+03	1.62E+02	7.61E+00	8.01E-02			2.02E+03
x2	2	5.21E-01	3.00E-01	-7.95E-01	5.35E-01			5.21E-01
x3	2	3.45E+01	1.16E+01	3.49E+00	3.27E-01			3.45E+01
x4	2	6.01E+02	6.01E+02	6.05E+00	8.33E-01			6.01E+02

deterministic parameters in limit-state function:
tp (1) = 7.000E-01
tp (2) = 1.100E+00

>>>> FIRST-ORDER RELIABILITY ANALYSIS <<<<

iteration number .....iter= 7
value of limit-state function..g(x)= 1.316E-03
reliability index .....beta= 2.0805
probability .....Pf1= 1.874E-02

var	design point		sensitivity vectors			
	x*	u*	alpha	gamma	delta	eta
x1	1.987E+03	-1.666E-01	-.0800	-.0800	.0817	-.0197
x2	9.051E-01	1.300E+00	.6247	.6247	-.4330	-.4153
x3	5.502E+01	1.590E+00	.7641	.7641	-.4774	-.9148
x4	3.338E+02	-2.901E-01	-.1398	-.1398	.2811	-.1132

>>>> SECOND-ORDER RELIABILITY ANALYSIS -- POINT FITTING <<<<

coordinates and ave. main curvatures of fitting points in rotated space

axis	u'i	u'n	G(u)	a'+i	u'i	u'n	G(u)	a'-i
1	2.024	2.136	-2.755E-05	2.690E-02	-1.996	2.162	-2.899E-06	4.077E-02
2	1.921	2.229	-3.830E-04	8.039E-02	-1.984	2.172	-9.648E-04	4.669E-02
3	2.075	2.086	-1.651E-07	2.575E-03	-2.075	2.085	-1.068E-06	2.306E-03

	improved Breitung	Tvedt's EI
generalized reliability index betag =	**2.1269**	**2.1276**
probability Pf2 =	**1.672E-02**	**1.669E-02**

JACKET BAY 3 - BROADSIDE LOADING

var	ids	mean	st. dev.	param1	param2	param3	param4	init. pt
x1	2	2.02E+03	1.62E+02	7.61E+00	8.01E-02			2.02E+03
x2	2	5.21E-01	3.00E-01	-7.95E-01	5.35E-01			5.21E-01
x3	2	3.45E+01	1.16E+01	3.49E+00	3.27E-01			3.45E+01
x4	2	6.01E+02	6.01E+02	6.05E+00	8.33E-01			6.01E+02

deterministic parameters in limit-state function:

tp (1) = 7.000E-01
tp (2) = 1.100E+00

>>>> FIRST-ORDER RELIABILITY ANALYSIS <<<<

iteration number .....iter= 7
value of limit-state function..g(x)= 1.316E-03
reliability index .....beta= 2.0805
probability .....Pf1= 1.874E-02

var	design point		sensitivity vectors			
	x*	u*	alpha	gamma	delta	eta
x1	1.987E+03	-1.666E-01	-.0800	-.0800	.0817	-.0197
x2	9.051E-01	1.300E+00	.6247	.6247	-.4330	-.4153
x3	5.502E+01	1.590E+00	.7641	.7641	-.4774	-.9148
x4	3.338E+02	-2.901E-01	-.1398	-.1398	.2811	-.1132

>>>> SECOND-ORDER RELIABILITY ANALYSIS -- POINT FITTING <<<<

coordinates and ave. main curvatures of fitting points in rotated space

axis	u'i	u'n	G(u)	a'+i	u'i	u'n	G(u)	a'-i
1	2.024	2.136	-2.755E-05	2.690E-02	-1.996	2.162	-2.899E-06	4.077E-02
2	1.921	2.229	-3.830E-04	8.039E-02	-1.984	2.172	-9.648E-04	4.669E-02
3	2.075	2.086	-1.651E-07	2.575E-03	-2.075	2.085	-1.068E-06	2.306E-03

		improved Breitung	Tvedt's EI
generalized reliability index betag =		**2.1269**	**2.1276**
probability	**Pf2 =**	**1.672E-02**	**1.669E-02**

JACKET BAY 4 - BROADSIDE LOADING

var	ids	mean	st. dev.	param1	param2	param3	param4	init. pt
x1	2	2.28E+03	1.82E+02	7.73E+00	7.98E-02			2.28E+03
x2	2	5.36E-01	3.10E-01	-7.68E-01	5.37E-01			5.36E-01
x3	2	3.45E+01	1.16E+01	3.49E+00	3.27E-01			3.45E+01
x4	2	1.85E+03	1.85E+03	7.18E+00	8.33E-01			1.85E+03

deterministic parameters in limit-state function:
tp (1) = 7.000E-01
tp (2) = 1.100E+00

>>>> FIRST-ORDER RELIABILITY ANALYSIS <<<<

iteration number .....iter= 8
value of limit-state function..g(x)= 5.077E-02
reliability index .....beta= 2.4163
probability .....Pf1= 7.840E-03

var	design point		sensitivity vectors			
	x*	u*	alpha	gamma	delta	eta
x1	2.239E+03	-1.630E-01	-.0672	-.0672	.0686	-.0163
x2	1.028E+00	1.482E+00	.6129	.6129	-.3690	-.5029
x3	5.904E+01	1.805E+00	.7468	.7468	-.4153	-1.0468

x4 7.974E+02 -5.972E-01 -.2494 -.2494 .5568 -.2572

>>>> SECOND-ORDER RELIABILITY ANALYSIS -- POINT FITTING <<<<

coordinates and ave. main curvatures of fitting points in rotated space

axis	u'i	u'n	G(u)	a'+i	u'i	u'n	G(u)	a'-i
1	2.366	2.465	-1.113E-04	1.756E-02	-2.359	2.472	-1.740E-05	1.996E-02
2	2.105	2.691	-1.294E-02	1.242E-01	-2.179	2.632	-7.859E-03	9.085E-02
3	2.382	2.450	4.728E-03	1.178E-02	-2.385	2.447	-2.263E-04	1.080E-02

	improved Breitung	Tvedt's EI
generalized reliability index betag =	**2.4773**	**2.4784**
probability Pf2 =	**6.619E-03**	**6.599E-03**

JACKET BAY 5 - BROADSIDE LOADING

var	ids	mean	st. dev.	param1	param2	param3	param4	init. pt
x1	2	2.92E+03	2.34E+02	7.98E+00	7.99E-02			2.92E+03
x2	2	5.38E-01	3.10E-01	-7.63E-01	5.35E-01			5.38E-01
x3	2	3.45E+01	1.16E+01	3.49E+00	3.27E-01			3.45E+01
x4	2	2.78E+03	2.78E+03	7.58E+00	8.33E-01			2.78E+03

deterministic parameters in limit-state function:
tp (1) = 7.000E-01
tp (2) = 1.100E+00

>>>> FIRST-ORDER RELIABILITY ANALYSIS <<<<

iteration number .....iter= 9
value of limit-state function..g(x)= 7.134E-02
reliability index .....beta= 2.7467
probability .....Pf1= 3.010E-03

var	design point		sensitivity vectors			
	x*	u*	alpha	gamma	delta	eta
x1	2.873E+03	-1.810E-01	-.0662	-.0662	.0676	-.0172
x2	1.143E+00	1.675E+00	.6101	.6101	-.3084	-.6043
x3	6.390E+01	2.047E+00	.7458	.7458	-.3572	-1.2164
x4	1.080E+03	-7.185E-01	-.2592	-.2592	.6013	-.2900

>>>> SECOND-ORDER RELIABILITY ANALYSIS -- POINT FITTING <<<<

coordinates and ave. main curvatures of fitting points in rotated space

axis	u'i	u'n	G(u)	a'+i	u'i	u'n	G(u)	a'-i
1	2.687	2.805	-5.700E-04	1.626E-02	-2.675	2.817	-1.215E-04	1.950E-02
2	2.349	3.094	-1.939E-02	1.259E-01	-2.448	3.016	-2.126E-02	8.986E-02
3	2.697	2.796	3.531E-02	1.345E-02	-2.704	2.789	-1.222E-03	1.142E-02

	improved Breitung	Tvedt's EI
generalized reliability index betag =	**2.8074**	**2.8084**
probability Pf2 =	**2.497E-03**	**2.490E-03**

FOUNDATION (LATERAL) - BROADSIDE LOADING

var	ids	mean	st. dev.	param1	param2	param3	param4	init. pt
x1	2	3.21E+03	2.56E+02	8.07E+00	7.97E-02			3.21E+03
x2	2	5.38E-01	3.10E-01	-7.63E-01	5.35E-01			5.38E-01
x3	2	3.45E+01	1.16E+01	3.49E+00	3.27E-01			3.45E+01
x4	2	2.95E+03	2.95E+03	7.64E+00	8.33E-01			2.95E+03

deterministic parameters in limit-state function:
tp (1) = 7.000E-01
tp (2) = 1.100E+00

>>>> FIRST-ORDER RELIABILITY ANALYSIS <<<<

iteration number .....iter= 9
value of limit-state function..g(x)= 9.166E-02
reliability index .....beta= 2.8420
probability .....Pf1= 2.242E-03

var	design point		sensitivity vectors			
	x*	u*	alpha	gamma	delta	eta
x1	3.148E+03	-1.890E-01	-.0668	-.0668	.0683	-.0179
x2	1.181E+00	1.736E+00	.6112	.6112	-.2902	-.6378
x3	6.548E+01	2.122E+00	.7471	.7471	-.3401	-1.2714
x4	1.141E+03	-7.256E-01	-.2527	-.2527	.5876	-.2841

>>>> SECOND-ORDER RELIABILITY ANALYSIS -- POINT FITTING <<<<

coordinates and ave. main curvatures of fitting points in rotated space

axis	u'i	u'n	G(u)	a'+i	u'i	u'n	G(u)	a'-i
1	2.777	2.906	-9.547E-04	1.655E-02	-2.763	2.919	-2.252E-04	2.026E-02
2	2.419	3.210	-1.834E-02	1.256E-01	-2.533	3.121	-2.813E-02	8.690E-02
3	2.791	2.892	9.047E-02	1.276E-02	-2.799	2.884	-1.614E-03	1.069E-02

	improved Breitung	Tvedt's EI
generalized reliability index betag =	**2.9018**	**2.9027**
probability Pf2 =	**1.855E-03**	**1.850E-03**

FOUNDATION (AXIAL) - BROADSIDE LOADING

var	ids	mean	st. dev.	param1	param2	param3	param4	init. pt
x1	2	7.70E+03	4.31E+03	8.81E+00	5.22E-01			7.70E+03
x2	2	5.40E-01	3.10E-01	-7.59E-01	5.34E-01			5.40E-01
x3	2	3.45E+01	1.16E+01	3.49E+00	3.27E-01			3.45E+01

deterministic parameters in limit-state function:
tp (1) = 8.100E-01
tp (2) = 7.000E-01
tp (3) = 1.100E+00

>>>> FIRST-ORDER RELIABILITY ANALYSIS <<<<

iteration number .....iter= 9
value of limit-state function..g(x)= 1.137E-05
reliability index .....beta= 2.6657
probability .....Pf1= 3.841E-03

var	design point		sensitivity vectors			
	x*	u*	alpha	gamma	delta	eta
x1	3.230E+03	-1.402E+00	-.5260	-.5260	1.0600	-.8858
x2	1.006E+00	1.433E+00	.5375	.5375	-.3367	-.4205
x3	5.812E+01	1.757E+00	.6592	.6592	-.3767	-.8938

>>>> SECOND-ORDER RELIABILITY ANALYSIS -- POINT FITTING <<<<

coordinates and ave. main curvatures of fitting points in rotated space

axis	u'i	u'n	G(u)	a'+i	u'i	u'n	G(u)	a'-i
1	2.666	2.666	7.921E-07	-1.080E-10	-2.666	2.666	1.511E-06	2.475E-09
2	2.666	2.666	-8.359E-07	6.449E-10	-2.666	2.666	9.216E-07	1.788E-09

	improved Breitung	Tvedt's EI
generalized reliability index betag =	**2.6657**	**2.6657**
probability Pf2 =	**3.841E-03**	**3.841E-03**

---

var	ids	mean	st. dev.	param1	param2	param3	param4	init. pt
x1	2	4.06E+03	1.26E+03	8.26E+00	3.03E-01			4.06E+03
x2	2	8.70E-01	5.00E-01	-2.82E-01	5.34E-01			8.70E-01
x3	2	3.45E+01	1.16E+01	3.49E+00	3.27E-01			3.45E+01

deterministic parameters in limit-state function:
tp (1) = 1.500E+00
tp (2) = 7.000E-01
tp (3) = 1.100E+00

>>>> FIRST-ORDER RELIABILITY ANALYSIS <<<<

iteration number .....iter= 8
value of limit-state function..g(x)= 4.626E-09
reliability index .....beta= 2.4931
probability .....Pf1= 6.332E-03

var	design point		sensitivity vectors			
	x*	u*	alpha	gamma	delta	eta
x1	3.007E+03	-8.417E-01	-.3376	-.3376	.4600	-.3692
x2	1.667E+00	1.484E+00	.5952	.5952	-.3577	-.4917
x3	5.929E+01	1.818E+00	.7292	.7292	-.4026	-1.0309

>>>> SECOND-ORDER RELIABILITY ANALYSIS -- POINT FITTING <<<<

coordinates and ave. main curvatures of fitting points in rotated space

axis	u'i	u'n	G(u)	a'+i	u'i	u'n	G(u)	a'-i
1	2.493	2.493	-2.963E-09	-5.540E-13	-2.493	2.493	1.311E-09	1.256E-12
2	2.493	2.493	1.986E-10	1.348E-12	-2.493	2.493	2.955E-09	-4.818E-13

	improved Breitung	Tvedt's EI
generalized reliability index betag =	**2.4931**	**2.4931**
probability Pf2 =	**6.332E-03**	**6.332E-03**

Appendix C ULSLEA
Ultimate Limit State Limit Equilibrium Analysis

User Manual

ULSLEA

Ultimate Limit State Limit Equilibrium Analysis

Contents

C1. Introduction

C1.1 Introduction

ULSLEA is the proto type of a simplified nonlinear structural analysis program developed for level 2 screening of steel, template-type offshore platforms. It is based on simplified load and capacity calculation procedures developed for the joint industry-Government sponsored research project called *"Screening Methodologies for Use in Platform Assessments and Requalifications"*.

This research has been performed at the University of California at Berkeley, Department of Civil Engineering by Research Assistant Mehrdad Mortazavi under supervision of Professor Robert Bea. The theoretical background of ULSLEA is documented in previous chapters of this report.

C1.2 Application Range of ULSLEA

ULSLEA can be applied to typical, symmetrical, jacket type platforms with generic geometries; 4-, 6-, 8-, and 12-leg platforms with up to 8 jacket bays (at present stage). The loading has been calibrated to platforms located in deep and intermediate water depths. At this stage, ULSLEA is expected to give some what conservative results in case of shallow water platforms. For information on other limitations of the program, please refer to next sections of this appendix.

C1.3 Program Structure

The program is developed using Microsoft Excel Spreadsheet Software. The following Excel files are linked together and comprise the program:

- ULSLEA.XLS
- CAP.XLS
- KIN.XLS
- LOAD.XLS
- TRASH.XLS
- INP.XLM

C1.4 Installation and Execution

It is strongly recommended to run ULSLEA on at least a 486 - 66MHz PC with 8MB of RAM. Otherwise the speed of the program will be significantly reduced.

The files on the floppy disk are in compressed (zipped) format. The unzipping program, PKUNZIP.EXE, is also included on the disk. Following steps need to be taken to install and run the program:

To install:

- Copy the files ULSLEA.ZIP and PKUNZIP.EXE into your computer's hard disk
- Unzip ULSLEA.ZIP by typing:

pkunzip ulslea.zip

To run:

- In Excel version 4.0, open the file ULSLEA.XLS (**password =TEST**). All other files will be automatically opened and a customized menu bar will appear, which includes all commands that are necessary to run the program.

To Exit:

- Choose EXIT from the FILE menu.

C2. Input Data

C2.1 Introduction

There are principally two ways of data input in the program:

a) by stepping through the input menu and defining the necessary parameters or

b) by opening an input file that has been originally created by stepping through the input menu and subsequently saved.

The data that needs to be defined by the user is subdivided into five principle categories:

- Environmental Conditions
- Global Parameters
- Local Parameters
- Material and Soil Properties
- Uncertainties and Biases

C2.2 Environmental Conditions

Under this category, the user is required to define the site specific environmental parameters which are then used to calculate the aero- and hydrodynamic forces acting on the platform. These include water depth, storm surge, wind, wave, and current parameters (Figure C3):

- Water Depth, Storm Surge (ft)
- Wind : velocity @ 30 ft elevation (mph)
- Wave: height (ft) and period (sec)
- Current: velocities (fps) @ SWL and mudline
  current profile: linear/quadratic/constant with depth:

If linear or quadratic current velocity profiles are specified, the profile is stretched from still water level up to the wave crest so that the water volume remains unchanged. If a constant current velocity profile is specified, the velocities will be equal to the specified velocity every where in the water column.

C2.3 Global Parameters

These include global data on platform (Figures C4 & C5):

- Number of supporting legs: (4,6,8 or 12)
- Number of jacket bays: (at this time =< 8)
- Total deck weight (kips)
- Deck and Cellar deck dimensions (ft)
- Base Centerline Width (ft): the horizontal distance between the central axis of the two outer jacket legs @ the base of the jacket

- Top Centerline Width (ft): the horizontal distance between the central axis of the two outer jacket legs @ the top of the jacket
- Middle Section Width (ft): the horizontal distance between the central axis of the two inner jacket legs (0 for 4- and 6-leg platforms)
- Bay Heights (ft)
- Total Number of Joints: the sum of the number of joints with different joint parameters in two orthogonal planes (End-on and Broadside) , n= < 50
- Total number of Diagonal Braces: the sum of the number of vertical diagonal braces in all planes at a given bay and with a given direction (end-on/broadside), n=<12 per jacket bay and direction

C2.4 Local Parameters

The input data file for local parameters is subdivided into the following sections:

- Decklegs and vertical diagonal braces
- Horizontal braces
- Joints
- Foundation
- Force Coefficients
- Boatlanding and appurtenances

C2.4.1 Decklegs and vertical diagonal braces

Deckleg diameter (in) and thickness (in) are to be specified first. Then, for each jacket bay, starting from top to the bottom of jacket, the following data is required (Figures C6 & C7):

- Jacket leg diameter
- Jacket leg thickness: only for the uppermost jacket bay
- Bracing information:
  For each vertical diagonal brace in a given bay the diameter, thickness, type of axial loading (tension/compression), position of the brace relative

to wave direction (left, center, right) and the brace configuration (S (Single)-braced, K-braced, and X-braced) are to be defined. Wave, current, and wind flow directions are assumed to be **from left to the right**. In addition, the identification number of the joints at the two ends of each brace element are required.

For damaged or repaired members, *Dent Depth* and *Out-of-Straightness* have to be defined. Please note that in this case, a given brace can be either *Damaged* or *Repaired.*

C2.4.2 Horizontal braces

For each horizontal framing, the total number of elements, including non-diagonal members, is to be defined; at this time n= <20. For each element the following information is required (Figure C14):

- Diameter (in)
- Length (ft)
- Angle (degree): is to be measured from an axis parallel to the end-on side of the platform, $\alpha = < 90^{\circ}$

C2.4.3 Joints

For each joint that the user wants to include in the analysis, the following information is to be specified (Figure C8):

- Joint type (K, Y, X): see API RP 2A (20th edition) for joint classifications
- Chord diameter (in)
- Chord thickness (in)
- Branch diameter (in)
- Gap in K-joints (in)
- Chord/branch angle (degree)

If a rigid-joint assumption is to be made for the analysis, at least one joint has to be defined. The joint parameters are then to be specified so that the joint capacity is larger than member capacity. The ID# of this joint is then to be used to define the joints at the end of each diagonal member.

A bias factor can also be defined for joint capacity (see Section C2.6).

C2.4.4 Foundation

The following data is to be specified by the user (Figure C12):

- Pile length (ft): the embedded pile length
- Pile diameter (in)
- Pile thickness (in): no variation over legnth possible at this time
- If legs are grouted? yes, if the pile/jacket leg annulus is filled with grout
- If piles are plugged? yes, if any kind of plug exists inside the piles

C2.4.5 Force Coefficients

The following coefficients need to be defined (Figure C10):

- Modification Factors: current blockage factor
  directional spreading factor
- Force Coefficients: drag force coefficient on deck elements
  drag force coefficient on jacket elements
- Global Load Factor: defines the magnitude of lateral loading given a fixed loading pattern (Default = 1.0)
- Marine Growth (in): the variation over depth can be specified (Figure C11)

C2.4.6 Boatlanding and appurtenances

An equivalent area (ft^2) for boatlanding is to be defined for both end-on and broadside directions. This area is assumed to be at SWL. An equivalent diameter (ft) for appurtenances (conductors, risers, etc.) is to be defined for deck bay and every jacket bay. In this case, user has to include marine growth thickness in estimating the equivalent diameter for appurtenances (Figure C13).

C2.5 Member Strength, Material and Soil Properties

The following material and element properties are to be specified (Figure C9):

- Steel Yield Stress (ksi)
- Steel Elastic Modulus (ksi)
- Brace Buckling Length Factor
- Brace Residual Strength Factor (Default = 1.0 : elastic perfectly plastic behavior)

At present stage, only one soil layer can be considered. Soil parameters to be specified are:

- Soil Type (Clay/Sand)
- Linear Variation of Undrained Shear Strength (ksf)
- Angle of Friction of Soil (degree)
- Submerged Specific Weight of Soil(kips/ft^3)
- Scour Depth (ft)

Bias factors can be specified for axial and lateral pile capacities in sand and clay (see Section C2.6)

C2.6 Uncertainties and Biases

The current Version 1.0 of ULSLEA includes a simplified first order second moment reliability analysis. Failure of each component is defined as the "lower bound" capacity of the component being reached. The resulting reliability indices are conditional on the specified environmental conditions (storm surge, wave, current, and wind). For information on other underlying assumptions, please refer to Chapter 7 of this report.

COV's and Biases have to be defined for loadings and capacities:

Loadings:

- Wave on Deck Load
- Wave on Jacket Load

Capacities:

- Tubular Braces: bias and COV of axial compressive capacity of tubular braces
- Tubular Joints at this point, the uncertainty associated with joint capacity is not included in the reliability analysis
- Foundation: bias and COV of axial and lateral pile capacities in sand and clay.

Biases for tubular joints and those for foundation capacities are also used in deterministic analysis to predict a "best estimate" capacity of a given platform. The default value for these biases is taken to be B=1.0.

C3. Output

C3.1 Introduction

The output of ULSLEA is in graphical format. The following charts are produced by the program:

- Kinematics: wave, current, and total velocities vs. platform elevation
- End-on loading: cumulative storm shear force and platform's shear capacity vs. platform elevation
- Broadside loading
- Axial pile performance: in form of RSR = pile axial capacity/pile axial load
- Risk Analysis: for end-on and broadside loading directions

C3.2 Interpretation of Output Data

The velocity profiles are plotted from mudline to the top of deck legs (bottom of cellar deck). Current velocity profile is based on the input data provided by the user. If linear or quadratic current velocity profiles are specified, the profile is stretched from still water level up to the wave crest so that the water volume remains unchanged. If a constant current velocity profile is specified, the velocities will be equal to the specified velocity every where in the water column. The water particle velocity due to wave motion is based on Stoke's

5^{th} order theory. The total velocity is the linear summation of velocities due to current and wave.

The cumulative storm shear at a given elevation, is the integrated aero- and hydrodynamic forces acting on the portions of platform above that elevation. The ordinate at the top of the plot (top of decklegs) corresponds to total wind, wave and current forces acting on decks of the platform. The ordinate at mudline is the total base shear. When the storm shear profile touches the platform shear capacity profile at any elevation, the corresponding total base shear defines the capacity of the platform.

The upper-bound capacity of a given bay is based on failure of all of the resisting elements. The lower bound capacity of a given bay is based on first member failure and is plotted in addition to upper-bound capacity for jacket bays only.

The failure mode for a given bay is independent from other failure modes. As a result, different analyses for a platform with and without "fixed" base are unnecessary. The load can always be increased to estimate the collapse base shear for any failure mode in deck, jacket or foundation.

The simplified risk analysis subroutine is partially based on the developments included in Chapter 7 of this report. For each principal orthogonal direction, ***FOSM*** reliability indices (β) are shown for all failure modes in graphical format. These indices are in general conditional on environmental conditions and in particular on the specified wave height.

C4. Example

C4.1 Example Platform

The input data and analysis results of a four legged platform (Verification Platform C - PMB Benchmark Platform) is included in this appendix.

The input file of this 4-leg platform is copied on the floppy disk under "EXAMPLE". You can run the analysis of this platform by opening the file ULSLEA.XLS, choosing EXAMPLE as your input file, and running the program.

C4.2 Input Data

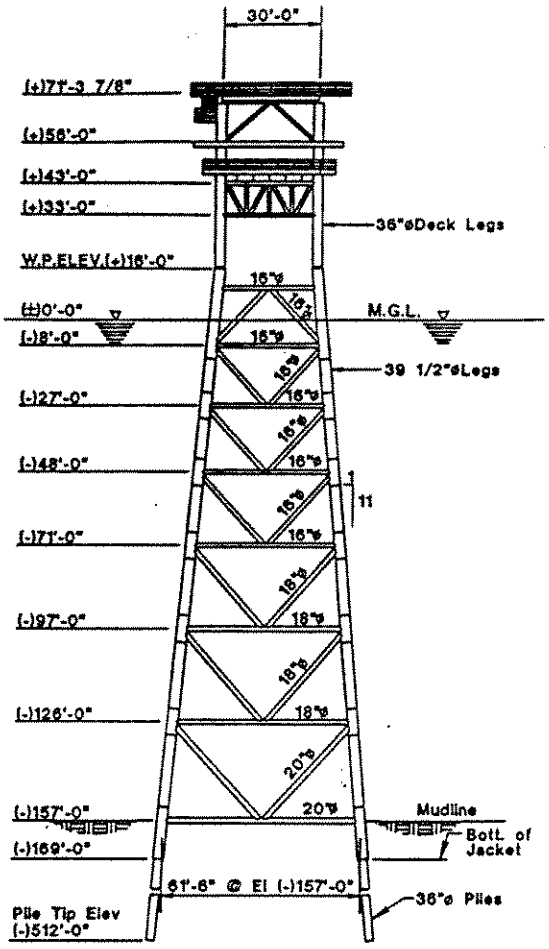

Figure C1: Platform C - Typical Elevation (Digre et. al., 1995)

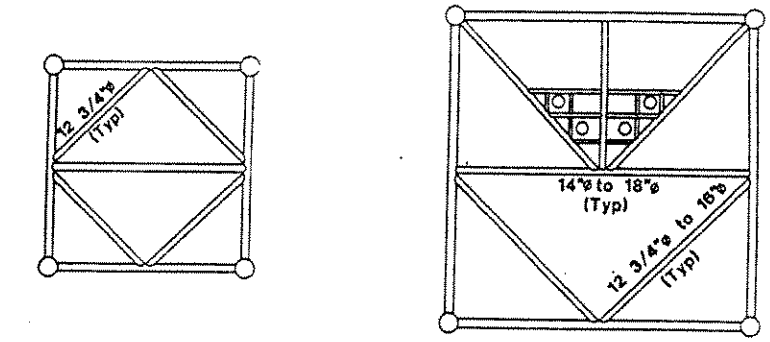

El.(-)8'-0", El(-)97'-0"

Other Jacket Elevations (Dia. Varies)

Figure C2: Platform C - Typical Horizontal Framings (Digre et. al., 1995)

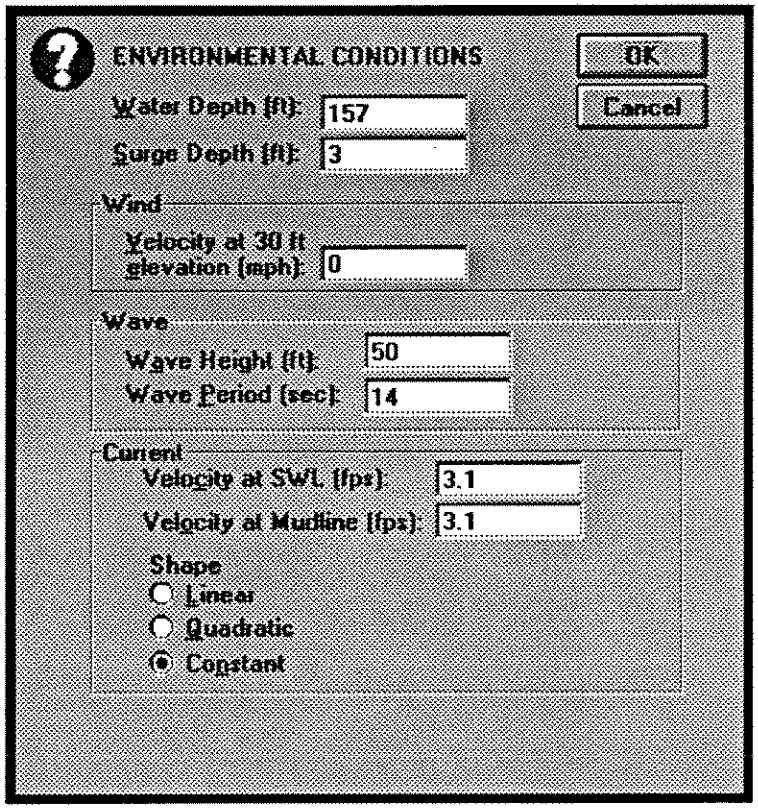

Figure C3: Platform C Input Data - Environmental Conditions

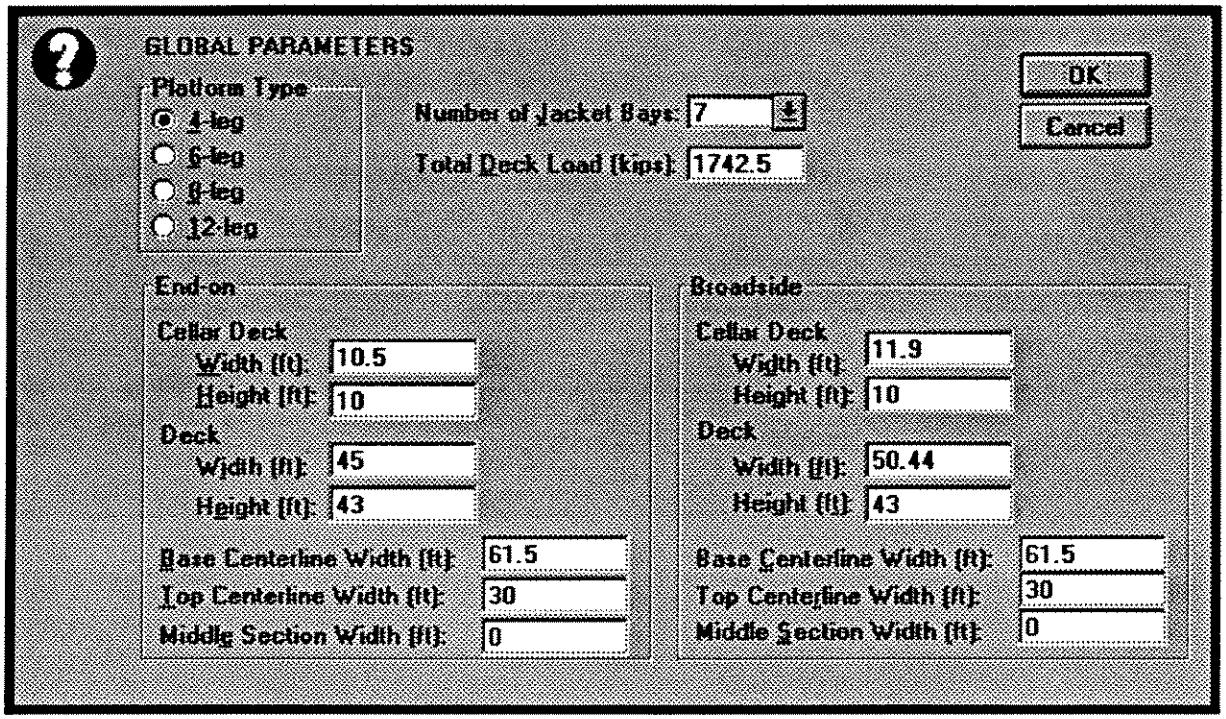

Figure C4: Platform C Input Data - Global Parameters

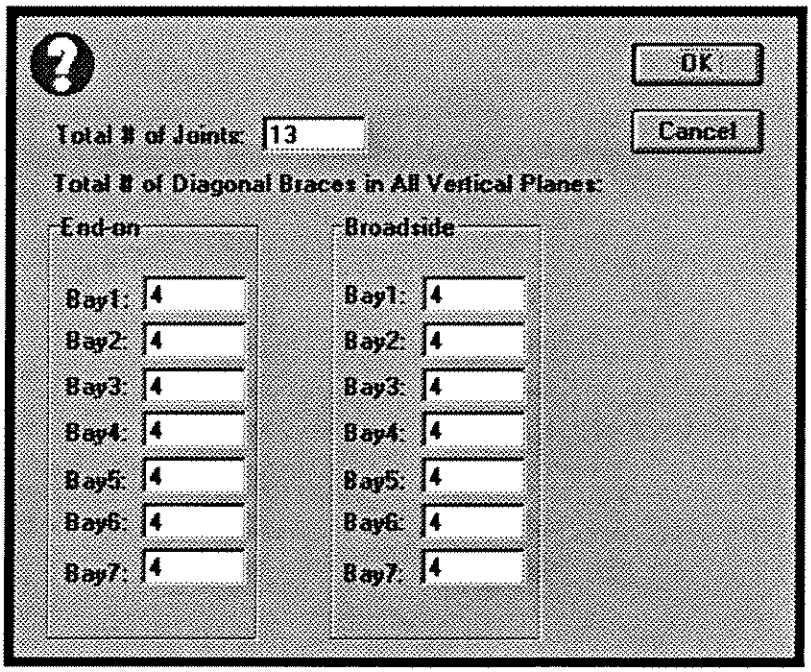

Figure C5: Platform C Input Data - Global Parameters

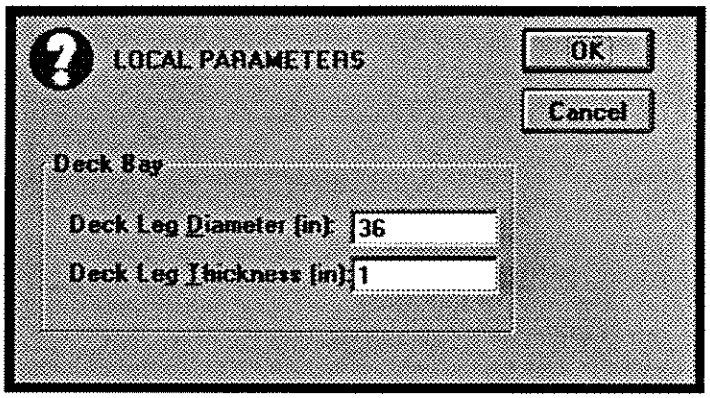

Figure C6: Platform C Input Data - Local Parameters

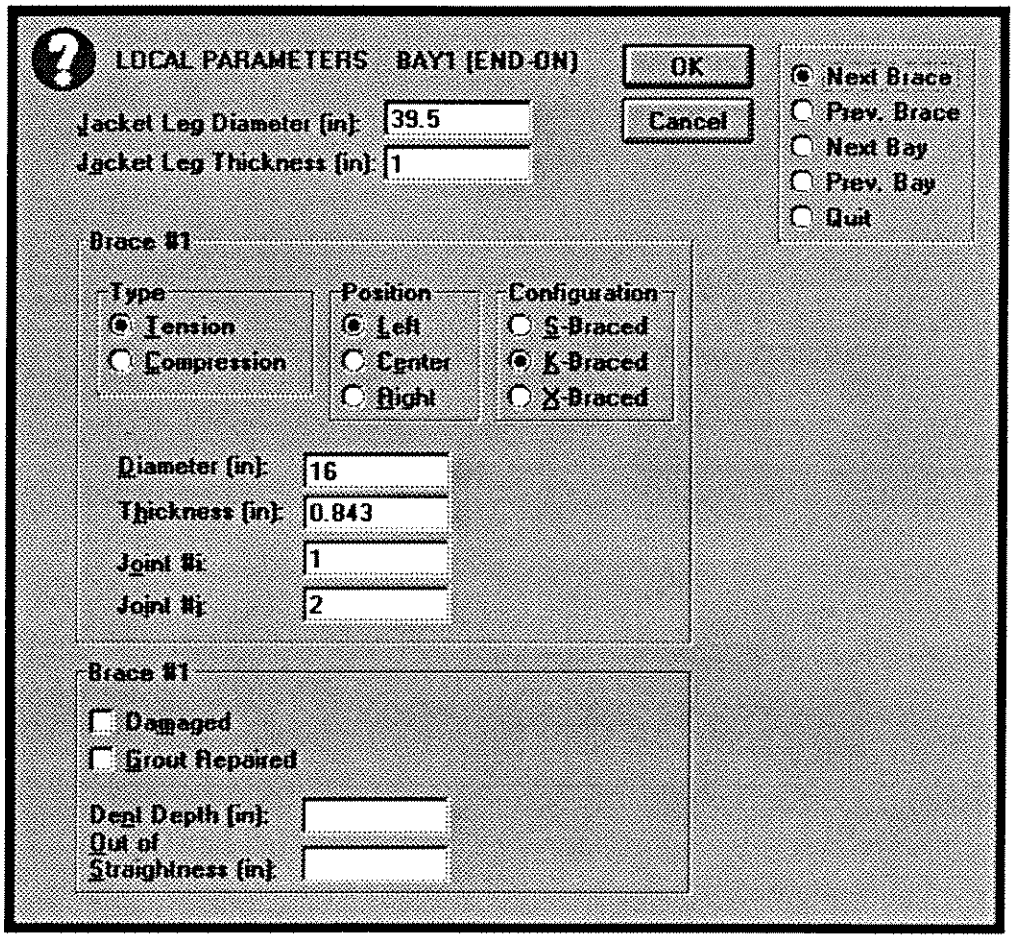

Figure C7: Platform C Input Data - Local Parameters (Vertical Diagonal Braces)

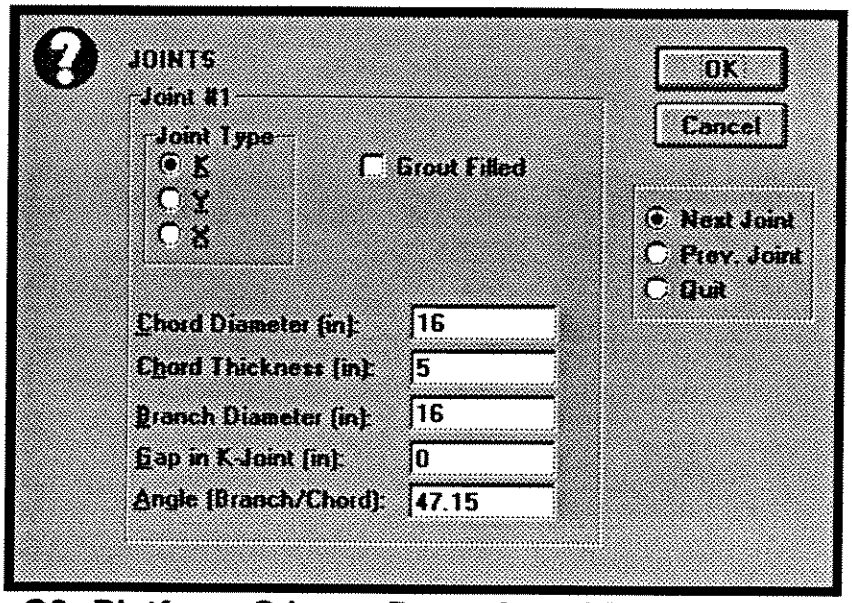

Figure C8: Platform C Input Data - Local Parameters (Joints)

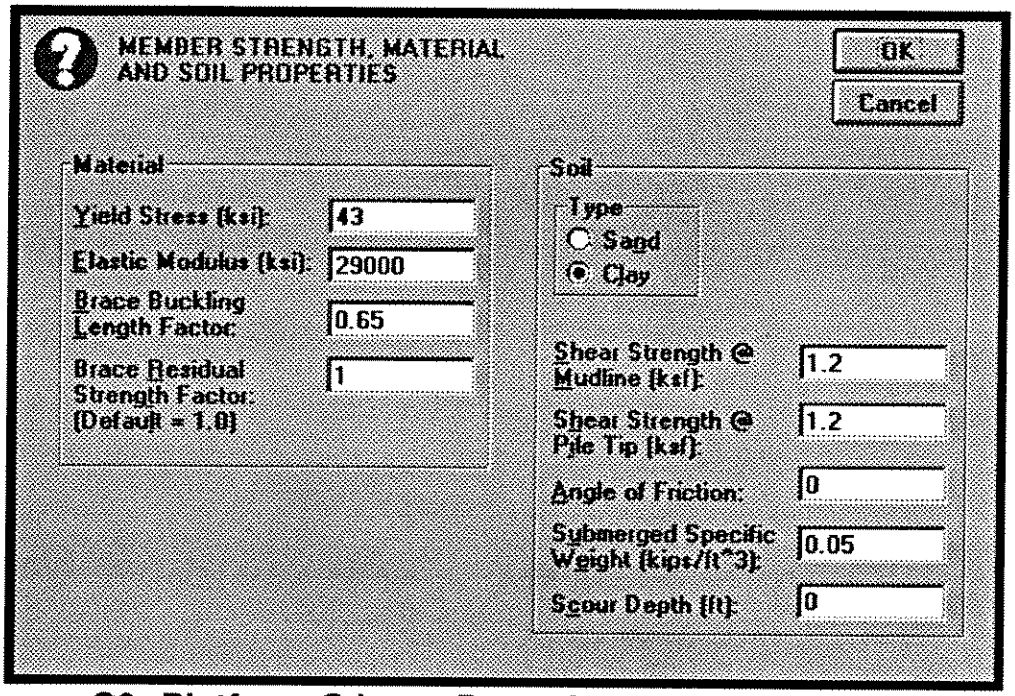

Figure C9: Platform C Input Data - Local Parameters (Member Strength, Material and Soil Properties)

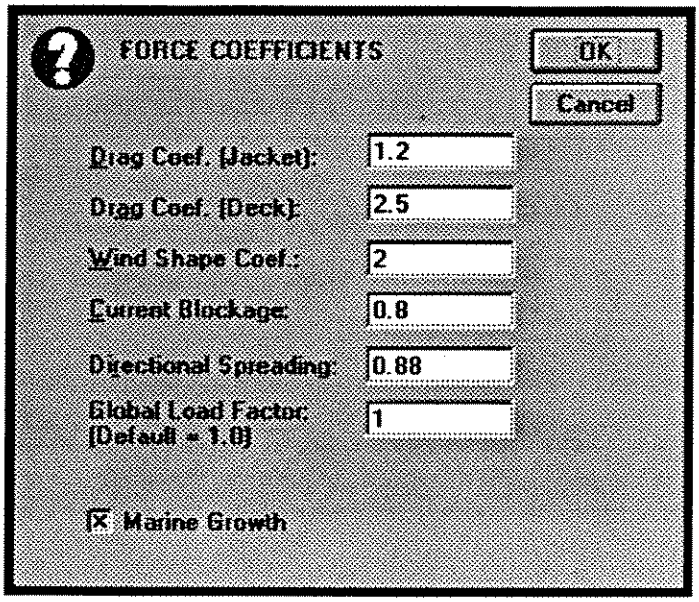

Figure C10: Platform C Input Data - Local Parameters (Force Coefficients)

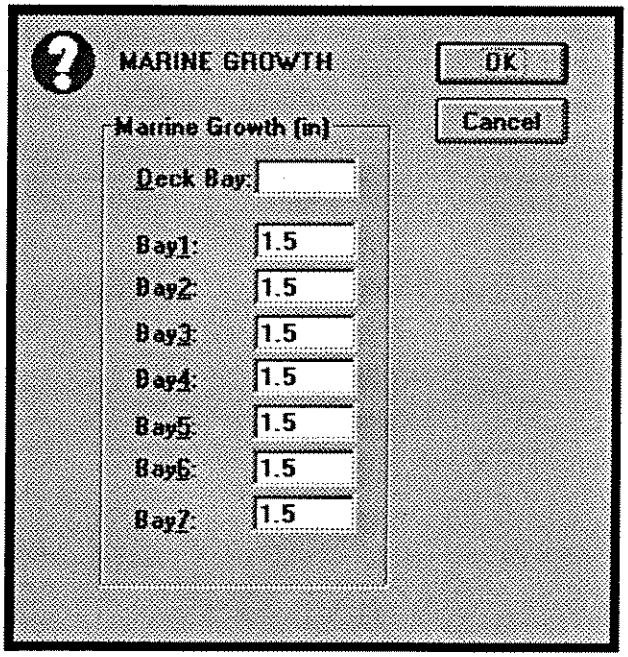

Figure C11: Platform C Input Data - Local Parameters (Marine Growth)

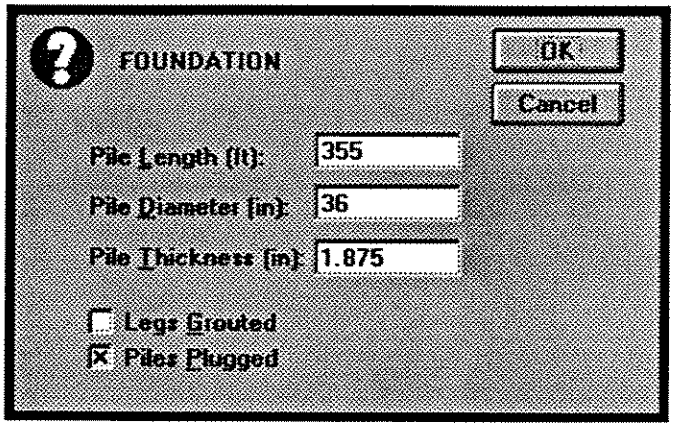

Figure C12: Platform C Input Data - Local Parameters (Foundation)

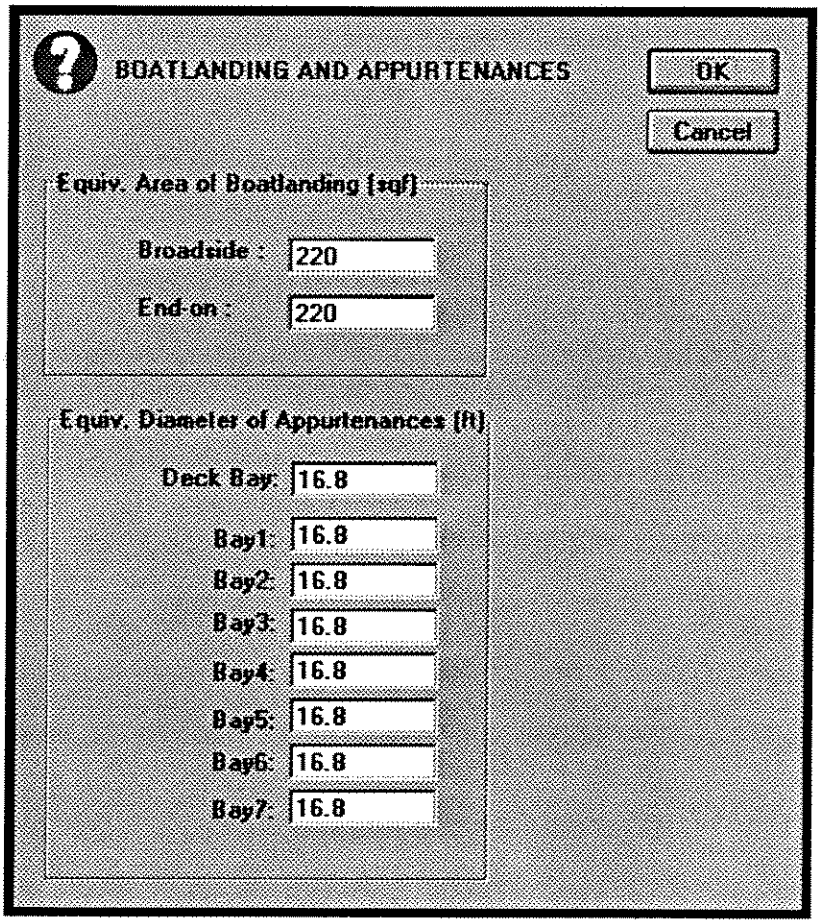

Figure C13: Platform C Input Data - Local Parameters (Boatlanding and Appurtenances)

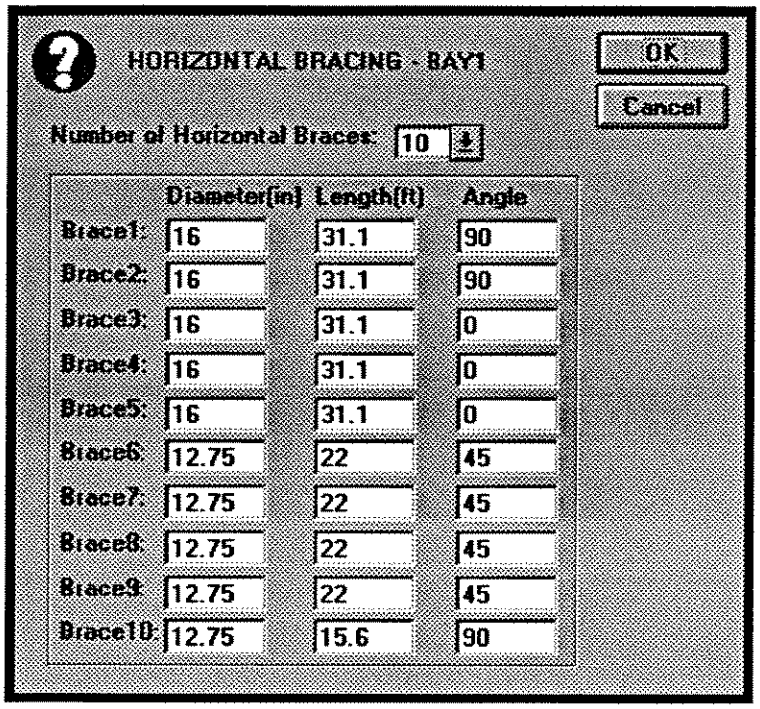

Figure C14: Platform C Input Data - Local Parameters (Horizontal Bracing - Bay1)

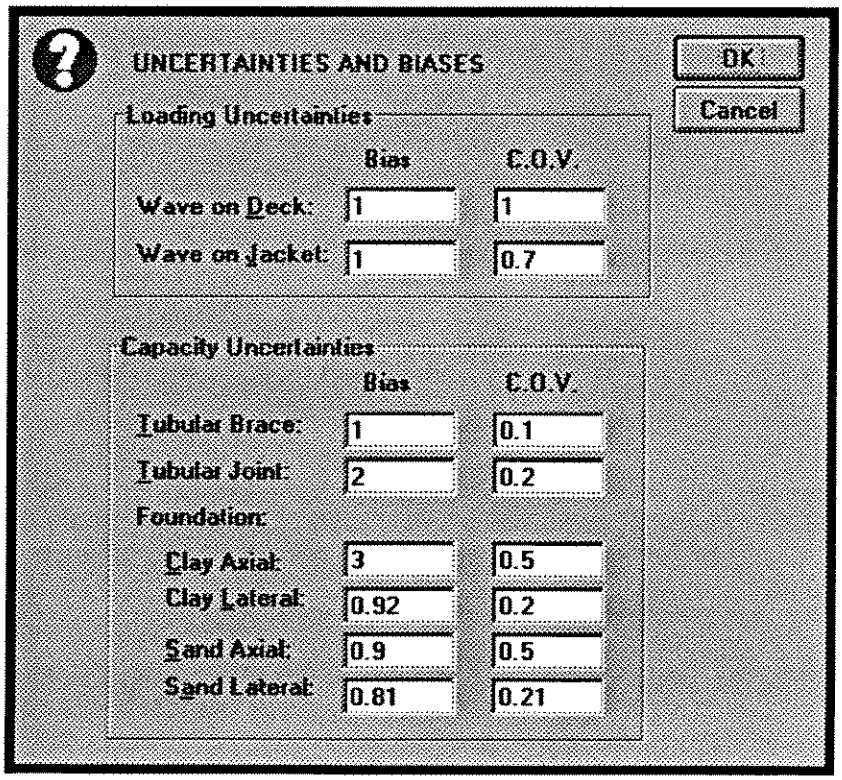

Figure C15: Platform C Input Data - Uncertainties and Biases

C4.3 Output

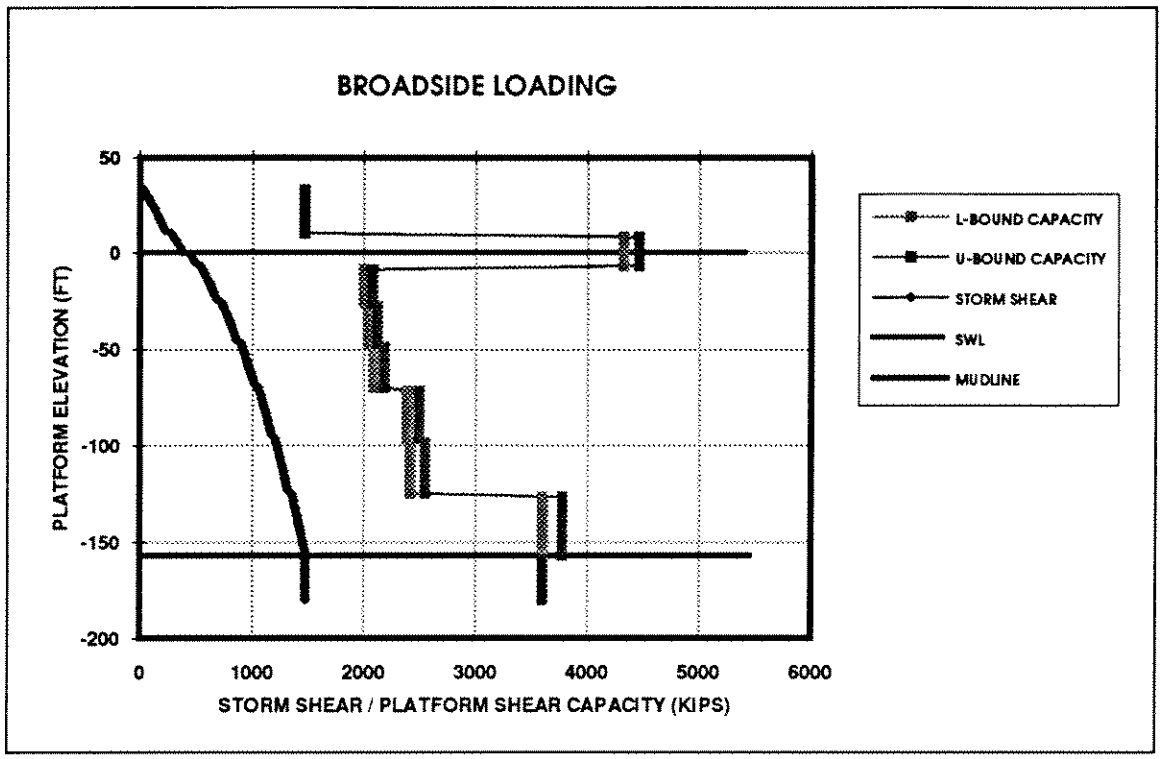

Figure C16: Platform C - Storm Shear vs Shear Capacity

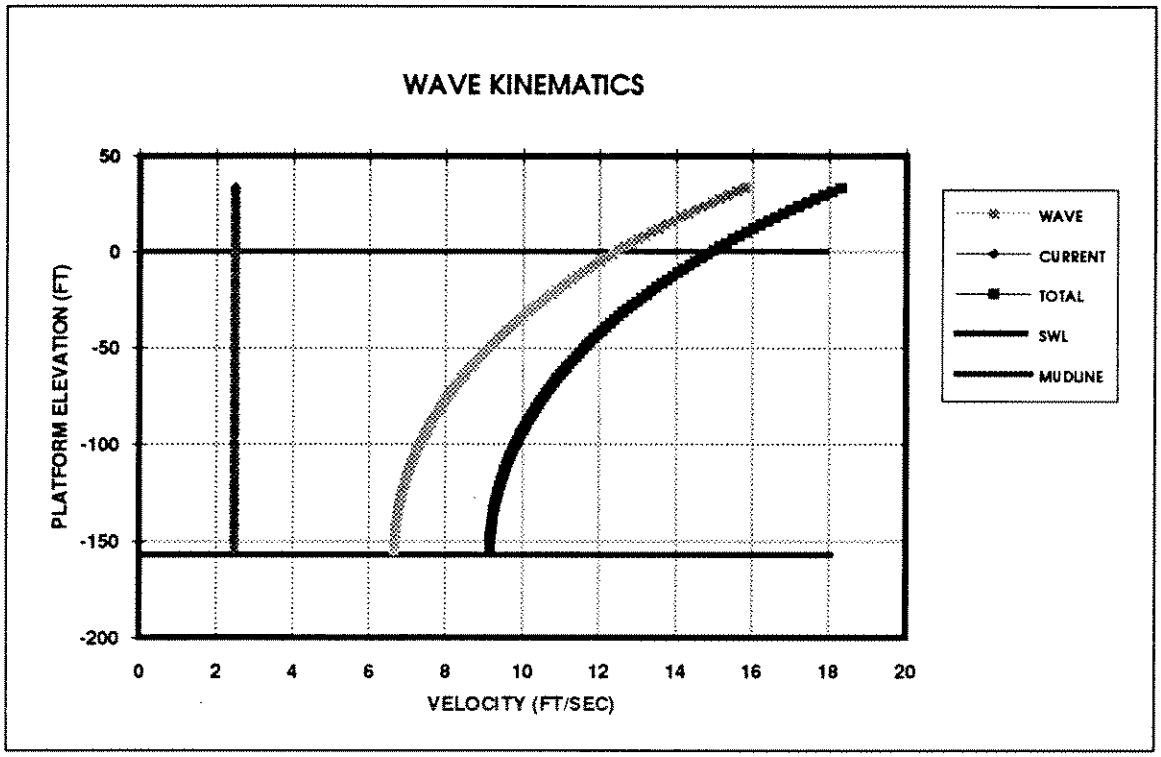

Figure C17: Platform C - Kinematics

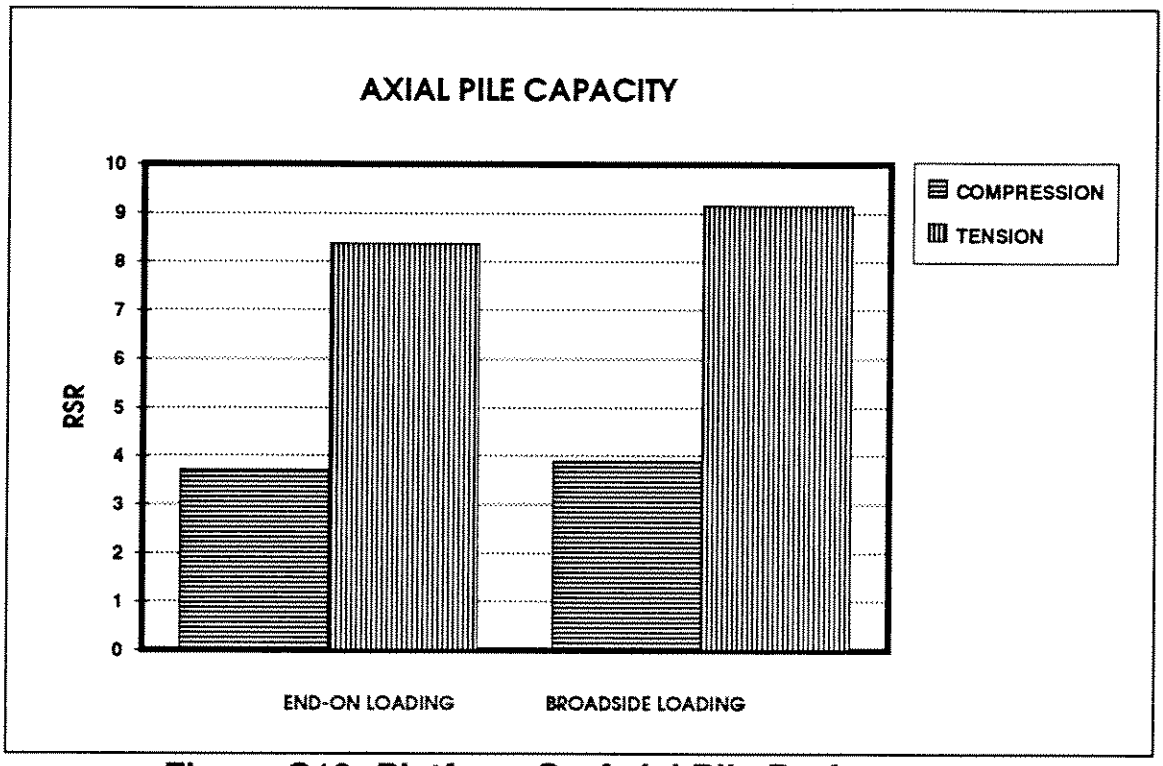

Figure C18: Platform C - Axial Pile Performance

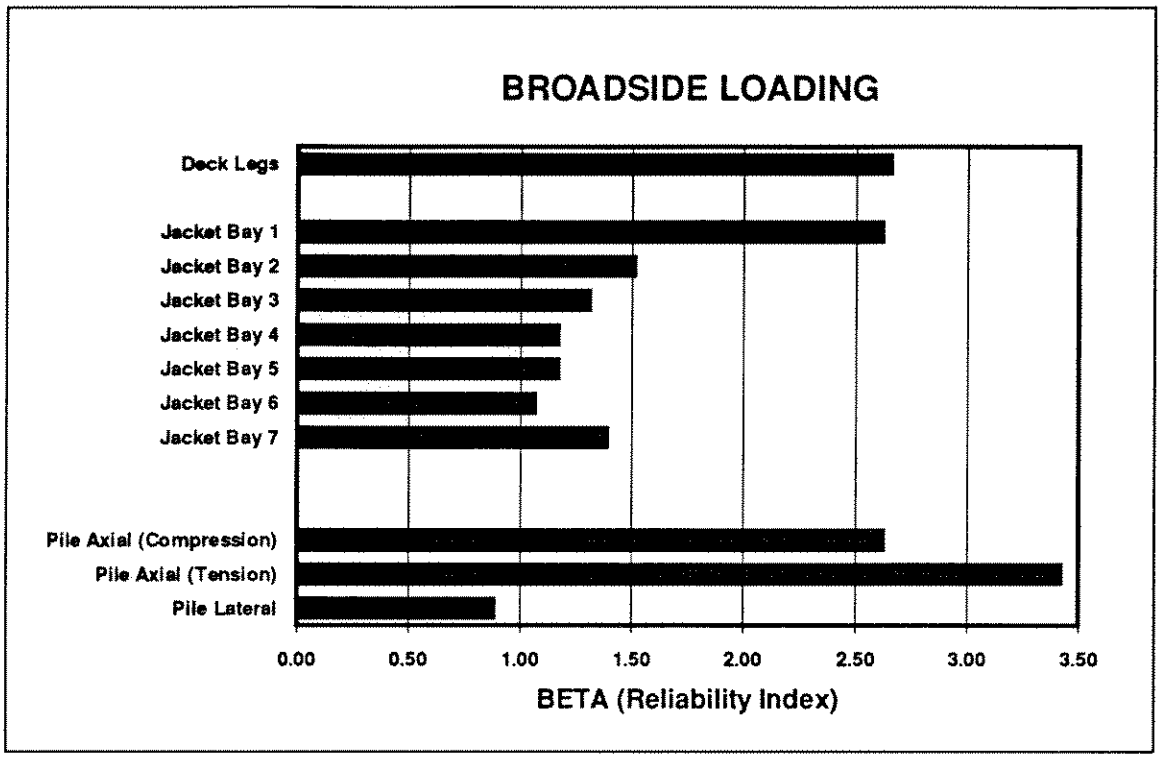

Figure C19: Platform C - Risk Analysis (Broadside Loading)